Technische Universiteit Delft

Control of Multi-Terminal VSC-HVDC for Offshore Wind Power Integration

M.Sc. thesis

Student:

Christian Ismunandar

Thesis committee:

Prof. ir. W. L. Kling
Dr. ir. M. Gibescu
ir. S. W. H. de Haan
ir. A. A. van der Meer

Electrical Power Systems

Department of Electrical Sustainable Energy
Faculty of Electrical Engineering, Mathematics and Computer Science
Delft University of Technology

August, 2010

Contact:

Christian Ismunandar
e-mail: ismunandar@gmail.com

Abstract

Wind power evolution in Northern Europe is foreseen to continue in the future with development of large-scale wind power plants (WPPs) on far offshore. Integration scheme of these WPPs to the onshore grids would grow from point-to-point connection to a transnational multi-terminal network where the transmission capacity serves both to evacuate the wind power and to facilitate power trading between countries. In such a situation, application of multi-terminal VSC-HVDC transmission is considered the favorable technological solution. A control strategy which capable of accommodating different dispatch schemes is however required.

This thesis presents a control strategy for dispatching power in the future transnational network situation. The control strategy is developed based on the voltage-margin method and is customized to comply with different dispatch schemes possibly be applied in the future transnational network. The control strategy is implemented on a multi-terminal VSC-HVDC network representing the future transnational network and its capabilities are confirmed through simulation studies for normal and abnormal operations. For normal operation, the capability to dispatch the offshore wind power as well as the traded power among the onshore grids is explored under wind speed changes. For abnormal operation, the capability to interchangeably control the direct voltage upon disconnection of a direct voltage controlling converter is examined. In addition, the compatibility of the control strategy to work with particular low voltage ride-through mechanisms is reported. The control strategy, the multi-terminal network and the simulation studies are implemented in MATLAB/Simulink.

Contents

1 Introduction

1.1 Background considerations

Demand of electricity is ever increasing. Over the past decades, the increment in electricity demand has been largely balanced by capacity development of conventional generations. However, further capacity development of these generations to balance demand of electricity is considered unsustainable mainly due to limited resource of their primary energies and due to negative impacts they introduce to the environment. In order to meet the future demand of electricity as well as to replace ageing existing generations, a number of new generation technologies i.e. wind power, solar thermal, solar photovoltaic, biomass, biodiesel, tidal power and wave power, which make use of the renewable energy resources e.g. wind, solar, biomass, biodiesel, tidal and wave energy as their primary energy, have been developed.

Wind power technology transforms kinetic energy in wind speed into electricity by utilizing a number of wind turbines. These wind turbines are installed in a particular area where the potency of wind energy is high and are linked together forming a wind power plant (WPP). In Europe, development of WPPs for electricity generation has been growing in past years and is expected to continue in the near future. At present, contribution of WPPs to electricity generation only covers a small percentage of the load. These WPPs are installed onshore and offshore close to the shore (less than 60 km). In the future, it is foreseen that a number of large capacity WPPs would be installed further offshore (more than 60 km) where high potency of wind energy and large space are available.

In order to integrate the future far offshore WPPs into the onshore grid, long cable transmission would be required. Moreover, regarding the capacity of these WPPs, large transmission capacity would be required. However, variability of the wind speed and thus variability of the power generated by WPPs would result in a relatively low capacity factor of the transmission and thus relatively high transmission cost per amount of energy delivered. The capacity factor can be increased if the transmission connects several offshore WPPs. Moreover, if the transmission is extended further, it may be used to facilitate power trading between countries in addition to evacuate power from the WPP. If these solutions were applied, several far offshore WPPs would be connected to multiple onshore grids and thus it would lead to the development of a transnational offshore network.

For such a multi-terminal offshore network, where large power would be transmitted over long distance, application of high-voltage alternating-current transmission (HVAC) technology may be difficult to implement due to large amount of reactive power compensation required. Thus, an alternative is to use high-voltage direct-current transmission (HVDC) technology. Moreover, since the offshore network may act as a power pool where power may be injected to and extracted from the network at different nodes, flexibility to control direction of power whilst maintaining voltage in the network is required. For such a situation, implementation of voltage sourced converter HVDC (VSC-HVDC) technology is favorable.

VSC-HVDC is capable of changing the direction of power whilst maintaining voltage in the dc network. Moreover, it is capable of performing independent active and reactive power control and of operating without necessarily depends on communication between the converters. Furthermore, since it is self commutated, it is inherently capable of

providing self restoration as well as providing black start for the connected grid or the connected offshore installation. In addition, it introduces a compact converter station for offshore application due to the reactive power compensator is not necessarily required, and the amount of filters is reduced compared to line commutated converter HVDC (LCC-HVDC).

Considering that the offshore network may serve not only to evacuate power from large capacity WPPs but also to facilitate power trade between countries, different dispatch schemes may be applied by connected countries in order to trade power or to share power from the WPPs, or both. Thus, a general control strategy would be required in order to regulate the power flows in the offshore network and the exchange of power with onshore power systems.

A number of control strategies have been proposed in the literature for operation of a multi-terminal VSC-HVDC network, such as a future transnational network. Generally, they are based on the direct-voltage droop method and the voltage-margin method. The direct voltage droop method has been shown capable of performing several dispatch schemes by implementing different droop characteristics among converters. However, determination of the droop characteristics needs to take into account the topology of the multi-terminal network. Thus, the droop characteristic of each converter may require adjustment whenever the network topology changes. On the other hand, the voltage-margin method has been shown capable of performing the direct voltage control interchangeably among assigned converters and may work without necessarily depending on the topology of the network. However, further exploration on the capability of the voltage-margin method to perform dispatch mechanisms whilst showing its degree of independency on the network topology is required.

1.2 Thesis project description

In this thesis project, a control strategy based on the voltage-margin method is developed. The capability of the control scheme to dispatch power in the future transnational network situation during normal operation as well as to control the direct voltage during disturbances is explored by simulating a number of case studies. Prior to the exploration, a multi-terminal network model representing a future transnational network is developed. The control strategy is then implemented in the multi-terminal test network. In simulating normal operation, the scenarios are taking into account several dispatch schemes and several possible changes in the network topology. In simulating disturbances, the scenarios are taken into account several severe disturbances i.e. voltage dip on an onshore grid and loss of an onshore converter. At the end, result of the simulations is presented and discussed. The entire model used for this project is developed in MATLAB/ Simulink, using the SimPowerSystems toolbox.

1.3 Thesis project objectives

The objectives of this thesis project are:

a. To develop a control strategy based on the voltage-margin method which is capable of dispatching power in future transnational grids.
b. To explore the capability of this control strategy to perform several dispatch schemes possibly be applied in the future transnational network.
c. To examine the capability of the control strategy to interchangeably control the direct voltage upon loosing the direct voltage controlling converter as well as the other onshore converter.

d. To study the compatibility of the control strategy to work with particular fault ride-through mechanisms (energy dissipation and frequency modulation) during a voltage dip in an onshore grid.

1.4 Thesis contributions

The contribution of this thesis is twofold. The first is the developed control strategy for dispatching power in a future transnational offshore network, with particular focus on the variable nature of wind. The second one is the compatibility of the control strategy with existing low-voltage ride-through mechanism.

1.5 Thesis layout

This thesis consists of seven chapters. Chapter 2 describes the detailed interesting developments which lead to the construction of the future transnational network. In Chapter 3, the model of the multi-terminal network is presented. The developed control strategy and its implementation in order to perform particular dispatch schemes are explained in Chapter 4. In Chapter 5, the implementation of the fault ride-through methods in the multi-terminal network model is described. In Chapter 6, the simulation results are reported and discussed. Finally, the conclusions of this thesis and recommendations for future work are given in Chapter 7.

2 Offshore Wind Power Integration

2.1 Emerging of renewable energy

Our modern society shows increasing dependency on the use of electricity. For many years, electricity has been the source of energy mainly used to support human activities e.g. for lighting, heating, cooling, telecommunication and manufacture. As technological advancement and modern life requirement for comfortableness and efficiency increase, the number of electrical appliances being used to support human activities is growing and thus results in increasing demand for electricity. Moreover, correlation between economic growth and electricity consumption shows that increased prosperity motivates society to make use more electric appliances. As a consequence, it is projected that over the next 20 years, the world dependency on electricity will increase further (Figure 2.1) [1].

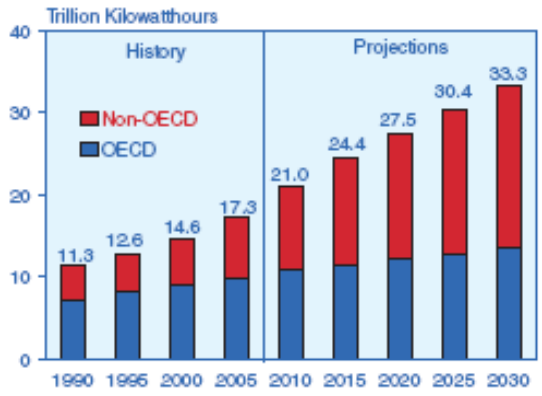

OECD: member of Organization for Economic Cooperation and Development

Figure 2.1 World net electricity generations, 1990-2030 [1]

Over the past decades, the increment in electricity demand has been largely balanced by capacity development of conventional generation plants which make use of fossil fuels, nuclear fission, hydro reservoir and geothermal as their primary energy to produce electricity. However, except for geothermal, further capacity development of these generation plants to balance the future electricity demand as well as to replace ageing ones is considered not sustainable. The resource of fossil fuels and uranium is limited and depleted. Besides, generation plants using fossil fuels release greenhouse gases which have negative impacts to the environment. Moreover, dependency on imported fossil fuels which supply often originated from conflicted and politically unstable part of the world may introduce uncertainty over its price and thus insecure electricity supply for the local society. High risk related to the operation of nuclear reactor and disposal of nuclear waste have made the development of new plant is difficult. Hydro power development is nearly reach it's stagnant since its potential has been largely exploited. Moreover, flooding large areas to create hydro reservoir has a devastating effect on local environment.

In order to meet the future demand of electricity as well as to replace ageing existing generation plants while avoiding the above disfavors, a number of new generation technologies i.e. wind power, solar thermal, solar photovoltaic, biomass, biodiesel, tidal power and wave power, which make use of the renewable energy resources e.g. wind, solar, biomass, biodiesel, tidal and wave energy as their primary energy, have been installed on parts of the world. They introduce several advantages above the conventional ones. Firstly, availability of their primary energy resources is abundant and sustainable

which would be adequate to cover the ever increasing demand of electricity. Secondly, although degree of potency varies from one region to another, their primary energy resources can be accessed or possibly be developed locally. Moreover, they introduce less negative impact to the environment.

2.2 Wind power technology

Wind power technology captures kinetic energy in wind speed for electricity generation by utilizing a number of wind turbines. These wind turbines are installed in a particular area where the potency of wind energy is high and are linked together forming a WPP. The power generated by the wind turbines is aggregated and delivered to the grid. Depending on their location e.g. onshore or offshore, their connection to the grid may directly or through a dedicated transmission. However, variability in wind speed introduces variability in WPP power both over short period e.g. minutes and long period e.g. hours or days. When a number of WPPs are connected to a grid, the variability in their power may complicate dispatch of other types of generation. The variability in WPP power over short period may decrease when the number of utilized wind turbines increases. The variability over long period however, may decrease only when location of the WPPs are dispersed over a wide area.

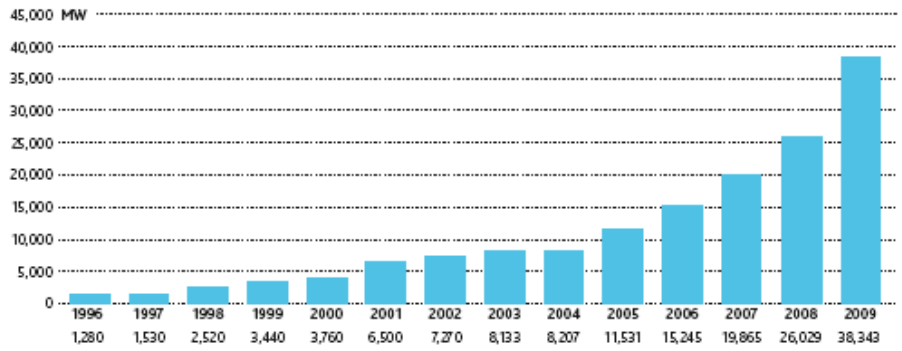

Figure 2.2 Global annual installed capacity of wind power, 1996 - 2009 [2]

Over the past decade, development of wind power in the world is rapidly growing (Figure 2.2). This rapid development is mainly influenced by technological advancement which has made possible to increase its turbine size to produce electricity at cost level approaching present market price. This factor also influences the increased size of WPP from utilizing tents of wind turbines to groups of up to hundreds of wind turbines. Moreover, its possibility to be installed offshore allows for development with capacity comparable to that of the conventional generation with less impact to the local society.

2.3 Wind power development in Europe

As well as other parts of the world, electricity demand in Europe is growing and accordingly the generation capacity must be increased in order to meet the future electricity demand as well as to replace the ageing generation plants. However, increasing the generation capacity by installing additional generation using fossil fuels or nuclear power would introduce several negative impacts and difficulties. On the other hand, potency of wind energy at some parts of Europe is high both onshore and offshore (Figure 2.3) [3]. Therefore, developing wind power technology for electricity generation is a promising solution.

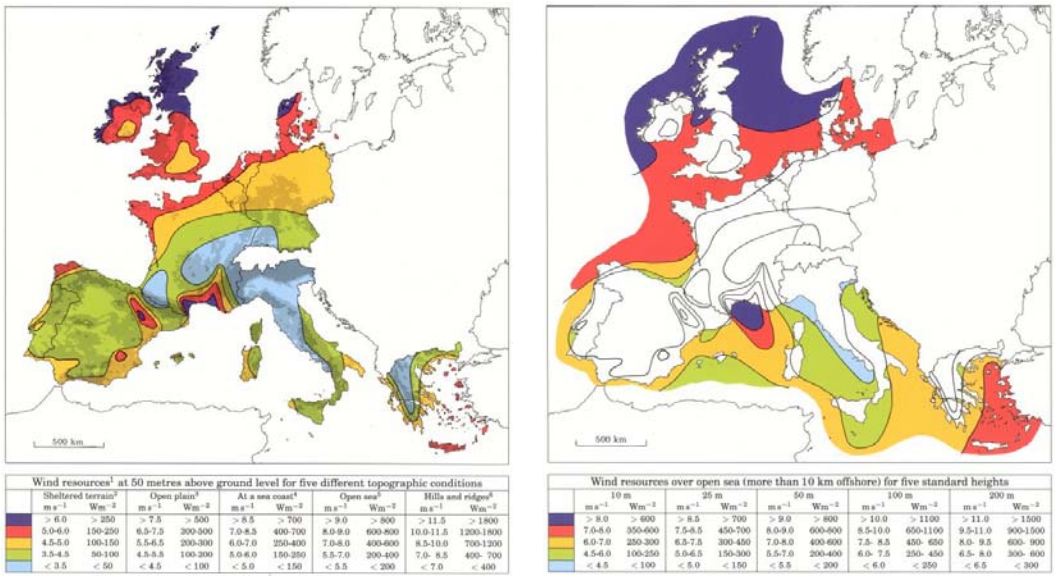

(a) (b)

Figure 2.3 Wind resources over Europe: (a) Onshore (b) Offshore [3]

Development of wind power in European Union (EU) has been rapidly growing during the past decade (Figure 2.4) [4]. Given its rapid growth over the past decade, however, its contribution to the total of electricity generation in EU is currently small, only about 4.2% during 2008 [5]. Nevertheless, wind power development is expected to continue in the future. It can be noticed from the 2008 European Commission target in which wind power contribution to the total of EU's electricity generation will be increased up to 12% by 2020 [6]. Moreover, wind power development to 2020 has been reported technically and economically feasible by several organizations e.g. the European Wind Energy Association (EWEA), the Global Wind Energy Council (GWEC) and the International Energy Agency (IEA).

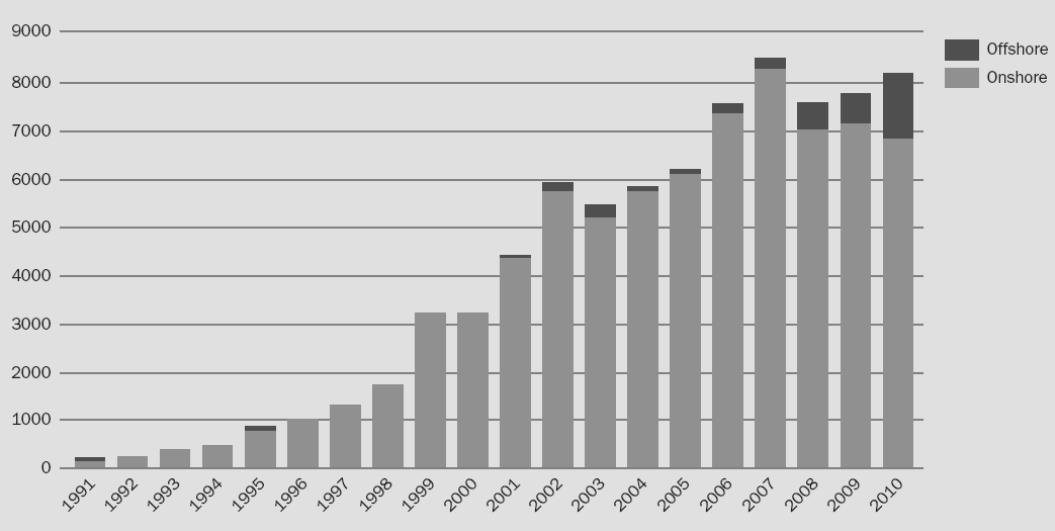

Figure 2.4 Annual wind power capacity in The EU (in MW), 1991 – 2010 [4]

At present, a large portion of the total installed WPP capacity is situated onshore and a small portion is situated offshore. In general, the onshore WPPs are directly connected to the main grid while the offshore WPPs are connected to the main grid through a dedicated offshore transmission. However, their capacity is relatively small compared to that of conventional generation. In order to increase its contribution to the total electricity generation, future development of wind power is foreseen to move toward development of a number of large capacity WPPs. This implies that the future WPP would be

constituted from hundreds of wind turbines and thus would require a large space. Moreover, due to large power involved, integrating a number of large capacity WPPs to the main grid would require a large transmission capacity at particular segments.

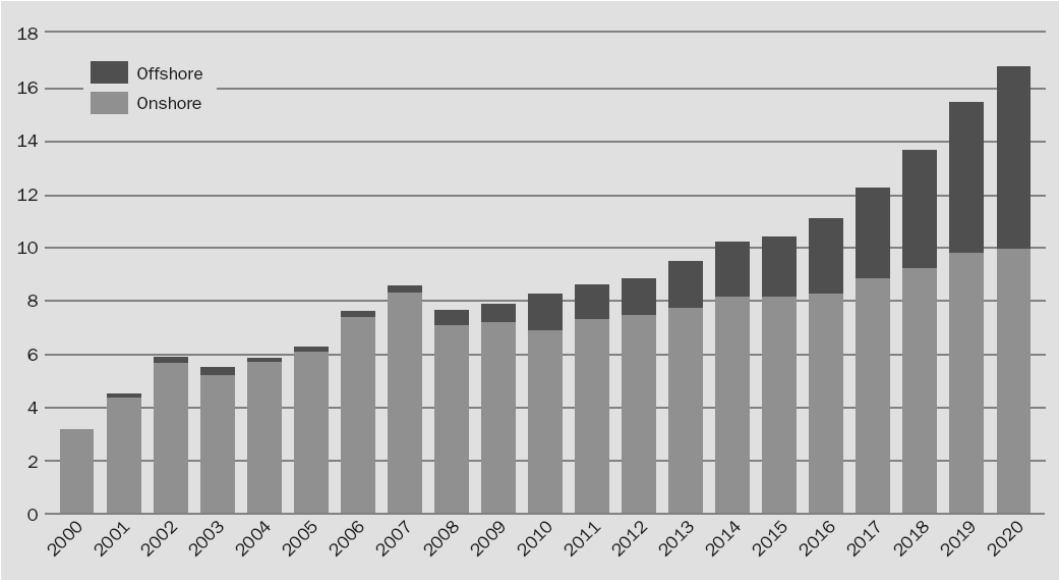

Figure 2.5 Wind power annual installations in The EU (in GW), 2000 – 2020 [4]

Regarding wind power development in the future, it is predicted that while the capacity of onshore WPP would still be the dominant, the capacity of offshore WPP would grow higher annually (Figure 2.5) [4]. It is due to, on one hand, developing a number of large capacity WPPs onshore may be limited to two factors. Firstly, acquiring large space to install large capacity WPP may be difficult due to land use conflicts. Moreover, visual and noise pollution as the results of wind turbines operation would become significant as the number of utilized wind turbines increase and thus may introduce unwanted impact to local society. Secondly, the existing transmission capacity between EU member states is currently at its limit [6]. Therefore transmission capacity at particular segments may need to be upgraded or developed for the grid to be able to share the excess power of the future WPPs from one country to the others. However, although it is technically possible, it may be difficult to acquire additional space for the grid reinforcement due to land use conflicts of right of way. On the other hand, developing future WPPs far offshore would introduce several benefits. Higher potency of wind energy and more space available far offshore have present option to develop larger capacity WPPs. Moreover, the visual and noise impact from utilizing hundreds of wind turbines would be negligible to the society on land. Furthermore, possibility to share the power from the far offshore WPP directly to the other countries, introduce alternative to the reinforcement of the onshore grid.

2.4 Connection aspects of offshore wind power

Higher potency of wind energy and more space available offshore have present option to develop large capacity WPP. Currently, a few offshore WPPs have been put into operation. In general, they are situated relatively close to the shore (< 60 km) and each of them is integrated to the onshore grid through a dedicated transmission. In the future, however, as the potency of wind energy is higher and the availability of space is larger far offshore, a number of WPPs with capacity comparable to that of conventional generation is foreseen to be installed far from the shore (> 60 km).

Nevertheless, implementing a dedicated transmission to connect the far offshore WPPs to the onshore grid would not always be a pleasant decision. There are two important issues

to be considered. First, installing WPP far offshore would involve longer cable transmission for connection to the onshore grid. Moreover, as far offshore wind power tends to be built with larger capacity, larger power would be transmitted to onshore grid and thus larger transmission capacity would be required. Second, when a WPP is connected to the onshore grid by a dedicated transmission, power delivered through the transmission would vary as the result of variability in the output power of the WPP due to variability of the wind speed. In such a circumstance, only a small percentage of the transmission capacity may be used over particular time. Moreover, as a large transmission capacity is involved, the variability in transmission capacity utilization may result in a low utilization factor and thus relatively high transmission costs.

The utilization factor of the transmission capacity may be increased in two ways. First, the utilization factor may be increased if several offshore WPPs are connected together. In such a way, the variability in the total output power of the WPPs would decrease and results in a decreased variability in the transmission capacity utilization. It is because, over particular time, the variability of the wind speed at geographically dispersed WPPs is different and thus variability in the output power of the WPP balances each other. Second, the utilization factor may be increased if, in addition to evacuate power from offshore WPP, transmission serves as an interconnector to facilitate power trade between countries. This can be realized by allocating an extra transmission capacity for power trading in addition to that used for the WPP power or by utilizing the spare transmission capacity for power trading during periods when the WPP power is low (e.g. when the wind speed is low) or by combining the previous two alternatives in which the capacity for power trading may be increased whenever the WPP output is low.

When those two alternatives are combined together, the connections may form a transnational offshore network linking several offshore WPPs to several onshore grids or countries. Not only a high utilization factor of the transmission capacity would be achieved in this way, but also the variability in power delivered to onshore grid would be decreased significantly, which is advantageous. Moreover, the possibility to interconnect the offshore WPPs with countries having large capacity of controllable hydro power would be an advantage to further compensate for the variability in power delivered by renewables in general. Besides, installing an offshore network which is designed for both for wind power integration and for trade interconnectors would be economically more beneficial than installing separate point-to-point connections.

2.5 Development of the future transnational offshore network

A number of bodies i.e. TradeWind, Airtricity, Greenpeace, Statnett, Imera and Mainstream Renewable Power have put forward different proposals regarding the development of a transnational offshore network [7]. Greenpeace, in their proposal, predicted that development of a future transnational network on the North Sea would grow in several stages [8]. First, the earlier stage would be initialized by the development of several far offshore WPPs where each of them may be connected to onshore grid of different countries (Figure 2.6). Next, several nearby WPPs may also be developed and connected to a common offshore node and thus make use a common offshore transmission to deliver power to the onshore grid.

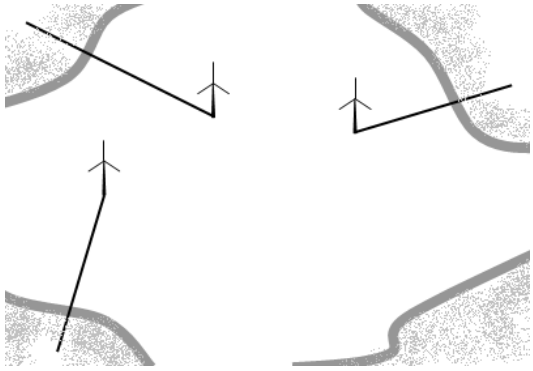

Figure 2.6 Earlier stage of the future transnational network development

Second, as the need for power trading between countries increases, the intermediate stage would be started by connecting a particular WPP to another country or by connecting two WPPs of different countries and utilizing part of the offshore connections capacity for power trading (Figure 2.7).

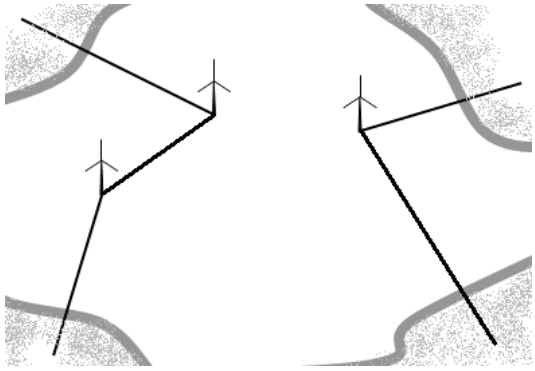

Figure 2.7 Second stage of the future transnational network development

Third, as the development of the far offshore WPPs and the need for power trading between countries further increase, connections linking several far offshore WPPs and several countries surrounding the sea would be developed (Figure 2.8).

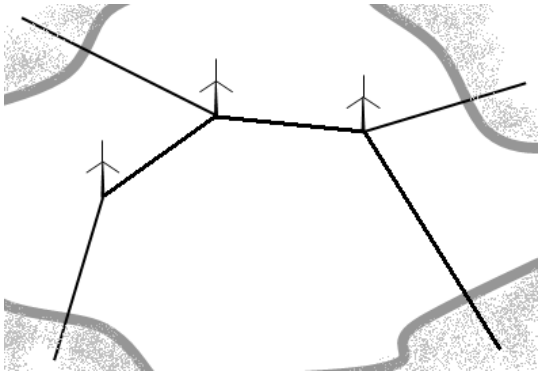

Figure 2.8 Third stage of the future transnational network development

2.6 Technological solution for the future transnational network

Future development of the offshore wind power would move toward the development of large capacity offshore WPPs. Location where the potency of wind energy and the availability of space sufficient for installing large capacity offshore WPP is far from the shore (>60 km). For such distance, integration of the offshore WPP to the onshore grid would employ a long cable transmission. Moreover, considering that in the future

transnational network not only far offshore WPPs are connected but also different countries, the length of the required transmission may be doubled or even longer. It means that the required transmission may involve distance of hundreds of km. Furthermore, considering that a future transnational network may serve not only to evacuate power from large capacity WPPs but also to facilitate power trade between countries, a large transmission capacity would be required.

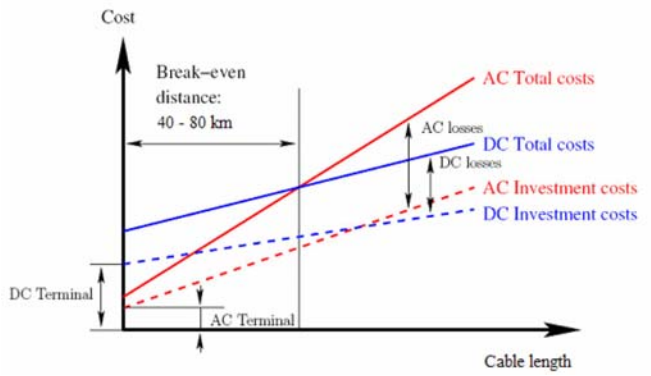

Figure 2.9 Comparison of cost for HVAC and HVDC cable transmission [9]

Regarding the transmission requirements, there are two options of cable transmission technology may be applied i.e. high-voltage alternating-current (HVAC) and high-voltage direct current (HVDC). Utilization of HVAC technology is more favorable than HVDC for short transmission distances. It is because, for such distance, HVDC technology introduces higher investment cost mainly due to its requirement to employ components for ac to dc conversion and vise versa. Contrarily, for long transmission, HVDC technology is preferable. It is due to, as the length increase, the amount of reactive power compensation required by HVAC transmission grows, and thus, for transmission longer than a particular distance, the total cost introduced by HVAC i.e. investment cost and cost due to reactive power compensation, would be higher than that by HVDC. The break even length between HVAC and HVDC transmission technology is relative and may vary depending on the capacity requirement of the transmission. Nevertheless, in general, the value lies between 40 km to 80 km [9]. Therefore, in the case of a future transnational network, implementation of HVDC transmission is preferable.

To specify which kind of HVDC technology is suitable for offshore networks, more technical characteristics must be taken into account. There are two kind of HVDC transmission technology i.e. line commutated converter based HVDC (LCC-HVDC) and voltage sourced converter based HVDC (VSC-HVDC). Both LCC-HVDC and VSC-HVDC employ switching commutation to different groups of semi-conductor switches in its converter in order to perform conversion from ac to dc (rectifying) or dc to ac (inverting). However, there is a main difference in how their switches commutated by which they further introduce disadvantages and advantages one over the other.

Switching commutation of LCC-HVDC is dictated by both the ac voltage of connected ac grid and the triggering pulse applied to its switches. The angle at which the triggering pulse applied to defines the power factor and the voltage at dc side of its converter and hence further defines the amount as well as the direction of power delivered between the rectifying and the inverting converters. The amount of power delivered is adjusted by adjusting the triggering angle and thus adjusting the voltage at dc side of its converter. As well, to change the direction of power, the triggering angle is further adjusted such that the voltage at dc side of its converter is changed in polarity. Therefore, between the converters, a communication link is required to control the triggering angle so that the power may be delivered correctly. These characteristics of LCC-HVDC introduce several disadvantages. LCC-HVDC can only perform conversion when ac voltage is available on

the ac side of its converter. In other words, it can not perform self restoration upon disconnection from the connected ac grid nor provide black start to the connected ac grid. Moreover, due to the triggering angle, it operates at lagging power factor and thus absorbs reactive power from the ac grid. Therefore reactive power compensator (e.g. shunt capacitors) is required on the ac side of its converter. Furthermore, its dependency on communication between converters has made it prone to failures due to the communication link.

On the other hand, switching commutation of VSC-HVDC is self-controlled by pulse-width modulation (PWM), which can be operated independently of ac voltage of the connected grid and of other converters. The use of PWM has made its converter to constitute a controlled ac voltage source where the amplitude, the phase angle and the frequency of its ac voltage can be controlled independently. Therefore, at the ac side of its converter, the reactive power can be controlled independently of the active power. Moreover, a dedicated reactive power compensator is not necessarily required. Furthermore, it can perform a self restoration upon a disconnection from the connected ac grid as well as provide a black start to the connected ac grid. In addition, it has the capability to operate without necessarily depending on communication between the rectifying and the inverting converters. When the rectifying converter injects an amount of power into dc link, the direct voltage will rise. The inverting converter, then, will notice the increase in the direct voltage and thus delivers the same amount of power to the connected ac grid.

As foreseen, a future transnational network will probably grow in stages from connecting one far offshore WPP to one onshore grid toward linking several far offshore WPPs to multiple onshore grids. The offshore network would then act as a power pool where power may be injected to and extracted from the network at different nodes. In such circumstances, flexibility to control the active and the reactive power in the network is required. Thus, implementing LCC-HVDC would be difficult due to its requirement to change the polarity of the direct voltage in order to change the direction of power. Therefore, implementation of VSC-HVDC is favorable. Moreover, the capability of VSC-HVDC to self restored, to provide black start and to operate without necessarily depend on communication between converters would be considered as advantages. In addition, implementation of VSC-HVDC in the network may result in a compact offshore converter station as the dedicated reactive power compensator is not necessarily required.

3 Multi-Terminal Network Model

3.1 Introduction

In this thesis, a control strategy based on the voltage-margin method is developed for controlling power in a future transnational network. In order to explore its capability, the control strategy is implemented in a multi-terminal VSC-HVDC network which represents the future transnational network situation. The topology of the multi-terminal network is depicted in Figure 3.1.

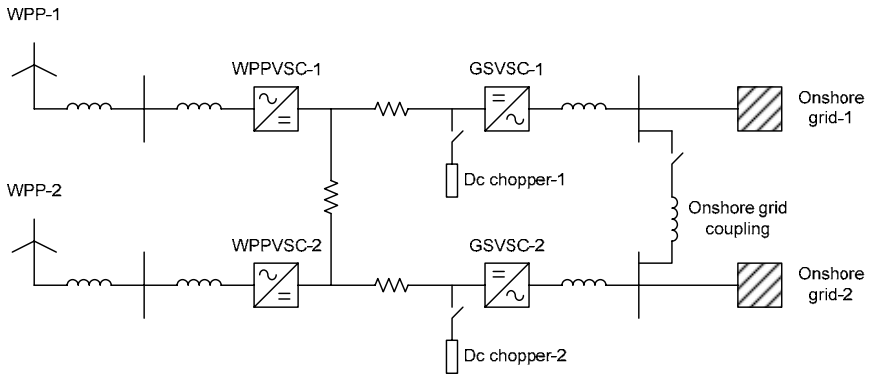

Figure 3.1 Multi-terminal network

The multi-terminal network consists of two offshore WPPs and two onshore ac grids connected through a multi-terminal VSC-HVDC offshore network. The offshore network consists of two WPP side VSCs (WPPVSC) and two grid side VSCs (GSVSC). The multi-terminal network is basically composed from two similar point to point VSC-HVDC connected one another at the dc and the ac side.

In this chapter, the model of the multi-terminal network will be presented in detail. The model of the VSC-HVDC will be described first whereas later the model of the WPP will be explained.

3.2 VSC-HVDC model

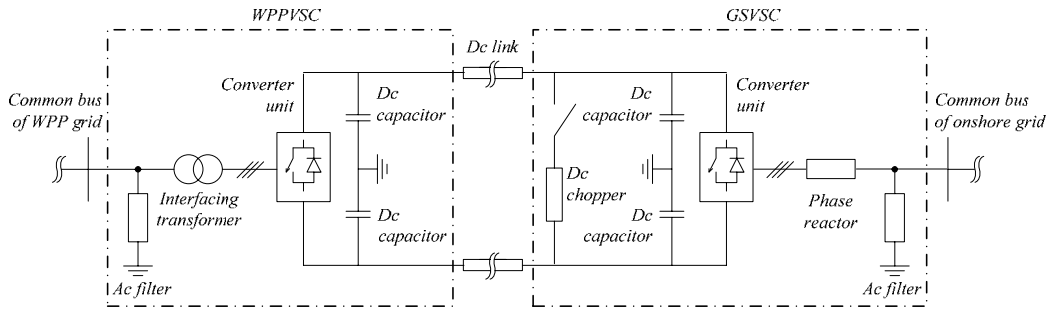

Figure 3.2 Topology of point to point VSC-HVDC

This section presents point to point VSC-HVDC model which constitutes the basic model for the multi-terminal network implemented in this thesis. Topology of the point to point

VSC-HVDC is shown in Figure 3.2. It connects the local ac grid of an offshore WPP to an onshore ac grid. It consists of a WPP side converter station (WPPVSC), a dc link and an onshore grid side converter station (GSVSC). The size of the two converter stations is the same i.e. 440 MVA, 150 kV. The size of the dc link is 440 MW, ± 150 kV. The WPPVSC is connected to the WPP grid at a common bus of 33 kV. The GSVSC is connected to the onshore grid at a common bus of 150 kV.

The model of the point–to-point VSC-HVDC described in this section is derived form the topology given in Figure 3.2. It consists of models of the two converter stations, model of the dc link and model of the control scheme. In the following sections, first, model of the WPPVSC, model of the dc link and model of the GSVSC are presented. Later, model of the control scheme for each of the converter stations is described.

3.2.1 WPPVSC model

WPPVSC model is depicted in Figure 3.3. The assumptions taken in determining the model are described subsequently in the following paragraphs for each of the main components.

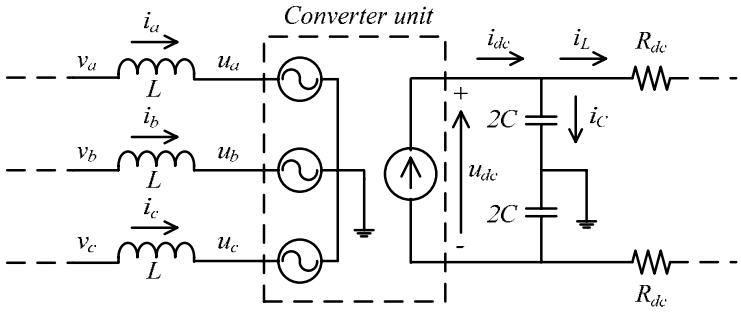

Figure 3.3 WPPVSC model

3.2.1.1 Interfacing transformer

The model of the interfacing transformer is represented by its leakage inductance. It is based on the following assumptions. First, in general, power transformer is build with very high magnetizing inductance and very low winding resistance to allow maximum flux be confined in the core and to allow high power to be transferred through the transformer. As the result, the power losses due to the winding resistance and due to the magnetizing inductance are very small compared to the rated power of the transformer. Thus, considering the objectives of this thesis, the series winding resistance and the magnetizing inductance are neglected and only the leakage inductance is included in the model. Second, the interfacing transformer may have a tap changer installed. In general, the objective of this tap changer is to support the reactive power control provided by the converter unit during a long term voltage dynamics. Therefore, within the time frame of interest of this thesis, the tap changer is not expected to react. Thus, it is considered not necessary to include the tap changer in the model.

The leakage inductance of the interfacing transformer is generally in the range of 0.1 pu to 0.2 pu [10]. In this thesis, the value of 0.15 pu of the rated capacity and voltage of the WPPVSC is applied.

3.2.1.2 Ac filter

In general, the ac filter is tuned to a characteristic frequency higher than the fundamental frequency in order to eliminate the high order harmonics. In such a way, the ac filter provides almost no attenuation to the fundamental frequency. Considering the objectives of this thesis, the effect of the ac filter to the fundamental frequency waveform is neglected and the ac filter is excluded from the model.

3.2.1.3 Converter unit

The ac side of the converter unit is modeled as a fundamental frequency controllable ac voltage source. Determination of the model is based on the following assumptions. First, the ac side of the converter unit generates ac voltage which can be controlled in amplitude, phase angle and frequency by modifying the control signals in the pulse width modulator. Thus, the ac side of the converter can be represented by a controllable ac voltage source. Second, the time taken to adjust the ac voltage by modifying the control signals in the pulse width modulator is almost instantaneously compared to the time frame of interest of this thesis (0.1s to 20s). Thus, the dynamics of the pulse width modulator and the corresponding switching mechanism can be excluded from the model. Third, by assuming that the converter unit employs sinusoidal pulse width modulation with high switching frequency and operates in the linear region, a voltage waveform close to sinusoidal is produced over the transformer in which only high order harmonics appear. By further assuming that the ac filter is tuned to the required characteristic frequency, the effect of the high order harmonics to the voltage waveform is negligible. Therefore, the effect of the higher order harmonics to the voltage waveform is neglected and only a fundamental frequency waveform of the ac voltage appears at the transformer terminal.

The dc side of the converter unit is modeled as a controllable direct current source in parallel with the dc capacitors where the direct current generated by the source is equal to the direct current delivered through the dc side of the converter. Determination of the model is based on the following assumption. Power losses in the converter due to switching losses and due to voltage drop across the switches and the anti parallel diodes are small compared to the rated power transferred through the converter. Thus, considering the objectives of this thesis, the power losses in the converter are not taken into consideration. As the result, the active power exchanged at the common bus is equal to the power exchanged at the dc side of the converter i.e.

$$P = P_{dc} = u_{dc} i_{dc} \tag{3.1}$$

and therefore,

$$i_{dc} = \frac{P}{u_{dc}} \tag{3.2}$$

where P is the active power exchanged at the common bus [W], P_{dc} is the power exchanged at the dc side of the converter [W], u_{dc} is the direct voltage across the dc capacitors [V] and i_{dc} is the direct current delivered through the dc side of the converter [A].

3.2.1.4 Dc capacitors

Switching actions in the converter unit introduces ripple in the direct voltage. In order to obtain a small ripple in the dc voltage, large dc capacitors are required. However,

application of large dc capacitors results in slow changes of the dc voltage in respond to changes in power exchanged at the dc side of the converter. On the other hand, application of small dc capacitors results in fast response to changes in instantaneous power exchanged but at the expense of larger ripple in the dc voltage. Thus, the total capacitance of the dc capacitors can be approximated by [10]

$$C = \frac{2\,\tau\,S_b}{u_{dc,b}^2} \tag{3.3}$$

where C the total capacitance of the dc capacitors [μF], τ is the time constant of the dc capacitors [ms], S_b is the rated capacity of the converter unit [VA] and $u_{dc,b}$ is the nominal direct voltage [V]. τ may be selected between 5 ms to 10 ms to obtain small ripple and fast response of the dc voltage upon changes in the power exchanged at the dc side of the converter. In this thesis, the capacitance of the dc capacitors is 58.7 μF which obtained using (3.3) based on the dc capacitors time constant of 6 ms.

3.2.2 Dc link model

The dc link is modeled as series resistance and shunt capacitance where the shunt capacitance is lumped to the capacitance of the dc capacitors. Thus, only the series resistance will appear in the dc link model. In this thesis, the resistance of 0.0073 Ω/km per pole is chosen for the series resistance of the dc link [11]. The length of the dc link circuit is 200 km.

The direct current flowing through the dc link is defined by the following equation i.e.

$$i_L = i_{dc} - i_C \tag{3.4}$$

where i_L is the direct current flowing through the dc link [A], i_{dc} is the direct current exchanged through the dc side of the converter [A] and i_C is the direct current flowing through the dc capacitors [A].

In steady state, there is no current flowing through the dc capacitors and thus the direct current flowing through the dc link is equal to the direct current exchanged at the dc side of the converter. However, when the direct current exchanged at the dc side of the converter is changed due to changes in the active power exchanged at the common bus, current will flow to the dc capacitors and thus the direct voltage over the capacitors is changed i.e.

$$u_{dc} = \frac{1}{C}\int i_C\,dt + u_{dc,0} \tag{3.5}$$

where u_{dc} is the direct voltage over the capacitors [V], C is the total capacitance of the dc capacitors [μF], i_C is the direct current flowing through the dc capacitors [A] and $u_{dc,0}$ is the initial direct voltage over the dc capacitors [V].

3.2.3 GSVSC model

The GSVSC employs the same set of main components as the WPPVSC except that in the GSVSC, a dc chopper is placed on the dc side and a phase reactor is used instead of an interfacing transformer. Thus, only the phase reactor model and the dc chopper model are described in this section.

A phase reactor is used based on the design of the VSC-HVDC described in section 3.2 in which the nominal voltage of the onshore grid is equal to the nominal voltage of the GSVSC. Therefore, installing an interfacing transformer is considered not necessary.

3.2.3.1 Phase reactor

The phase reactor is modeled as a series inductance. The inductance of the phase reactor is usually about 0.15 pu [10]. In this thesis, a value of 0.15 pu of the GSVSC rated capacity is applied. GSVSC model is therefore similar to the WPPVSC model shown in Figure 3.3.

3.2.3.2 Dc chopper

The dc chopper acts to prevent the direct voltage rise to an endangering value during power imbalance in the dc link by dissipating the excess power. The dc chopper model and its implementation on the multi-terminal network model will be described in Chapter 5.

3.2.4 Control scheme model

3.2.4.1 GSVSC control scheme

In order to be able to control the active and reactive power independently, the control scheme implemented on the GSVSC is developed based on the *vector control* method. In the control scheme, the actual *abc* quantities measured at the common bus i.e. voltage and current are first transformed to the *dq0* components by applying the Clark and the Park transformations. In this transformation, the magnitude of the quantities in *dq* is made equal to the peak phase value of the corresponding *abc* quantities and, using the phase locked loop (PLL), the *d*-axis component of the common bus voltage (v_d) is aligned in phase with the phase *a* of the common bus voltage (v_a). The quantities in the *dq0* components are then manipulated in such a way so that the active and reactive power control can be decoupled.

The active and reactive power calculated from the *abc* quantities measured at the common bus are

$$P = v_a i_a + v_b i_b + v_c i_c \tag{3.6}$$

$$Q = \frac{1}{\sqrt{3}}(v_{ab} i_c + v_{bc} i_a + v_{ca} i_b) \tag{3.7}$$

where P is the active power exchanged at the common bus [W], Q is the reactive power exchanged at the common bus [var], v_a is the phase *a* of the common bus voltage [V], v_b is the phase *b* of the common bus voltage [V], v_c is the phase *c* of the common bus voltage [V], i_a is the phase *a* of the current flowing at the ac side of the converter [A], i_b is the phase *b* of the current flowing at the ac side of the converter [A] and i_c is the phase *c* of the current flowing at the ac side of the converter [A].

Transforming (3.6) and (3.7) to the *dq0* components and writing the results in pu of the converter rated capacity leads to

$$P = v_d i_d + v_q i_q + 2 v_0 i_0 \tag{3.8}$$

$$Q = v_q i_d - v_d i_q \tag{3.9}$$

By knowing that for a balanced three phase system the *0* components are equal to zero, and moreover, by considering that v_d is aligned in phase with v_a so that v_q is zero, (3.8) and (3.9) can be rewritten as

$$P = v_d i_d \tag{3.10}$$

$$Q = -v_d i_q \tag{3.11}$$

where v_d is the *d*-axis component of the common bus voltage [pu], v_q is the *q*-axis component of the common bus voltage [pu], v_0 is the *0*-axis component of the common bus voltage [pu], i_d is the *d*-axis component of the current flowing at the ac side of the converter [pu], i_q is the *q*-axis component of the current flowing at the ac side of the converter [pu] and i_0 is the *0*-axis component of the current flowing at the ac side of the converter [pu]. Thus, from (3.10) and (3.11), it can be seen that the active power and the reactive power are now decoupled. In other words, the active power can be controlled independent of the reactive power by regulating i_d. Likewise, the reactive power can be controlled independent of the active power by regulating i_q.

GSVSC control scheme is depicted in Figure 3.4. In the control scheme, two groups of cascaded controllers i.e. the outer controllers and the inner controller, are employed. Each of the outer controllers compares the corresponding measured quantity to the ordered value and produces current reference value i.e. i_d* or i_q* for the inner controller. The inner controller tracks the current reference values and generates voltage reference values i.e. u_d* and u_q*. The voltage reference values are then transformed to the *abc* quantities and fed as inputs to the controlled voltage source. Detailed description of the inner and the outer controllers is given in the following sections.

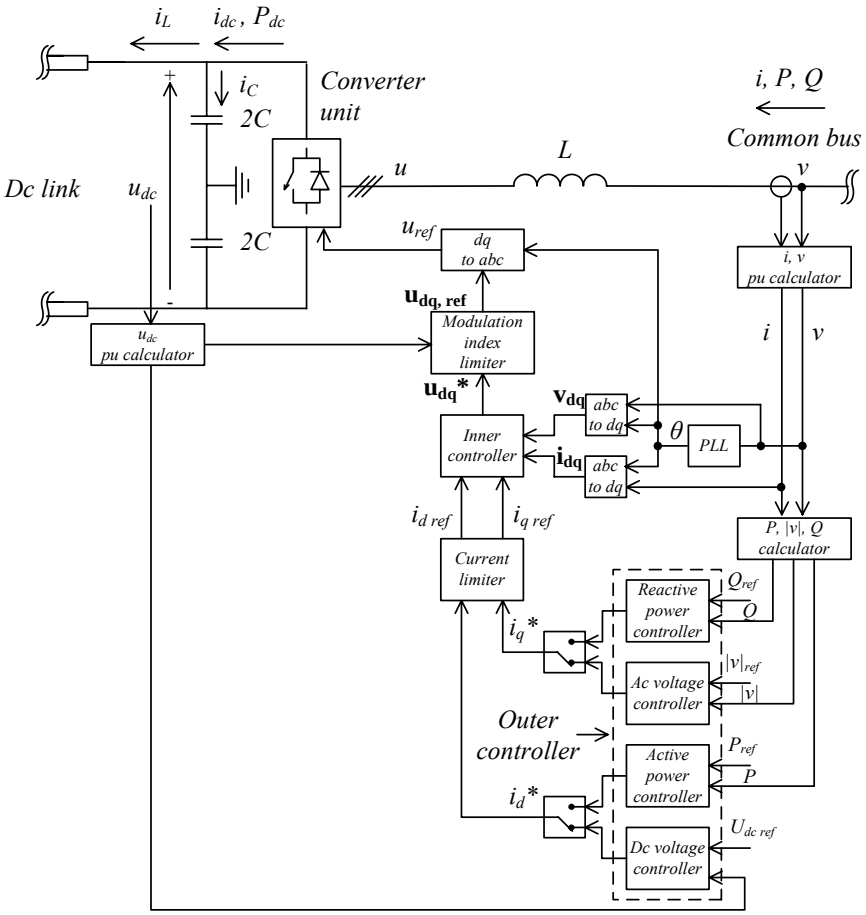

Figure 3.4 GSVSC control scheme

3.2.4.1.1 Inner controller

The objectives of the inner controller are to track the current reference values given by the outer controllers and to generate voltage reference values i.e. u_d* and u_q* fed to the controlled voltage source.

From Figure 3.4, the quantities at the ac side of the converter are related by

$$v = L\frac{di}{dt} + u \tag{3.12}$$

Rewriting (3.12) in the Laplace domain leads to

$$v = sLi + u \tag{3.13}$$

Transforming (3.13) to the dq components results in

$$v_d = sLi_d - \omega Li_q + u_d \tag{3.14}$$

$$v_q = sLi_q + \omega Li_d + u_q \tag{3.15}$$

where v is the voltage at the common bus [V], L is the leakage inductance of the phase reactor [H], i is the current flowing at the ac side of the converter [A], u is the voltage generated by the converter [V], s is the Laplace operator, v_d is the d-axis component of the common bus voltage [pu], v_q is the q-axis component of the common bus voltage [pu], i_d is the d-axis component of the current flowing at the ac side of the converter [pu], i_q is the q-axis component of the current flowing at the ac side of the converter [pu], u_d is the d-axis component of the voltage generated by the converter [pu] and u_q is the q-axis component of the voltage generated by the converter [pu].

The speed voltage terms i.e. ωLi_q and ωLi_d introduce cross coupling between d-axis quantities in (3.14) and q-axis quantities in (3.15). This cross coupling makes controlling the reactive power independently to the active power difficult. In other words, when i_q is regulated to control the reactive power, v_d will be altered, and thus, according to (3.10), the active power will also change. In order to eliminate the cross coupling, v_d and ωLi_q are fed forward on the d-axis controller while v_q and ωLi_d are fed forward on the q-axis controller. The results are shown in Figure 3.5.

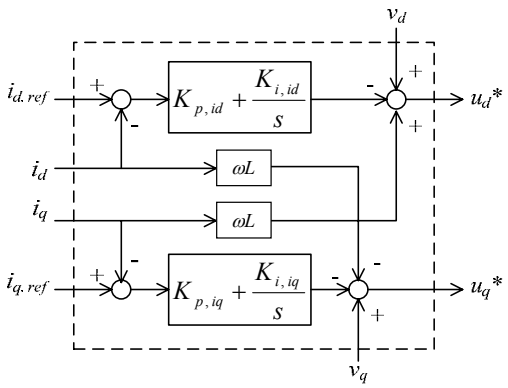

Figure 3.5 Inner controller

3.2.4.1.2 Direct voltage controller

The objective of the direct voltage controller is to maintain the direct voltage at the given reference value by regulating the active power exchanged at the common bus. That is, by modifying the value of i_d*.

Referring to (3.2) and (3.10), the active power exchanged at the common bus is defined as

$$u_{dc} i_{dc} = v_d i_d \tag{3.16}$$

Rewriting (3.16) and solving for i_d results in

$$i_d = \frac{u_{dc}}{v_d} i_{dc} \tag{3.17}$$

Substituting (3.4) into (3.17) and knowing that at steady state operation $i_C = 0$, gives

$$i_d = \frac{u_{dc}}{v_d} i_L \tag{3.18}$$

where u_{dc} is the direct voltage over the dc capacitors [pu], i_{dc} is the direct current exchanged at the dc side of the converter [pu], v_d is the d-axis component of the common bus voltage [pu], i_d is the d-axis component of the current flowing at the ac side of the converter [pu], i_C is the current flowing to the dc capacitors [pu] and i_L is the current flowing through the dc link [pu].

Therefore, (3.18) forms the initial value $i_{d,0}$* for the direct voltage controller. Scheme of the direct voltage controller is depicted in Figure 3.6.

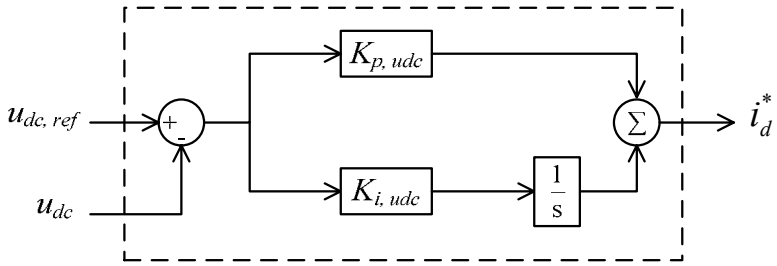

Figure 3.6 Direct voltage controller

3.2.4.1.3 Active power controller

The objective of the active power controller is to regulate the active power exchanged at the common bus to match the given reference value by modifying i_d*.

Rewriting (3.10) and solve for i_d results in

$$i_d = \frac{P}{v_d} \tag{3.19}$$

where i_d is the d-axis component of the current flowing at the ac side of the converter [pu], P is the active power exchanged at the common bus [pu] and v_d is the d-axis component of the common bus voltage [pu].

Thus, (3.19) constitutes the initial value $i_{d,0}$* for the active power controller. Scheme of the active power controller is shown in Figure 3.7.

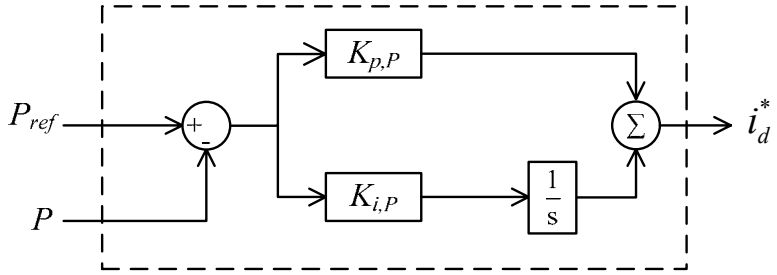

Figure 3.7 Active power controller

3.2.4.1.4 Reactive power controller

The objective of reactive power controller is to govern the reactive power exchanged at the common bus to match the given reference value by modifying i_q*.

Rewriting (3.11) and solve for i_q results in

$$i_q = -\frac{Q}{v_d} \tag{3.20}$$

where i_q is the q-axis component of the current flowing at the ac side of the converter [pu], Q is the reactive power exchanged at the common bus [pu] and v_d is the d-axis component of the common bus voltage [pu].

Hence, (3.20) constitutes the initial value $i_{q,0}$* for the reactive power controller. Scheme of the reactive power controller is pictured in Figure 3.8.

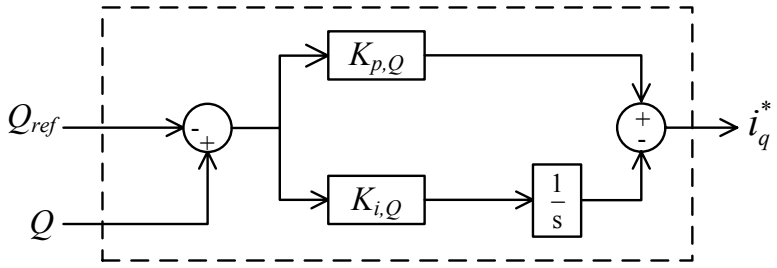

Figure 3.8 Reactive power controller

3.2.4.1.5 Ac voltage controller

The objective of the ac voltage controller is to regulate the amplitude of the ac voltage at the common bus to be equal to the given reference value by modifying i_q*. This implies that the controller governs the converter to generate an amount of reactive power so that

the voltage at the common bus matches the given reference value. Figure 3.9 pictures the scheme of the ac voltage controller.

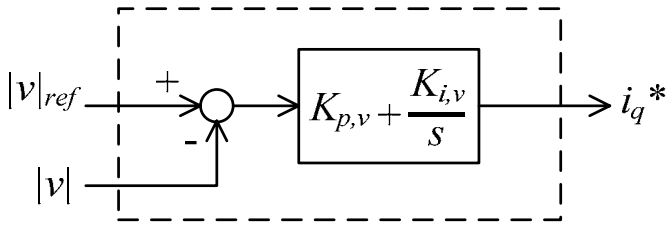

Figure 3.9 Ac voltage controller

3.2.4.1.6 Current limiter

In practice, current delivered or absorbed by the converter is flowing through the semiconductor switches and the anti parallel diodes in the switching bridges. These devices have maximum current carrying capability and thus may be broke down by an excessive current flowing through the converter. In this thesis, to avoid an excessive current, a current limiter is implemented in the control scheme.

Current limiter compares the magnitude of the current reference value generated by the outer controllers with the maximum permitted value. If the magnitude of the current reference value exceeds the maximum permitted value, then the magnitude of the current reference value is limited to the maximum permitted value. The magnitude of the current reference value generated by the outer controllers is

$$|i| = \sqrt{i_d^{*2} + i_q^{*2}} \tag{3.21}$$

where $|i|$ is the magnitude of the current reference value [pu], i_d* is the d-axis current reference value [pu] and i_q* is the q-axis current reference value [pu].

There are three options of limiting strategy may be applied in the current limiter when $|i|$ exceeds the maximum permitted value. First is to give priority to i_d* (Figure 3.10a) [12]. Second is to give precedence to i_q* (Figure 3.10b). Third is to equal scaling the i_d* and the i_q* (Figure 3.10c) [12]. In this thesis, all of the three limiting strategies are implemented in the control scheme. However, only the limiting strategy which gives priority to i_d* is used during the simulations reported in this thesis.

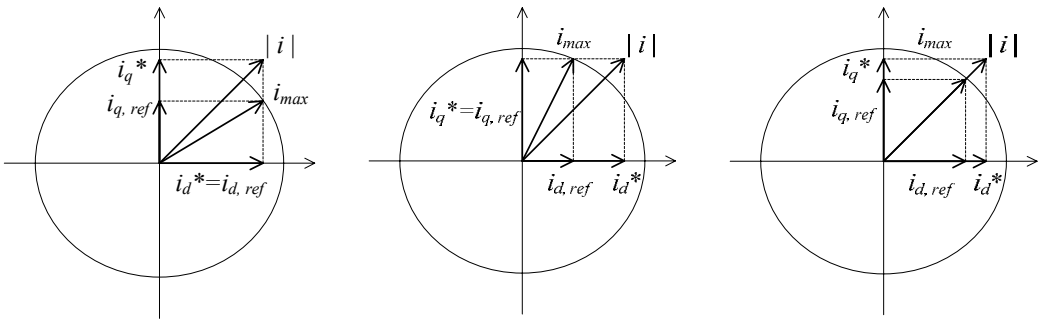

Figure 3.10 Current limiting strategies

3.2.4.1.7 Modulation index limiter

The magnitude of the converter voltage is linearly related to the direct voltage over the dc capacitors by

$$|\hat{u}_{ph}| = m_a \frac{u_{dc}}{2} \qquad \text{for } 0 \le m_a \le 1 \qquad (3.22)$$

where $|\hat{u}_{ph}|$ is the peak phase value of the converter voltage [V], m_a is the modulation index and u_{dc} is the direct voltage over the dc capacitors [V].

In order to maintain the converter operation in the linear region ($0 \le m_a \le 1$), a modulation index limiter is implemented in the control scheme. The scheme of the modulation index limiter is depicted in Figure 3.11.

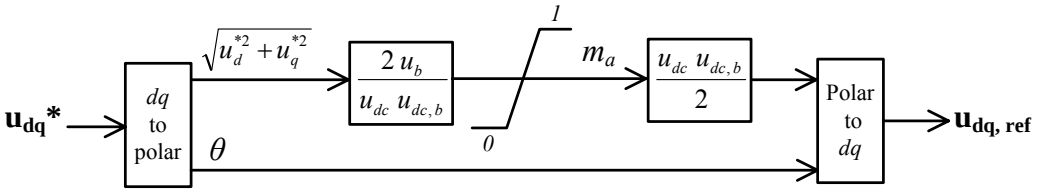

Figure 3.11 Modulation index limiter

The modulation index limiter model is based on

$$m_a = \frac{2\,u_b\,\sqrt{u_d^{*2} + u_q^{*2}}}{u_{dc}\,u_{dc,b}} \qquad \text{for } 0 \le m_a \le 1 \qquad (3.23)$$

where m_a is the modulation index, u_b is the base value of the converter voltage [V], u_d* is the *d*-axis converter voltage reference value [pu], u_q* is the *q*-axis converter voltage reference value [pu], u_{dc} is the direct voltage over the dc capacitors [V] and $u_{dc,\,b}$ is the base value of the direct voltage [V].

3.2.4.2 WPPVSC control scheme

In this thesis, the WPPVSC has three objectives. The first is to absorb power delivered by the WPP, whereas the second is to provide and to maintain voltage at the common bus at constant amplitude and angle. The third is to modulate frequency in the WPP local grid when the direct voltage rises to an endangering value. The control scheme of the WPPVSC is therefore developed based on those objectives.

Since the WPPVSC is not performing either the active power control or the direct voltage control, the corresponding controllers are thus not considered in the control scheme. Moreover, since the voltage at the common bus is provided by the WPPVSC, it is not necessary to include the PLL in the control scheme. The control scheme of the WPPVSC therefore consists of only an ac voltage controller, a frequency modulator and a modulation index limiter. The modulation index limiter implemented in the WPPVSC is similar to that implemented in the GSVSC. The ac voltage controller is however different and thus will be described in the following section. The control scheme of the WPPVSC is depicted in Figure 3.12.

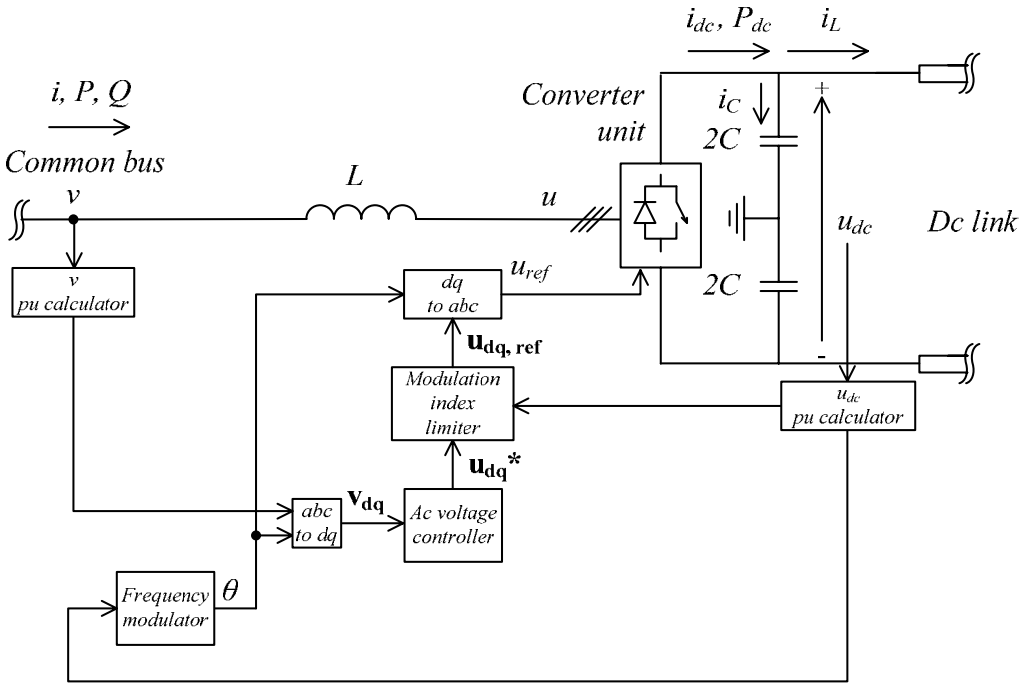

Figure 3.12 WPPVSC control scheme

3.2.4.2.1 Ac voltage controller

One of WPPVSC objectives is to absorb power delivered by the WPP. It can be achieved by operating the converter unit as a stiff voltage source. However, due to the transformer inductance, the voltage at the common bus is altered each time the power delivered by the WPP changes. Therefore, an ac voltage controller is applied to provide and to maintain voltage at the common bus at constant amplitude and angle. The scheme of the ac voltage controller is given in Figure 3.13.

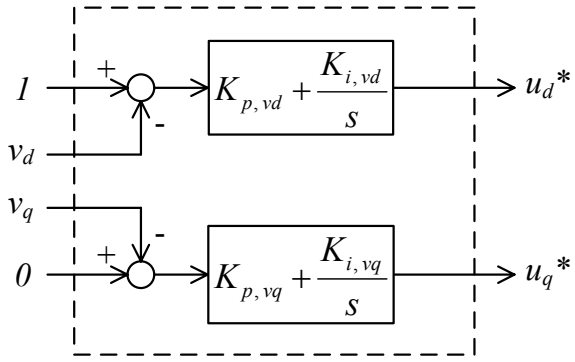

Figure 3.13 Ac voltage controller

3.2.4.2.2 Frequency modulator

The objective of the frequency modulator is to maintain a constant frequency in the local WPP grid during normal operation and to increase the frequency when the direct voltage rises above a given reference value. The frequency is increased in order to signal the

WPP to reduce its power to avoid a direct voltage rise to an endangering value. The frequency modulator model will be described in Chapter 5.

3.3 Offshore WPP model

As discussed in Chapter 2, a number of large scale WPPs are envisioned to be installed offshore far from the shore where the potential of wind energy is high and more space is available. For such a situation, it would be favorable to employ large capacity wind turbines in the WPP to be able to maximize the energy captured from the wind. From the three major concepts of currently developed wind turbine technologies i.e. fixed speed wind turbine with squirrel cage induction generator (FSIG); variable speed wind turbine with doubly-fed induction generator and power electronic converter (DFIG); and, variable speed wind turbine with induction or synchronous generator and fully rated power electronic converter (FCG); it is likely that one of the variable speed wind turbines technologies would be employed in the future large scale offshore WPP. The FSIG concept uses squirrel cage induction generator which speed can only be varied for a small range. This characteristic results in relatively low energy capture since maximum power from the wind can only be extracted for a small range of wind speed variation. On the other hand, utilization of power electronic converter makes the generator speed of the DFIG and the FCG concepts variable over a wide range of wind speed variation and thus results in high energy capture.

This section describes the offshore WPP model and the WPP local grid model implemented in this thesis. The size of the offshore WPP is 440 MVA and is developed based on aggregation of 200 units, 2.2 MVA, 0.69 kV wind turbines of the FCG concept. In the following sections, the FCG wind turbine model will be explained first. Later, the aggregated WPP model and its connection to the common bus with WPPVSC are described.

3.3.1 FCG wind turbine model

The model of the FCG wind turbine consists of models of its main components and model of wind speed as shown in Figure 3.14. The model is developed from [13] and [14].

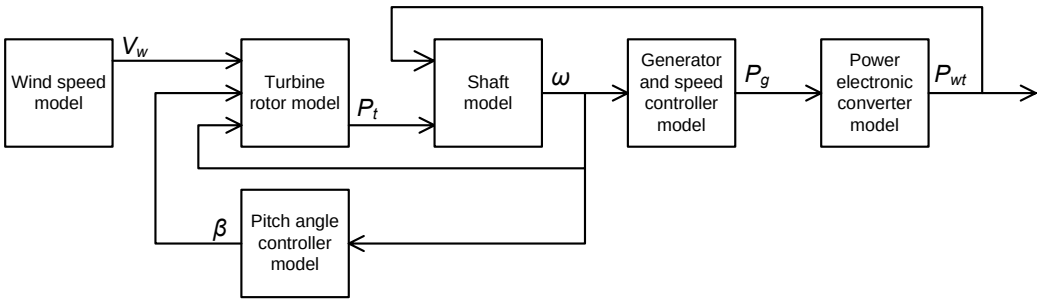

Figure 3.14 FCG wind turbine model

3.3.1.1 Wind speed model

The wind speed model implemented in this thesis is developed from [14]. There, the wind speed model has four components i.e. base component, ramp component, gust component and turbulence component. The base component represents a single value wind speed; the

ramp component represents a steady increase in the wind speed; the gust component represents a gust wind; and, the turbulence component represents turbulence in the wind speed. In this thesis, however, the turbulence component is neglected in order to simplify the wind speed model. It is based on consideration that the turbulence in the wind is much lower offshore than onshore due to relative less roughness on sea surface [15]. Moreover, the turbulence effect on the aggregated output power of a WPP decreases as the number of incorporated wind turbines increases and in case where variable speed wind turbine is used, turbulence is hardly reflected in the output power [16]. Furthermore, the gust component will not be used in this thesis and thus is also excluded from the wind speed model. Hence, the wind speed model implemented in this thesis consists of only the first two components i.e.

$$v_w = v_{aw} + v_{rw} \tag{3.24}$$

where v_w is the wind speed applied to the wind turbine [m/s], v_{aw} is the base component [m/s] and v_{rw} is the ramp component [m/s]. The base component is modeled as a constant. The ramp component is modeled using the following equations,

$$v_{rw} = \begin{cases} 0 & for \quad t \le t_{sr} \\ A_{rw,\max} \dfrac{t - t_{sr}}{t_{er} - t_{sr}} & for \quad t > t_{sr} \\ A_{rw,\max} & for \quad t \ge t_{er} \end{cases} \tag{3.25}$$

where $A_{rw,max}$ is the maximum ramp amplitude [m/s], t_{sr} is the time the ramp start and t_{er} is the time the ramp end.

3.3.1.2 Turbine rotor model

The turbine rotor captures power in the wind and converts it into mechanical power. The turbine rotor model thus consists of equations describing the mechanical power generates by the turbine rotor i.e.

$$P_t = 0.5 \rho \pi r^2 v_w^{\,3} C_p(\lambda, \beta) \tag{3.26}$$

where P_t is the mechanical power generates by the turbine rotor [W], ρ is the air density [kg/m^3], r is the radius of the turbine rotor [m], v_w is the wind speed [m/s] and $C_p(\lambda, \beta)$ is the turbine rotor power coefficient as a function of the blade tip speed ratio λ and the blade pitch angle β [degree]. The numerical approximation of the $C_p(\lambda, \beta)$ is based on the following formulas [13],

$$C_p(\lambda, \beta) = 0.5176\left(\frac{116}{\lambda_i} - 0.4\beta - 5\right)e^{-\frac{21}{\lambda_i}} + 0.0068\lambda \tag{3.27}$$

for which,

$$\lambda_i = \frac{1}{\dfrac{1}{\lambda + 0.08\beta} - \dfrac{0.035}{\beta^3 + 1}} \tag{3.28}$$

$$\lambda = \frac{\omega r}{v_w} \tag{3.29}$$

where ω is the rotational speed of the shaft [rad/s].

3.3.1.3 Shaft model

In power system studies, the main objective of developing a detailed model of the shaft in wind turbine model is to study the effect of the shaft torsional oscillations on the grid where the wind turbine is connected. The effect of the shaft torsional oscillations appears as harmonics in the electrical power supplied by wind turbine [17]. Study results reported in [18] has shown that by applying particular controller, the shaft torsional oscillation can significantly be damped. In this thesis, however, the effect of harmonics is neglected and only the fundamental frequency of the electric quantities is considered. Moreover, detailed interaction between the wind turbines and the local grid is outside the objectives of this thesis. Therefore, in this thesis, by assuming that the wind turbine is equipped with such controller and moreover by assuming that the controller works perfectly, the shaft is modeled as a single lumped mass. The equation describing the shaft model is thus the equation of motion where the inertia of turbine rotor and inertia of the generator rotor is lumped together i.e. [19]

$$\omega_{pu} = \frac{1}{2H_{pu}} \int (T_{t,\,pu} - T_{g,\,pu}) + \omega_{0,\,pu} \tag{3.30}$$

in which,

$$\omega_{pu} = \frac{\omega}{\omega_b} \tag{3.31}$$

$$H_{pu} = H_{t,\,pu} + H_{g,\,pu} \tag{3.32}$$

$$T_{t,\,pu} = T_t \frac{\omega_b}{S_b} \tag{3.33}$$

$$T_t = \frac{P_t}{\omega} \tag{3.34}$$

$$T_{g,\,pu} = T_g \frac{\omega_b}{S_b} \tag{3.35}$$

$$T_g = \frac{P_{wt}}{\omega} \tag{3.36}$$

$$\omega_{0,\,pu} = \frac{\omega_0}{\omega_b} \tag{3.37}$$

where ω_{pu} is per unit rotational speed of the shaft [pu], ω_b is base rotational speed of the shaft [rad/s], $\omega_{0,\,pu}$ is per unit initial rotational speed of the shaft [pu], ω_0 is initial rotational speed of the shaft [rad/s], H_{pu} is total inertia of the turbine rotor and the generator rotor [s], $H_{t,\,pu}$ is inertia of the turbine rotor [s], $H_{g,\,pu}$ is inertia of the generator rotor [s], $T_{t,\,pu}$ is per unit mechanical torque of the turbine rotor [pu], T_t is mechanical torque of the turbine rotor [Nm], S_b is rated capacity of the wind turbine [VA], $T_{g,\,pu}$ is per unit electrical torque of the generator rotor [pu], T_g is electrical torque of the generator rotor [Nm] and P_{wt} is electrical power delivered by the wind turbine [W].

3.3.1.4 Generator and speed controller model

In FCG wind turbines, the generator is decoupled from the grid by the power electronics converter. Only the active power produced by the generator is passed to the grid while the generator terminal voltage and frequency variation will not affect the grid during normal operation of the wind turbine. Since in this thesis, disturbance will not be implemented

either on the wind turbine or on the local grid where it is connected, the generator therefore is modeled only as a power source while the other electrical quantities interacting with the local grid are provided by the power electronics converter.

The wind turbine is assumed to employ a speed controller which function is to adjust electrical power produced by the generator so that the rotational speed of the generator rotor is always proportional to the wind speed at normal operation. In other words, at normal operation, the speed controller acts to maintain blade tip speed ratio (λ) at its optimum value so that maximum value of turbine rotor power coefficient (C_p) is always obtained and maximum energy capture is achieved. In this thesis, by assuming that this controller works perfectly, the generator and the speed controller model is therefore represented by the following equations,

$$P_g = \begin{cases} 0 & for \quad \omega \le \omega_{\min} \\ 0.5\rho\pi r^5 \dfrac{C_{p,\max}}{\lambda_{opt}^{\ 3}}\omega^3 & for \quad \omega_{\min} < \omega < \omega \\ P_{g,rated} & for \quad \omega \ge \omega_{rated} \end{cases} \tag{3.38}$$

where, ω_{min} is cut-in speed of the wind turbine [rad/s], ω_{rated} is rated speed of the wind turbine [rad/s], $C_{p,\,max}$ is the maximum value of the turbine rotor power coefficient and λ_{opt} is the optimum value of the blade tip speed ratio of the turbine rotor.

3.3.1.5 Pitch angle controller model

The objective of pitch angle controller is to reduce mechanical power by pitching the blades of the turbine rotor when the shaft speed increases above a certain value. Depending on the size of the wind turbine, the maximum rate of change of the pitch angle may vary between 3 to 10 deg/s [14]. In this thesis, it is assumed that the pitch controller starts to act at 1.02 pu of rated shaft speed and the rate of change of the pitch angle is 3 deg/s. In addition, it is assumed that the maximum pitch angle is 30 deg. The model of the pitch angle controller is shown in Figure 3.15.

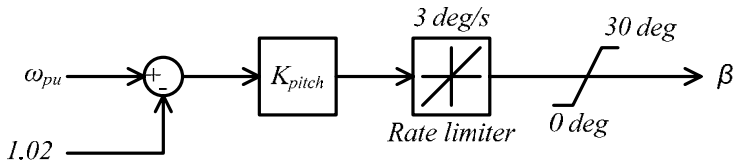

Figure 3.15 Pitch angle controller model

3.3.1.6 Power electronic converter model

In this thesis, the FCG wind turbine employs a back-to-back VSC for the power electronic converter. The model of the power electronic converter is developed from the point-to-point VSC-HVDC model described earlier in this chapter with several minor modifications. Here, the control and the protection schemes of the generator side VSC is assumed to work perfectly so that during normal operation, the power delivered by generator to the generator side VSC is always equal to that received at the grid side VSC. Therefore, model of the wind turbine power electronic converter can be represented only by the grid side VSC, where its power reference for the active power controller is equal to

the power produced by the generator. The scheme of the power electronic converter model is depicted in Figure 3.16.

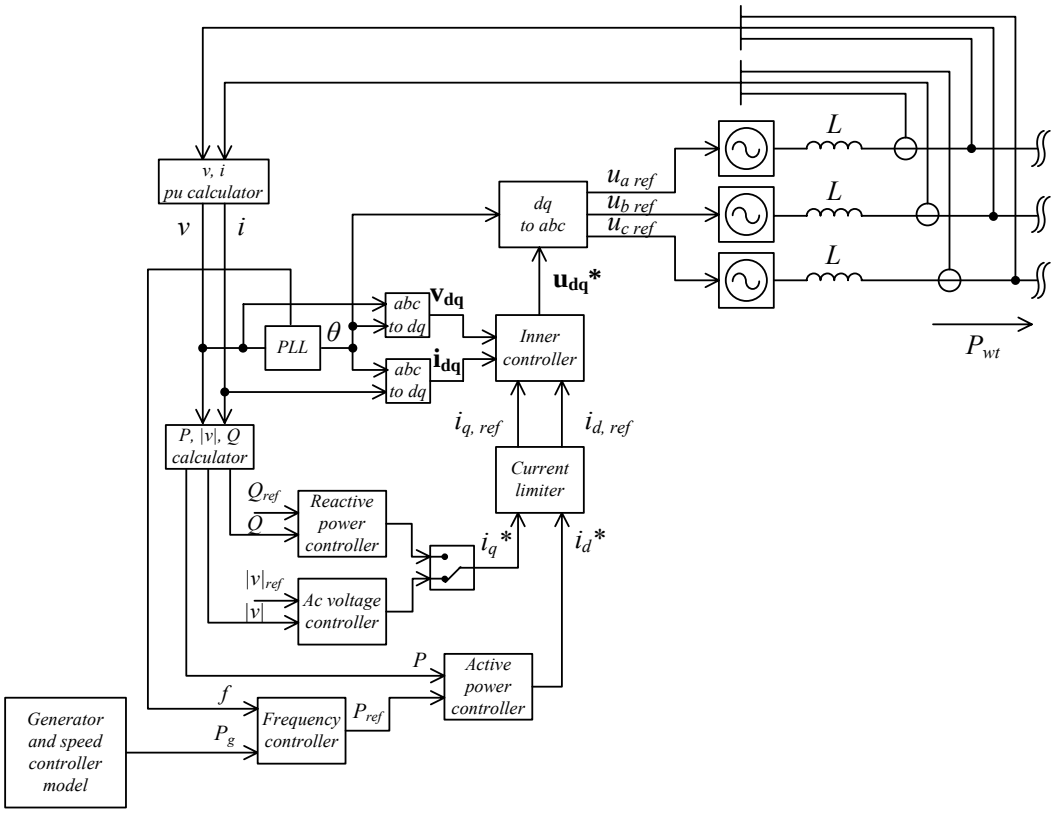

Figure 3.16 Power electronic converter model

In section 3.2.4.2.2, it is described that a frequency modulator is applied in the WPPVSC in order to signal the WPP to reduce its power when the direct voltage rises to an endangering value. To cope with the frequency modulation scheme, a frequency controller is added in the power electronic converter model. The model of the frequency controller will be described in Chapter 5.

3.3.2 Aggregated WPP model

The WPP model is based on aggregation of 200 units of the FCG wind turbine. The applied approach for developing the model is developed from [16]. In this thesis, however, the WPP detailed layout is not defined and therefore it is difficult to determine the individual wind speed applied to each wind turbine and to specify how the wind turbines are connected to each other in the WPP and to the common bus of the local grid. Therefore, for simplicity, it is assumed that each of the wind turbines experiences the same individual wind speed. Moreover, it is assumed that all of the wind turbines are connected to the common bus in parallel to each other. Based on those assumptions, the WPP model can be represented by one FCG wind turbine model where the mechanical power, electrical power and the rated capacity of the generator and the power electronic converter of the WPP model equals to those of the individual FCG wind turbine model multiplied by the number of wind turbines i.e.

$$P_{t,WPP} = n\,P_t \tag{3.39}$$

$$P_{g,WPP} = n\,P_g \tag{3.40}$$

$$P_{WPP} = n\,P_{wt} \tag{3.41}$$

$$S_{b,WPP} = n S_b \tag{3.42}$$

where, $P_{t,WPP}$ is the turbine rotor mechanical power of the WPP model [W], $P_{g,WPP}$ is the generator electric power of the WPP model [W], P_{WPP} is the power delivered by the WPP model [W], P_{wt} is the power delivered by a wind turbine [W], $S_{b,WPP}$ is the rated capacity of the WPP model [VA], and n is the number of wind turbines aggregated.

3.3.3 WPP connection

The aggregated WPP model is linked to the WPPVSC station at the common bus. The WPP model is connected to the common bus through a 440 MVA, 0.69/33 kV step-up transformer. The transformer model is represented by its leakage inductance based on assumptions similar to those described in section 3.2.1.1. The leakage inductance of the transformer is chosen 0.15 pu of its rated capacity and voltage. The WPP connection with the WPPVSC station is depicted in Figure 3.17.

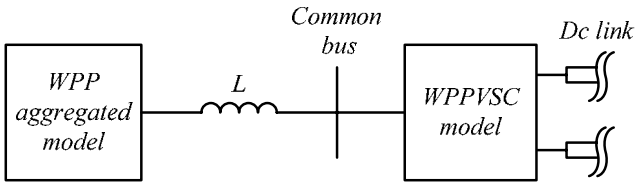

Figure 3.17 WPP connection with WPPVSC

4 Control Strategy for Multi-Terminal Network Operation

4.1 Introduction

In future transnational offshore networks, several offshore WPPs and several countries are connected together and different market dispatch schemes may be applied among the countries to share power from the offshore WPPs as well as to perform power trade. In general, there are three dispatch mechanisms that may be applied i.e. fixed power sharing, priority power sharing and proportional power sharing. In fixed power sharing, one country receives a fixed amount of power while the other country(s) balances the variability in WPPs power. In priority power sharing, one country gets the first priority to obtain WPPs power to a particular limit while the other country(s) receives the excess power. In proportional power sharing, several countries share WPPs power in particular proportion.

In order to comply with such a situation, a general control strategy capable of performing different market dispatch schemes in the future transnational network is required. Beside capable of performing different market dispatch schemes during normal operation, the control strategy should be capable of performing acceptable operation during and after a temporary or a severe disturbance e.g. voltage dip at an onshore grid or disconnection of a converter, notably the direct-voltage controlling converter. Moreover, it is also required that the control strategy to be independent of the network topology to avoid incorrect operation upon changes in the network topology, for instance, due to addition of a new transmission segment or removal of an existing transmission segment for maintenance purposes. Furthermore, if in order to perform the dispatch schemes, the control system requires communication with an outer remote controller such as a supervisory dispatch controller, it is important that the control strategy is capable to perform acceptable operation during communication delays or failure.

Considering the requirements above, there are two control strategies available in the literature which possibly to be applied in future transnational networks i.e. the direct voltage droop method and the voltage-margin method. Capability of the direct voltage droop method to perform priority and proportional power sharing as well as to perform acceptable operation during and after voltage dip at an onshore grid and disconnection of a direct voltage controlling converter has been explored and shown in [20], [21] and [22]. However, this method introduces disadvantages regarding its difficulty to perform fixed power sharing and to be independent of the network topology using a simple control strategy. Direct voltage droop method employs a proportional controller which represents a droop characteristic describing a unique relation between direct voltage and power delivered by the assigned converter. That way, the controller adjusts the power delivered by the assigned converter according to the immediate level of the direct voltage. This basic principle makes the direct voltage droop method difficult to perform constant power control in fixed power sharing. Moreover, since the droop characteristic is valid only for a given network topology, the correct operation of the control strategy therefore can not be achieved using the same droop characteristic if the network topology is changed.

On the other hand, voltage-margin method employs a proportional-integral controller where the output of the controller is limited to particular upper and lower value. That way, the controller adjusts the power delivered by the assigned converter by maintaining the direct voltage at a given reference value as long as the power is between the limits.

The unique relation between the direct voltage and the power delivered by the assigned converter defined by the network topology is not necessary considered for the controller to operate correctly. The correct operation of the controller therefore can be achieved for any given direct voltage reference value independently of the network topology. However, further exploration on the capability of the voltage-margin method to perform the dispatch schemes independently of the network topology for normal and disturbed operation is required.

4.2 Basic Principle of VMM

The voltage-margin method (VMM) implemented in this thesis is developed from [23], [24] and [25]. In this thesis, the basic control strategy of the VMM consists of a direct voltage controller and a limiter as shown in Figure 4.1. The direct voltage controller employs a proportional-integral (PI) controller similar to that described in Chapter 3. The limiter is applied to limit the *d*-axis current reference value to an upper value and a lower value in order to limit the power flowing through the converter to an upper and a lower value. In such an arrangement, the controller will maintain the direct voltage equal to the reference value as long as the power flowing through the converter is between the limits.

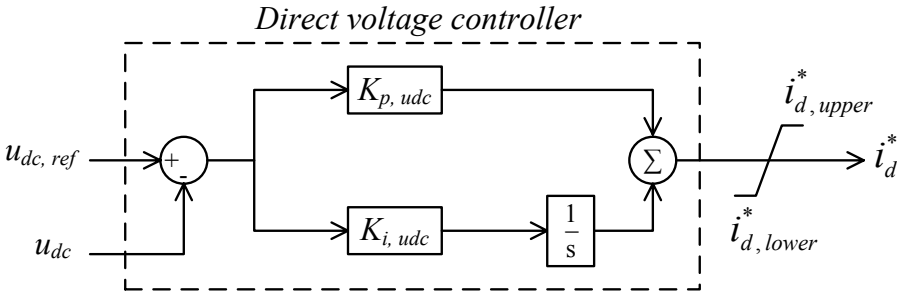

Figure 4.1 VMM basic scheme

The relation between the upper limit of the *d*-axis current reference value and the upper value of power flowing through the converter is

$$i^*_{d,upper} = \frac{P_{upper}}{v_d} \tag{4.1}$$

and the relation between the lower limit of the *d*-axis current reference value and the lower value of power flowing through the converter is

$$i^*_{d,lower} = \frac{P_{lower}}{v_d} \tag{4.2}$$

where $i_{d,}{}^*_{upper}$ is the upper limit value of the *d*-axis current reference value [pu], $i_{d,}{}^*_{lower}$ is the lower limit value of the *d*-axis current reference value [pu], P_{upper} is the upper value of power delivered by the converter [pu], P_{lower} is the lower value of power delivered by the converter [pu] and v_d is the *d*-axis component of the common bus voltage [pu].

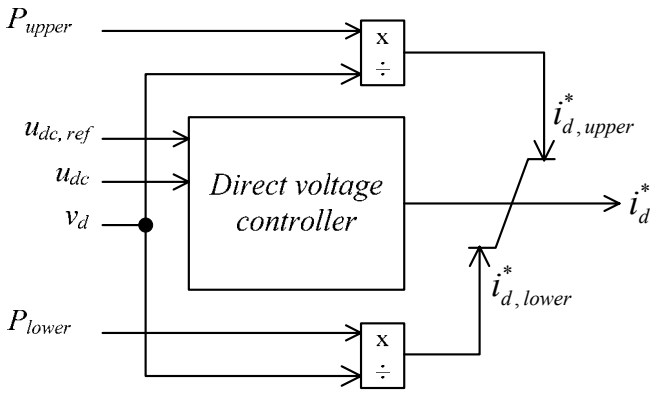

Figure 4.2 VMM basic scheme with adjustable limits

The upper and the lower value of the limiter are adjustable and their values may be set directly at the converter station or sent from a remote supervisory dispatch controller as shown in Figure 4.2. By applying the scheme shown in Figure 4.2, the maximum and the minimum power flowing through the converter can be controlled by adjusting the upper limit and the lower limit to the required value. Furthermore, by adjusting the upper limit equal to the lower limit, the converter can perform a constant power control. It should be noted, however, that the converter is not able to control the direct voltage during period when the power flowing through the converter is equal to one of the limits.

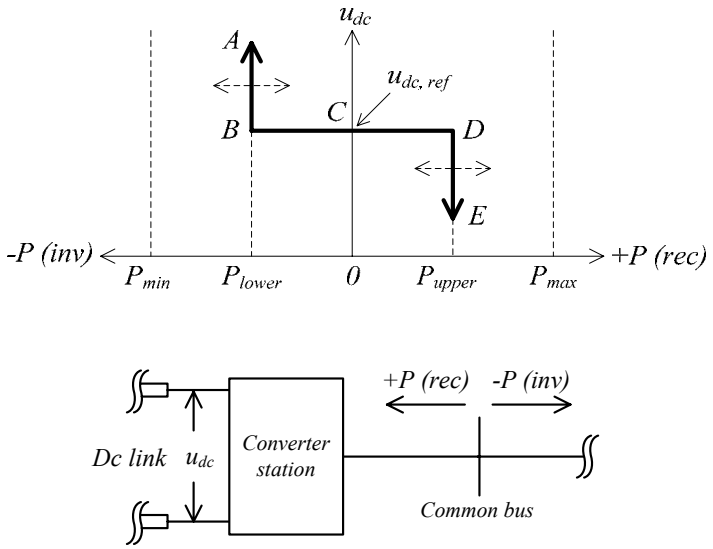

Figure 4.3 Converter operation characteristic:
(a) u_{dc}-P characteristic (b) power direction reference

When the scheme depicted in Figure 4.2 is applied to a converter, the converter will perform operation according to the u_{dc}-P characteristic as shown by the *A*-*B*-*C*-*D*-*E* line in Figure 4.3.a. The u_{dc}-P characteristic shows that the converter will maintain the direct voltage equal to the reference value and thus will perform operation in the *B*-*C*-*D* line as long as the power flowing through the converter is between the limits. The converter is performing inversion when it operates in the *B*-*C* line and is performing rectifying when it operates in the *C*-*D* line. However when the power flowing through the converter is equal to the lower limit, the controller is no longer able to control the direct voltage and while the power is maintained constant, the direct voltage may rise following the *B*-*A* line. Similarly, when the power flowing through the converter is equal to the upper limit,

the controller is no longer able to control the direct voltage and while the power is maintained constant, the direct voltage may drop following the *D-E* line.

It should be noted that for a point-to-point operation, the limiter may not be required. In such a situation, the upper and the lower value of the limiter can be set equal to the rated capacity of the converter.

For multi-terminal network operation, the scheme depicted in Figure 4.2 may be implemented in two or more direct voltage controlling converters by assigning different direct voltage reference value among the converters. The direct voltage reference value of each converter is set different one to the others by a particular voltage margin. The voltage margin should be set slightly larger than the expected voltage drop between a converter pair. In such a way, one converter will control the direct voltage after the other. An example of the u_{dc}-P characteristics of two converters operating with a voltage margin are given in Figure 4.4.

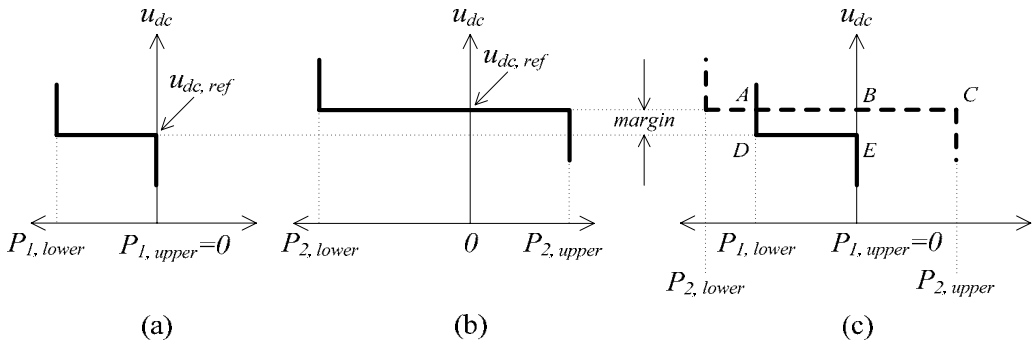

Figure 4.4 u_{dc}-P characteristic of two converters:
(a) converter-1 (b) converter-2 (c) converter-1 and 2

From Figure 4.4, it can be seen that the direct voltage reference value of the two converters are displaced by a particular margin. When the actual direct voltage is at E, converter-1 will control the direct voltage in the network and will perform inversion operation in the D-E line. However when converter-1 reach its lower limit at point D, it no longer be able to control the direct voltage and thus the direct voltage will rise following the D-A line. When the direct voltage reaches point A, converter-2 will start to control the direct voltage. A similar process will follow when converter-1 is suddenly out of operation and thus unable to control the direct voltage.

4.3 Two-stage direct voltage controller

In the example shown in Figure 4.4, converter-2 will perform direct voltage control when converter-1 has reached its limit or is suddenly out of operation. However, in the case when converter-1 has reached its limit and converter-2 is suddenly out of operation, there will be no converter controlling the direct voltage unless the lower limit of the converter-1 is adjusted further to the left hand side of its characteristic. In such a situation, however, it is not likely that the limit can be adjusted very quickly through signaling from a remote supervisory controller. As the result, the direct voltage may rise uncontrollable and the whole network may be taken out of operation. To avoid such situation, a two-stage direct voltage controller is applied to both of the converters. The scheme of the two-stage direct voltage controller is given in Figure 4.5.

In Figure 4.5, the two direct voltage controllers are identical. The only difference is the direct voltage reference value of the second controller is set higher at a particular margin

than that of the first controller. In such a way, during normal operation, the first controller will maintain the direct voltage equal to its reference value and perform operation in the first stage (the D-E line in Figure 4.6.b). During abnormal operation when the direct voltage rises above the reference value of the second controller, the second controller will automatically adjust the lower value of the first limiter further to the left hand side of the u_{dc}-P characteristic and will start to control the direct voltage at the second stage. The converter thus will perform operation in the B-C line (Figure 4.6.c).

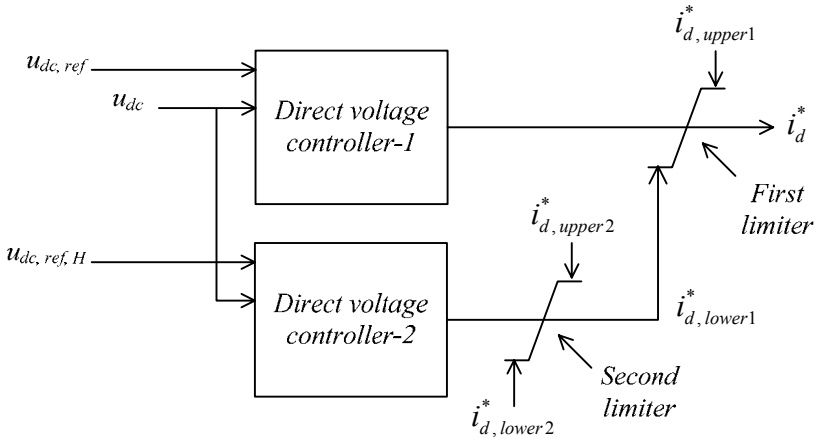

Figure 4.5 Two-stage direct voltage controller

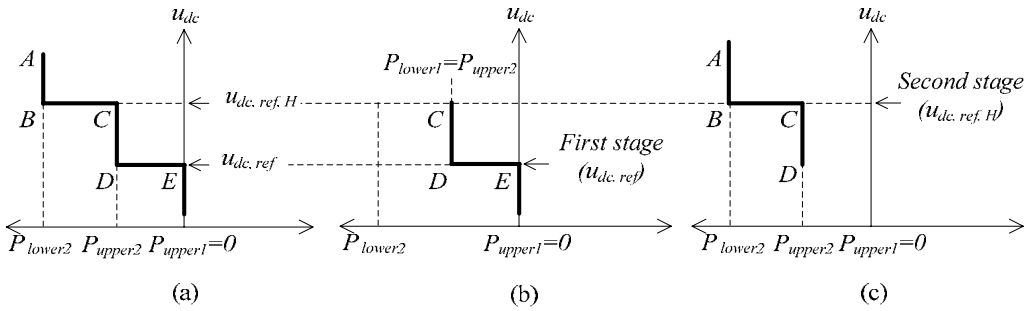

Figure 4.6 u_{dc}-P characteristic of the two-stage direct voltage controller:
(a) u_{dc}-P characteristic (b) first stage operation (c) second stage operation

The upper value of the first limiter and the upper and the lower values of the second limiter are also adjustable and may be set in the same way as described in the previous section. If the upper and the lower values of the second limiter are set equal, a u_{dc}-P characteristic similar to that shown in Figure 4.3 is obtained. The lower value of the second limiter however must be set equal to the rated capacity of the converter. It is based on consideration that during abnormal operation when the direct voltage in the network raises high due to a direct voltage controlling converter is suddenly out of operation, the back up converter must be able to extract as much power as possible from the network in order to restore the power balance.

An example of the u_{dc}-P characteristics of two converters using the two-stage direct voltage controller is shown in Figure 4.7. The upper and the lower value of the second limiter in converter-1 are set differently while the upper and the lower value of the second limiter in converter-2 are set equal. It can be seen that when converter-1 is at its limit, converter-2 will control the direct voltage and will operate at the A-B-C-D line. If, converter-2 is suddenly out of operation, the direct voltage will rise. When the direct voltage rises above the reference value of the second controller in converter-1, the

controller will adjust the lower limit of converter-1 further to the left hand side and will start to control the direct voltage in the E-F-I line.

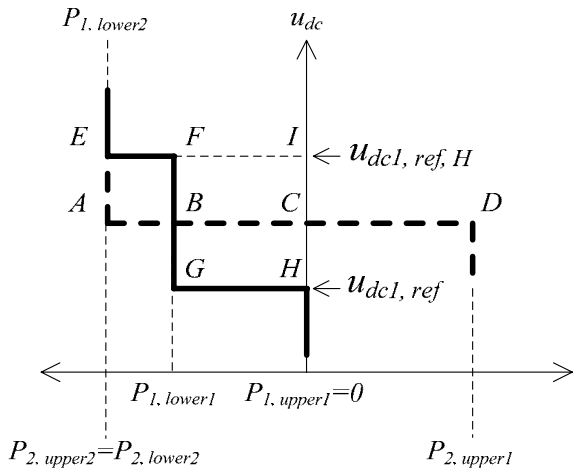

Figure 4.7 u_{dc}-P characteristic of two converters using the two-stage direct voltage controller: converter-1 (E-F-G-H); converter-2 (A-B-C-D)

4.4 Three-stage direct voltage controller

So far, only a situation where the converter is performing the inversion operation is discussed in the previous sections. In the future transnational network situation, however, a converter may have to perform the inversion as well as the rectifying operation. If the two-stage direct voltage controller is implemented in two converters performing rectifier operation, the direct voltage may drop uncontrollable when the direct voltage controlling converter is suddenly out of operation while the other converter is operating at its upper limit. To avoid such situation, a three-stage direct voltage controller is proposed in this thesis and applied to both converters. The scheme and the u_{dc}-P characteristic of the three-stage direct voltage controller is depicted in Figure 4.8 and Figure 4.9.

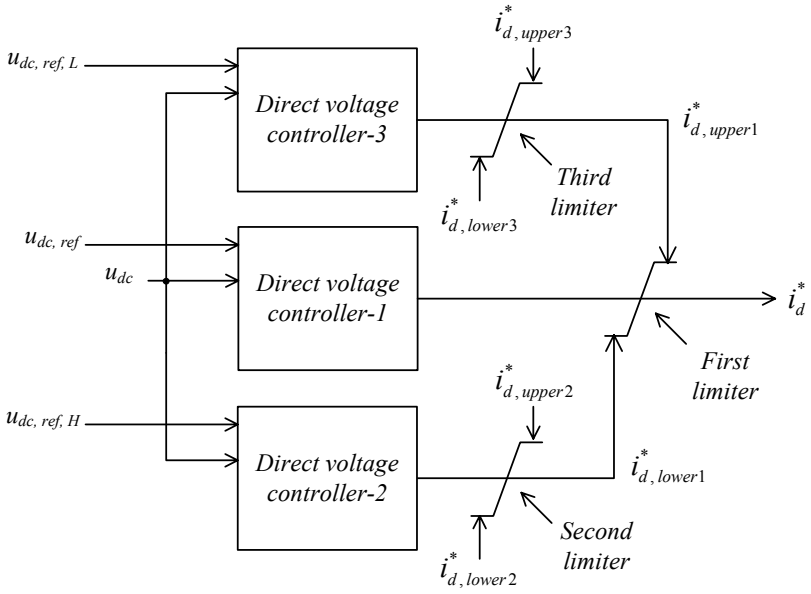

Figure 4.8 Three-stage direct voltage controller

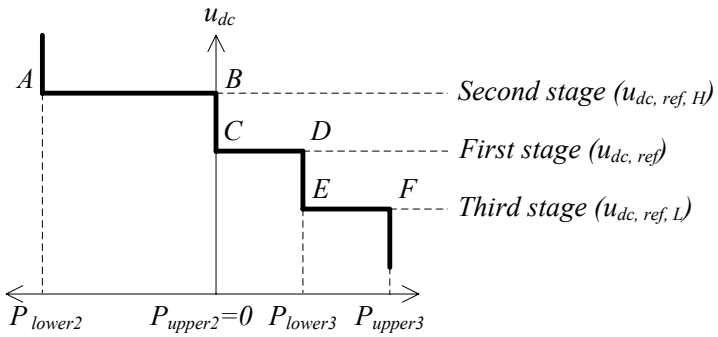

Figure 4.9 u_{dc}-P characteristic of the three-stage direct voltage controller

4.5 Implementation of the control strategy

In this thesis, the three-stage direct voltage controller is used and is applied at the GSVSCs in the multi-terminal network. The three-stage direct voltage controller replaces the direct voltage controller in the GSVSC control scheme described in section 3.2.4.1.

In the following sections, implementation of the control strategy at each GSVSC for each of the general market dispatch schemes is described. In the description, only two GSVSCs is considered for simplicity.

4.5.1 Fixed power sharing

In fixed power sharing, one country receives a fixed amount of power. The source of the power may be from the offshore WPPs or from the other countrie(s) or both. In the case of the fixed power sharing is applied among two countries, one country will balance the variability of the WPPs power. The u_{dc}-P characteristics of two GSVSCs performing fixed power sharing are given in Figure 4.10.

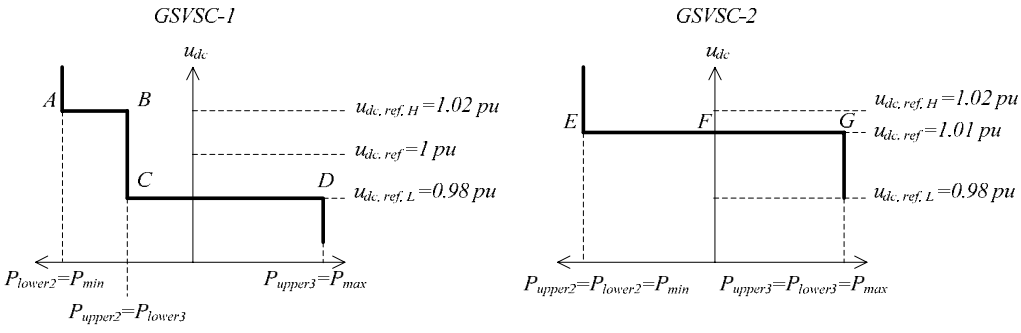

Figure 4.10 u_{dc}-P characteristics of two GSVSCs performing fixed power sharing

4.5.2 Priority power sharing

In priority power sharing, one country gets the first priority to obtain WPPs power to a particular limit while the other country(s) receives the excess power. In other words, as long as the power delivered to the first prioritized country has not reach the limit, the second prioritized country will not receive power from the WPPs. The u_{dc}-P

characteristics of two GSVSCs performing priority power sharing are depicted in Figure 4.11.

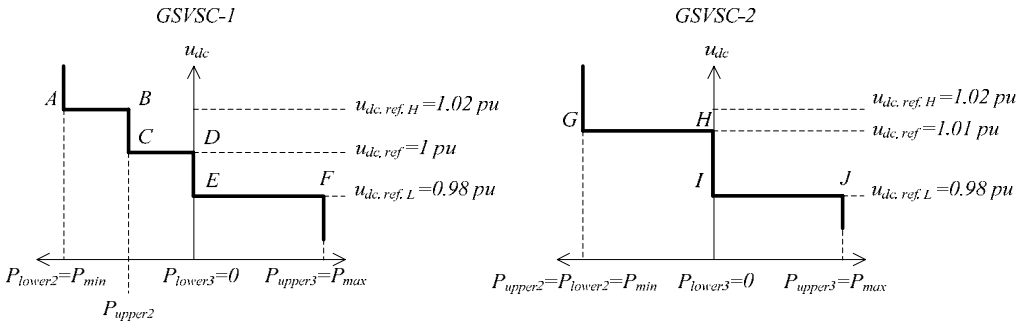

Figure 4.11 u_{dc}-P characteristics of two GSVSCs performing priority power sharing

4.5.3 Proportional power sharing

In proportional power sharing, the two countries share the WPPs power in a particular proportion. It should be noted here that it is difficult for the control strategy based on the VMM to perform proportional power sharing independently. In order to perform the proportional power sharing, collaboration between the control strategy in the GSVSC and a remote supervisory controller is required.

In this thesis, the supervisory controller is assumed to perform the following tasks subsequently: measures the WPP power received at each WPPVSC; summing the measured quantity to obtain the total power received at the WPPVSCs; dividing the total power according to the scheduled portion for each GSVSC; transforming the power portion into per unit value of the rated capacity of the corresponding GSVSC; and, signaling the per unit power portion to the corresponding GSVSC. At the corresponding GSVSC, the per unit power portion is used to adjust the upper value of the second limiter. The u_{dc}-P characteristics of two GSVSCs performing proportional power sharing are shown in Figure 4.12.

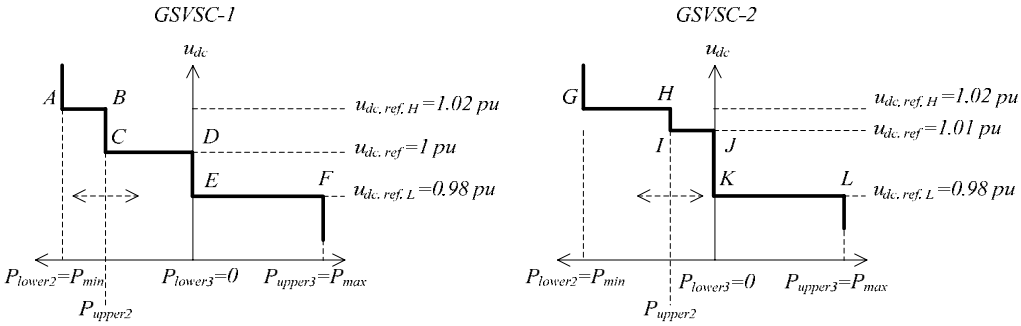

Figure 4.12 u_{dc}-P characteristics of two GSVSCs performing proportional power sharing

5 Fault Ride-Through of Multi-Terminal Networks

5.1 Introduction

As the capacity of modern WPPs is approaching that of the conventional generation and the number of WPPs integrated to the grid is growing, the influence of the WPPs power on the grid operation has become significant. An abrupt disconnection of a WPP delivering a large amount of power may significantly disturb the power balance in the grid. To minimize the occurrence of such an event, most grid codes impose fault ride-through (FRT) requirements in which the WPPs have to remain connected during a temporary voltage dip caused by a fault in the grid.

Typical FRT requirements demand that the WPPs must be capable of withstanding a voltage dip to a certain percentage of the nominal voltage at the connection point and for a specified duration. Moreover, it is also required that the WPPs are capable of restoring the active and the reactive power to the pre-fault values subsequently after the voltage returns to the normal operating level. In addition, some grid codes necessitate that the WPPs increase its reactive power generation during the voltage dip in order to provide voltage support.

The FRT requirements of various grid codes are pointed by the colored lines in Figure 5.1. The WPP should remain connected to the grid as long as the voltage dip occurs within the area above the line of the corresponding grid code. It can be noticed that some grid codes allow severe voltage dip down to 100% of the nominal voltage at the connection point. Particularly for the Germany and the UK grid codes, the severe voltage dip is allowed for 150 ms.

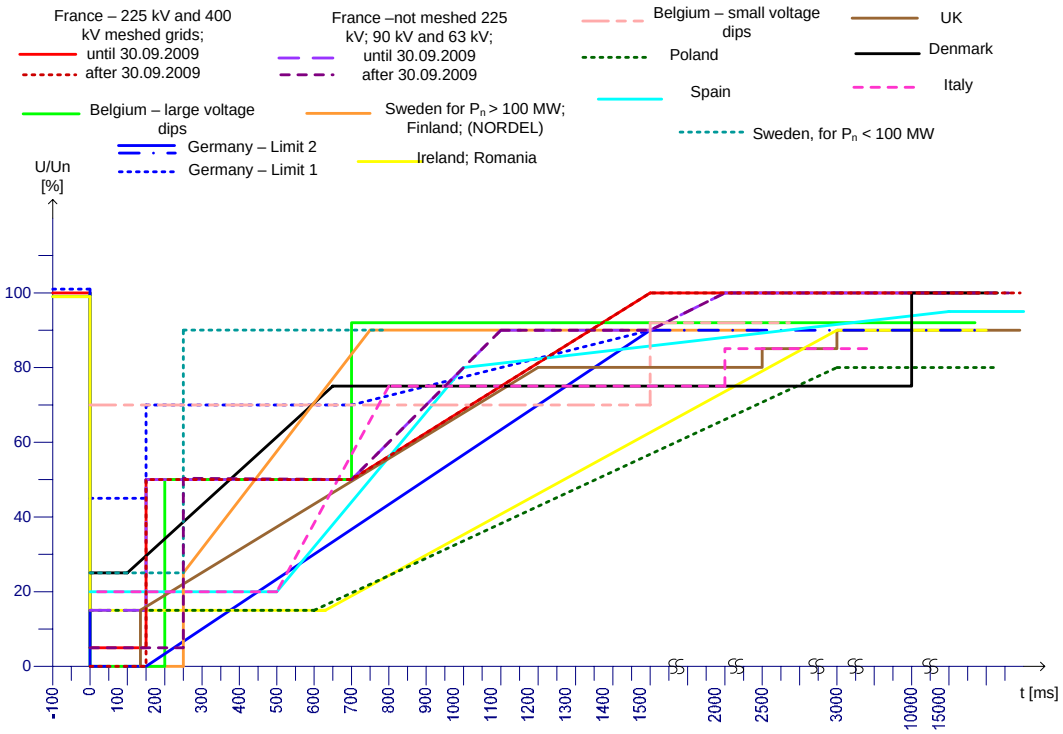

Figure 5.1 The FRT requirements of various grid codes [26]

For WPP which is connected to the grid directly or through an ac transmission, the FRT capability is provided by the control and protection systems in the WPP. However for a WPP which is connected to the grid by VSC-HVDC, the FRT requirements are accomplished by collaboration between the control and protection systems in the WPP and in the VSC stations.

5.2 Existing FRT methods for VSC-HVDC connected WPP

In a situation where the WPP is connected via a point–to-point VSC-HVDC transmission, such as during a voltage dip at the grid connection, the WPP power delivered by the corresponding inverting converter is reduced significantly. While the WPP is continuously injecting power into the dc link, the power imbalance will occur in the link. During power imbalance, the excess power in the dc link is stored in the dc capacitors and as the result the direct voltage will rise. The increase in the direct voltage may reach an endangering value if no preventive action is subsequently taken.

In order to prevent the direct voltage rises to a dangerously high value in the aforementioned situation, FRT methods as listed in [27] and [28] may be applied i.e. energy dissipation and WPP power reduction. In the first method, a dc chopper is applied to dissipate the WPP excess power in a resistor during the voltage dip. The second method is accomplished by reducing the WPP power in order to restore the power balance in the dc link and can be achieved by fast signaling, voltage reduction and frequency modulation.

Fast signaling is established between the WPPVSC and the WPP through a communication link. During a voltage dip, the control systems in the WPPVSC sense the endangering increase in the direct voltage and signal the control systems in the WPP to quickly reduce the WPP power. For a severe voltage dip, the direct voltage may rise very quickly and thus a fast execution is required. However, due to the use of communication, the signaling process experiences a communication delay and thus a fast execution may be difficult to achieve.

WPP power reduction by voltage reduction is accomplished by quickly reducing the WPP bus voltage. This is done by the control systems in the WPPVSC and can be performed as long as the WPPVSC is assigned to control the WPP bus voltage and the WPP employs wind turbine with power electronic converter. The power electronic converter of this wind turbine commonly has current limit slightly above its rated current [28]. When the direct voltage rises above a threshold value, the voltage controller in the WPPVSC quickly reduces the amplitude of the converter voltage in order for the WPPVSC to absorb the reactive power from the local WPP grid. This action causes the WPP bus voltage to drop. The WPP is thus operated at its current limit and the power it delivers is reduced. It should be noted that for the method to work properly, the capability of the wind turbine power electronic converter to provide voltage support should be disabled.

In the frequency modulation method, the frequency of the WPP local grid is increased when the direct voltage level increases above the threshold value. This action is performed by the frequency modulator in the WPPVSC. As in the case of the voltage reduction method, this method is applied for a WPP consisted of wind turbine with power electronic converter. In the wind turbine power electronic converter, a PLL is commonly employed to continuously measure the actual phase angle of the bus voltage required for the transformation of the phase quantities into the *dq* quantities and vise versa [29]. The same PLL can be used to continuously measure the actual WPP grid frequency. A controller, say the frequency controller, which translates the frequency increment into

power reduction order is required to be installed in the wind turbine power electronic converter for the WPP to sense the changes in frequency. The output of this controller is applied to reduce the active power reference value for the active power controller in the wind turbine power electronic converter.

It should be pointed that the implementation of the voltage reduction method may be limited if there is other electric installation (such as an offshore oil platform) connected to the WPP bus since during deep voltage reduction the installation may not be able to work properly. Moreover, in the case when the WPP power is required to be decreased to zero, the voltage would be reduced to zero and this may effect the installation even worse. On the other hand, the gain of the frequency controller used in the frequency modulation method can be adjusted so that to achieve WPP power reduction to zero, only small frequency alteration is applied. If the frequency alteration is bounded within the normal operation range, its effect to the operation of other installation in the WPP local grid would be insignificant.

In comparison to the other methods, the energy dissipation method is the most robust, whereas the fast signaling method is least robust due to its dependence on communication. However, implementation of the energy dissipation method would be more costly due to the addition of dc chopper to the VSC-HVDC installation. Moreover, in the case when the WPP is connected via a point-to-point VSC-HVDC transmission, the capacity required for the dc chopper is equal to the rated capacity of the WPP. On the other hand, application of the frequency modulation method or the voltage reduction method requires only additional control loops or adjustment of the existing control systems in the WPP and in the WPPVSC [28].

5.3 FRT methods for multi-terminal VSC-HVDC

In the multi-terminal VSC-HVDC case, the occurrence of a voltage dip on one of the grid connections does not necessarily lead to an abnormal rise in the direct voltage since it is possible that there is more than one converter assigned to compensate for power imbalance in the dc link. However, since the task specified for the converters may change during operation, implementation of FRT method is still required.

In this thesis, the energy dissipation method and the frequency modulation method are implemented in the multi-terminal network model. It is based on the following considerations. First, the energy dissipation method is robust. Moreover, by installing the dc chopper at the GSVSC, the capacity required for the dc chopper may not be as large as the rated capacity of the WPP but is more dictated by the rated capacity of the GSVSC. Second, considering the reliability of the FRT method, one of the WPP power reduction methods is added. Third, in a future transnational network, it might be possible that some electric devices are required to be installed in the WPPVSC to acquire controllability of the wind turbine connections remotely from the shore. The operation of the devices may depend on the actual voltage of the WPP bus. In such a situation, the application of the frequency modulation method is more favorable than the voltage reduction method.

In a future transnational offshore network, it is possible that two grids are connected onshore via an ac tie line. In the case when the grids are strongly connected, a voltage dip occurring at one grid may influence a voltage dip on the other grid. Thus, during the voltage dip, the direct voltage at the GSVSCs of the corresponding grids may rise high. The action of a dc chopper installed at one of the GSVSCs may not be to control the direct voltage at both GSVSCs. The direct voltage at the other GSVSC may still be high especially if the two GSVSCs are spaced by a long dc transmission. Based on that consideration, in a multi-terminal network model, the dc chopper is installed on each of

the GSVSCs while the frequency modulation method is implemented at each of the WPPs and the WPPVSCs.

5.4 Implementation of the FRT methods

5.4.1 Dc chopper

In practice, dc chopper mainly consists of voltage triggered power electronic switches and resistors. When the direct voltage rises above the threshold value of the dc chopper, the power electronic switches start to work and part of current flowing in the dc link is dissipated through the dc chopper resistor. The amount of current dissipated depends on the duty ratio of the switches and thus depends on the level of the direct voltage. The amount of current dissipated is, however, limited to the rated voltage and the rated capacity of the dc chopper.

In this thesis, dc chopper is modeled as a voltage controlled direct current source where the current injected by the current source is controlled by the duty ratio controller. The rated capacity of the dc chopper is 440 MW (1 pu of the rated converter capacity) and the rated voltage is 360 kV (1.2 pu of the rated dc link voltage). The scheme of the duty ratio controller is shown in Figure 5.2.

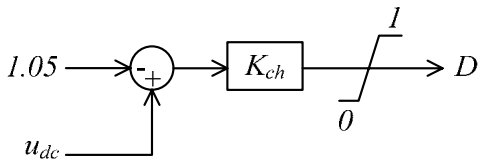

Figure 5.2 Duty ratio controller

The current injected by the current source is

$$i_{ch} = \frac{D\,P_{ch,\,rated}}{U_{ch,\,rated}} \tag{5.1}$$

where i_{ch} is the current injected by the current source [A], D is the duty ratio, $P_{ch,\,rated}$ is the rated capacity of the dc chopper [W] and $U_{ch,\,rated}$ is the rated voltage of the dc chopper [V].

5.4.2 Frequency modulator

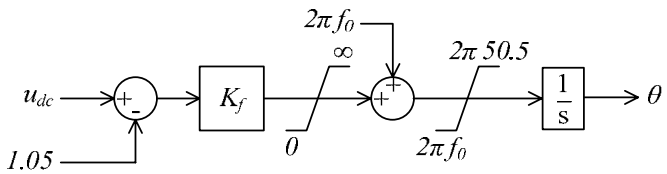

Figure 5.3 Frequency modulator

The scheme of the frequency modulator is shown in Figure 5.3. During normal operation, the frequency modulator generates frequency reference value for the WPPVSC. When the direct voltage rises above 1.05 pu of the rated value, the frequency reference value is increased proportional to the rise of the direct voltage. The gain of the frequency

modulator is defined such that when the direct voltage reaches 1.2 pu, the generated frequency reference value is equal to 50.5 Hz. The frequency reference value is limited to 50.5 Hz for the consideration discussed in section 5.2.

5.4.3 Frequency controller

The frequency controller acts to reduce the power reference value for the active power controller when the frequency in the WPP grid increases. The scheme of the frequency controller is given in Figure 5.4.

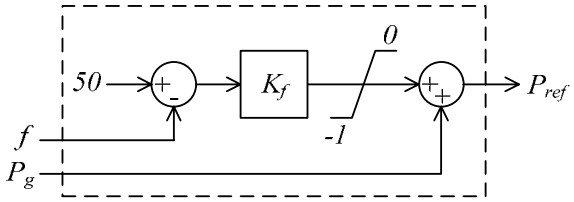

Figure 5.4 Frequency controller

6 Simulation Results

6.1 Introduction

In this chapter, simulation results based on particular case studies will be presented and discussed. Simulation results shown are chosen based on particular case studies which demonstrate the capability of the developed control strategy in performing general market dispatch scheme during normal operation as well as the response of the control strategy in regaining normal operation after experiencing a voltage dip at an onshore grid and in obtaining a new operating point after loosing an onshore converter.

The case studies and simulation results to be presented and discussed are divided into three major sections. In the first section (section 6.2), the capability of the control strategy in performing the three market dispatch schemes (i.e. fixed, priority and proportional power sharing) during normal operation is demonstrated. The second section (section 6.3) will present the response of the control strategy in obtaining a new operating point after loosing an onshore converter. The response of the control strategy in regaining normal operation after experiencing voltage dip at an onshore grid is pointed in the third section (section 6.4).

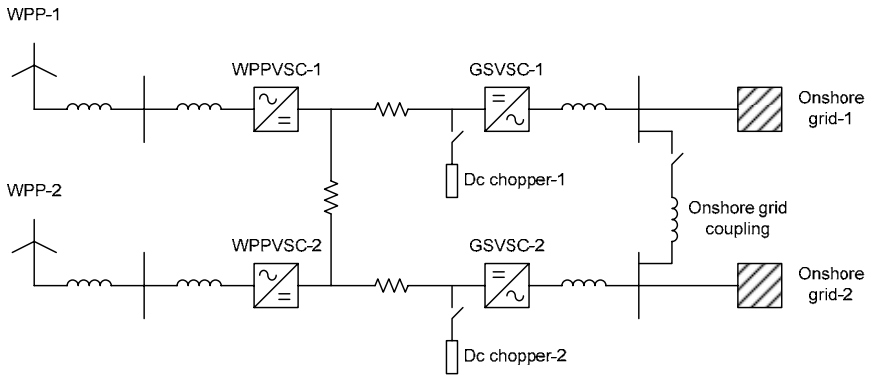

Figure 6.1 Multi-terminal network-1

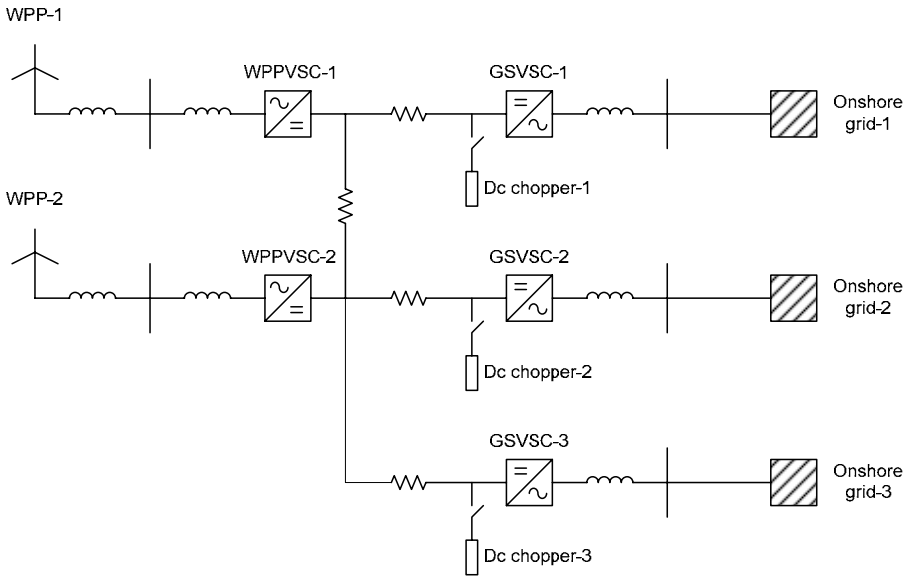

Figure 6.2 Multi-terminal network-2

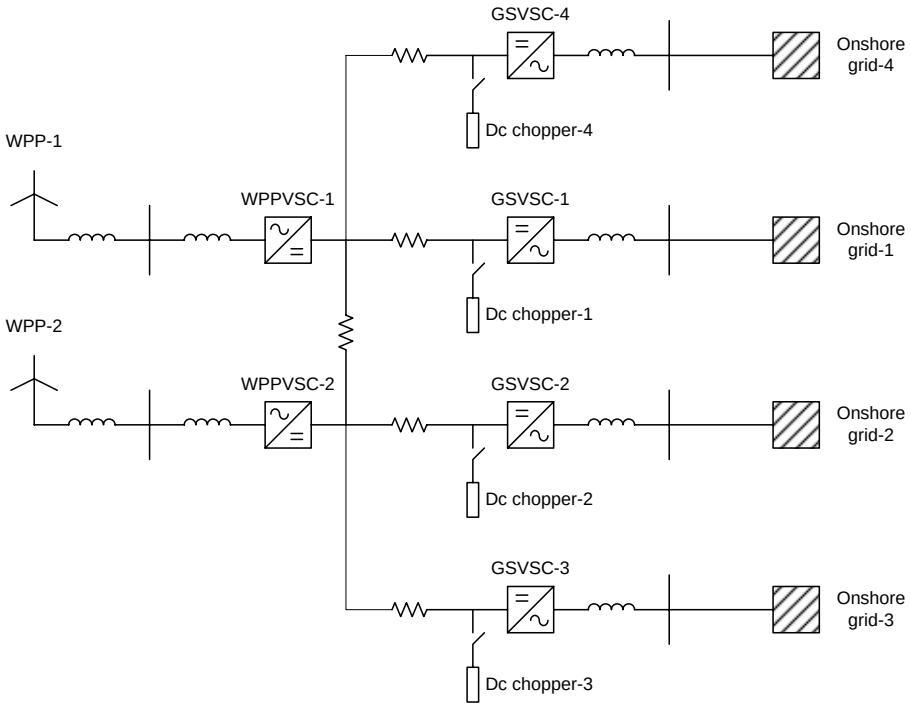

Figure 6.3 Multi-terminal network-3

The multi-terminal network developed in Chapter 3 (reprinted in Figure 6.1) is used for most of the study cases. For particular study cases, the third and the fourth GSVSC will be add to form the second and the third multi-terminal network as depicted in Figure 6.2 and Figure 6.3.

In the multi-terminal network-1, the control strategy is applied to the GSVSCs. The voltage margin between the GSVSC-1 and the GSVSC-2 is fixed to 0.01 pu of the rated direct voltage which is slightly higher than the expected voltage drop between them. The direct voltage reference value for the GSVSC-1 is set to 1 pu whereas that for the GSVSC-2 is set to 1.01 pu. The proportional and the integral controller gains for the direct voltage controller are chosen such that the highest direct voltage rise during normal operation is below 1.05 pu. Subsequent to the addition of the third and the fourth GSVSC, these parameters will not be changed in order to show that the existing converters are capable of maintaining normal operation upon particular changes in the network topology i.e. addition of new converters.

For each simulation results, three important points will be the focus of the discussion. First is the performance of the control strategy in dispatching power among the onshore grids. Second is the reaction of the direct voltage in the offshore network. Third is the response of the control strategy to the reaction of the direct voltage. In some simulation results, where the direct voltage rises significantly high, the response of the dc chopper, the frequency modulation and the WPP rotor speed are observed and thus will also be included in the discussion.

6.2 Market dispatch

In this section, the capability of the control strategy to perform fixed and priority power sharing without communication is assessed. Collaboration between the control strategy and outer dispatch controller is applied for proportional power sharing. In order to have a clear picture on the performance of the control strategy and the response of the offshore

network, first, each of the market dispatch scheme will be presented exclusively one of the others. Next, the capability of the control strategy to perform altogether fixed and priority power sharing will be presented. Later, the collaboration between the control strategy and a supervisory dispatch controller to perform altogether the fixed and the proportional power sharing as well as to perform altogether the three market dispatch schemes will be shown. The case studies are listed in Table 6.1.

Table 6.1. Case studies for section 6.2

	Fixed power sharing	Priority power sharing	Fixed and priority power sharing	Proportional power sharing	Fixed and proportional power sharing	Fixed, priority and proportional power sharing
Test network-1	√	√		√	√	
Test network-2			√			
Test network-3						√

6.2.1 Fixed power sharing

Simulation scenario

Onshore grid-1 is scheduled to receive a fixed amount of power of 200 MW. The source of power delivered to the onshore grid-1 may from the WPPs or the onshore grid-2. Initially, GSVSC-1 delivers 200 MW fixed power to the onshore grid-1. WPPs deliver 100 MW to the offshore network and therefore GSVSC-2 injects 100 MW to the offshore network. GSVSC-2 controls the direct voltage at 1.01 pu. At 2s, power from WPPs increases to 150 MW. Power injected by GSVSC-2 decreases to 50 MW. At 6s, power from WPPs increases to 300 MW. GSVSC-2 now delivers 100 MW to the onshore grid-2.

Simulation results

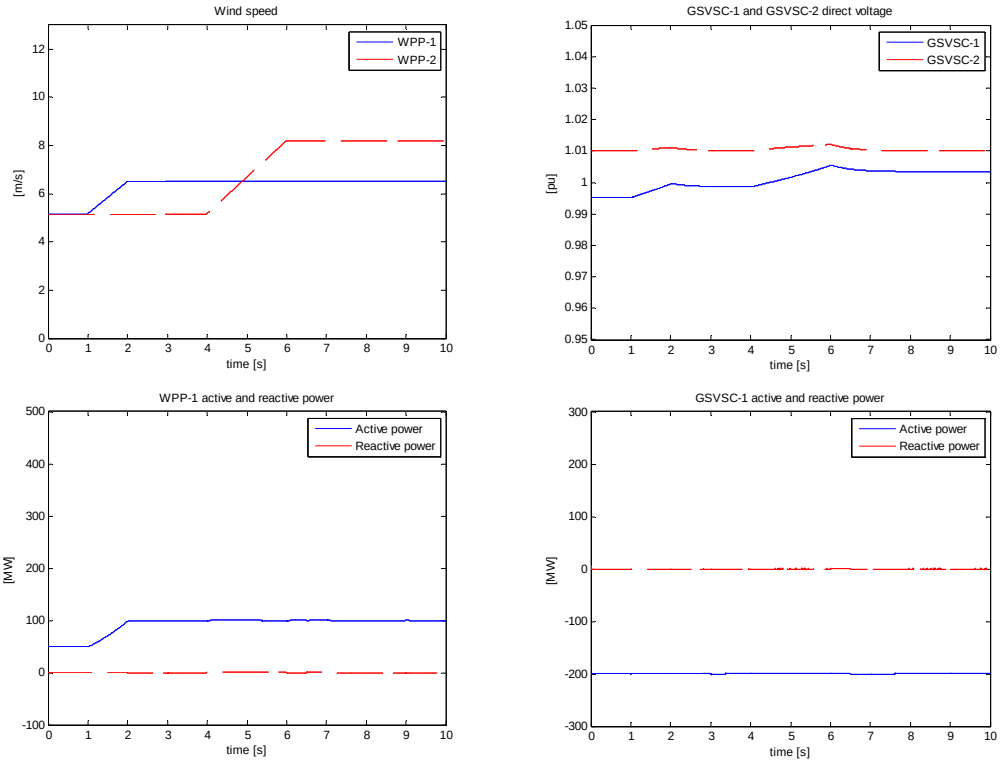

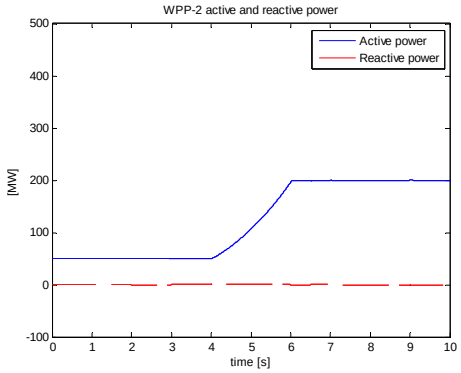

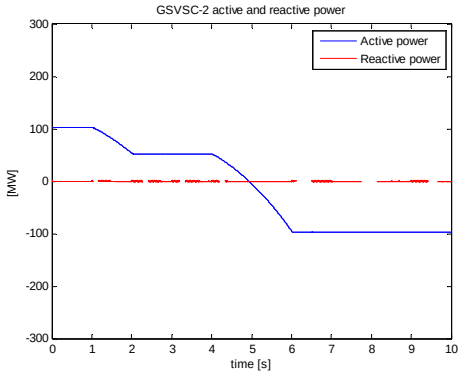

6.2.2 Priority power sharing

Simulation scenario

Power from WPPs is shared among two onshore grids in priority order. Onshore grid-1 is pre-scheduled to receive the first 200 MW. The excess power will be delivered to the onshore grid-2. Initially, WPPs deliver 100 MW to the offshore network and GSVSC-1 delivers 100 MW to the onshore grid-1. No power is delivered to the onshore grid-2. GSVSC-1 controls the direct voltage at 1.0 pu. At 2s, Power from WPPs increases to 150 MW. GSVSC-1 delivers 150 MW to the onshore grid-1. No power is delivered to the onshore grid-2. At 6s, Power from WPPs increases to 300 MW. GSVSC-1 reaches its power order limit (200 MW) and maintains 200 MW delivered to the onshore grid-1. GSVSC-2 now controls the direct voltage at 1.01 pu and delivers 100 MW to the onshore grid-2.

Simulation results

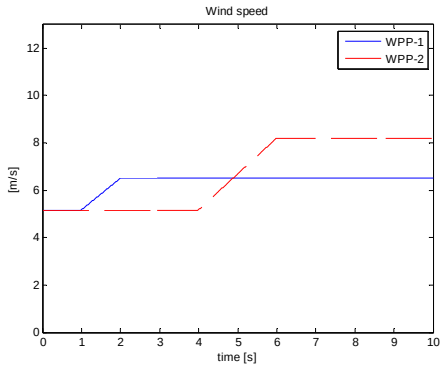

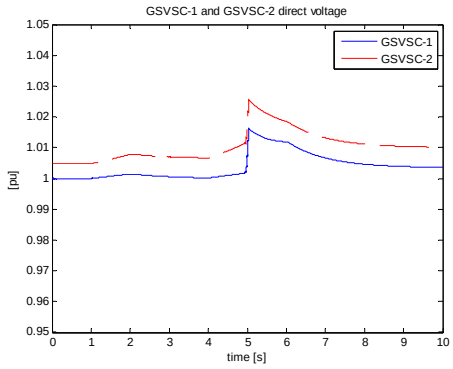

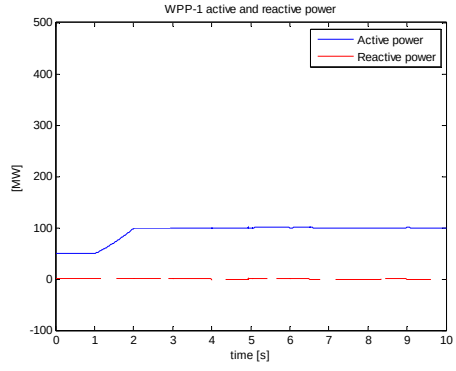

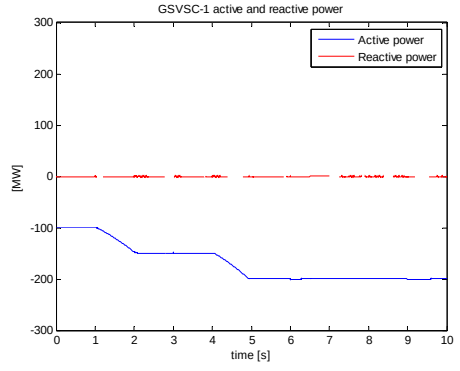

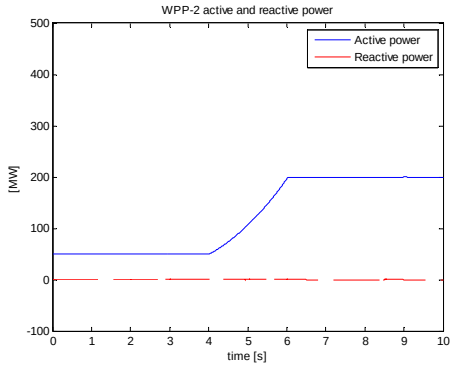

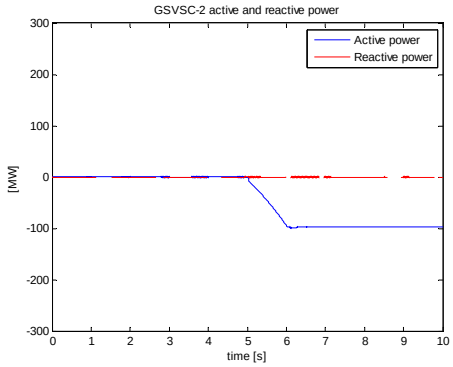

6.2.3 Fixed and priority power sharing

Simulation scenario

Onshore grid-1 is pre-scheduled to receive fixed power of 200 MW. The source of power delivered to the onshore grid-1 may from the WPPs or the onshore grid-2. The excess power from WPPs is shared to onshore grid-2 and 3 in priority order. Onshore grid-2 gets the first priority of the first 200 MW of the excess power. Initially, GSVSC-1 delivers 200 MW fixed power to the onshore grid-1. WPPs deliver 100 MW to the offshore network and therefore GSVSC-2 injects 100 MW to the offshore network. No power is delivered to onshore grid-3. GSVSC-2 controls the direct voltage at 1.01 pu. At 5s, Power from WPPs increases to 300 MW. GSVSC-2 delivers 100 MW to the onshore grid-2. At 8s, Power from WPPs increases to 500 MW. GSVSC-2 reaches its power order limit and GSVSC-3 now controls the direct voltage at 1.015 pu and delivers 100 MW to the onshore grid-3.

Simulation results

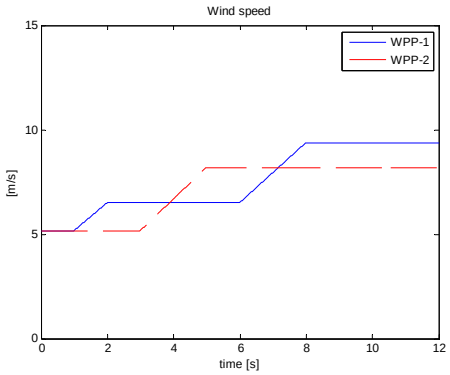

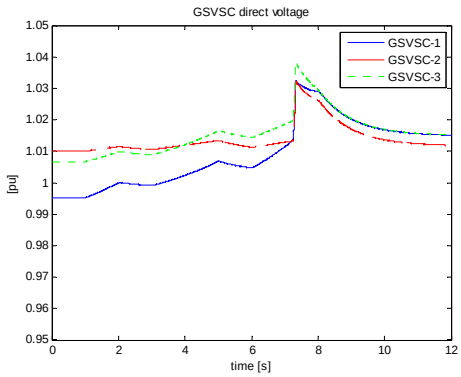

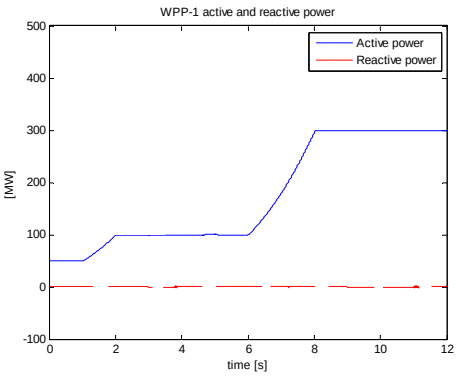

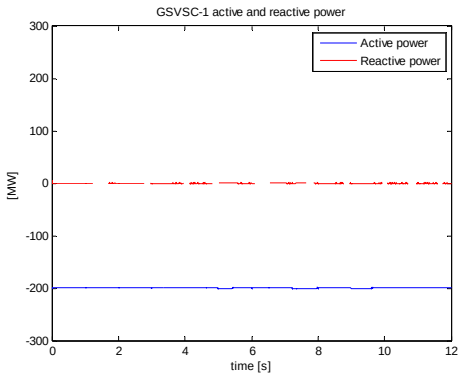

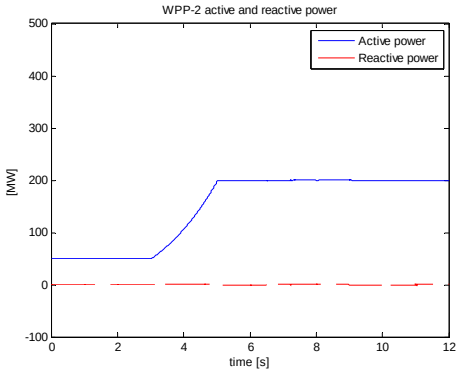

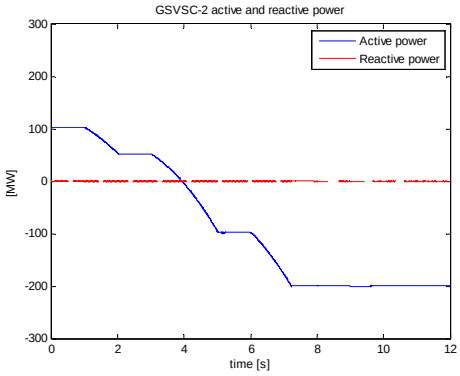

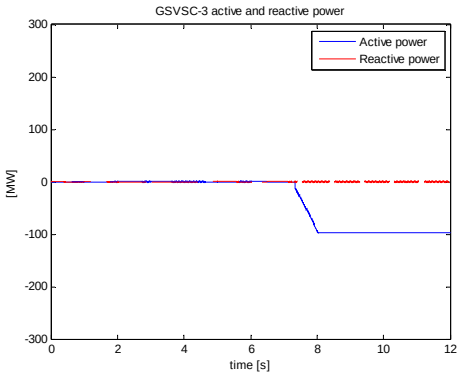

6.2.4 Proportional power sharing

Simulation scenario

Power from WPPs is shared among two onshore grids in proportion. Onshore grid-1 and onshore grid-2 are pre-scheduled to receive 75% and 25% of power from the WPPs respectively. Initially, the WPPs deliver 100 MW to the offshore network. Onshore grid-1 receives 75 MW while onshore grid-2 receives nearly 25 MW. GSVSC-1 has reached its power order limit (75 MW) and therefore GSVSC-2 controls the direct voltage at 1.01 pu. At 2s, WPPs deliver 150 MW to the offshore network. Onshore grid-1 receives 112.5 MW while onshore grid-2 receives nearly 37.5 MW. At 6s, the power from WPPs increases to 300 MW. Onshore grid-1 receives 225 MW while onshore grid-2 receives nearly 75 MW.

Simulation results

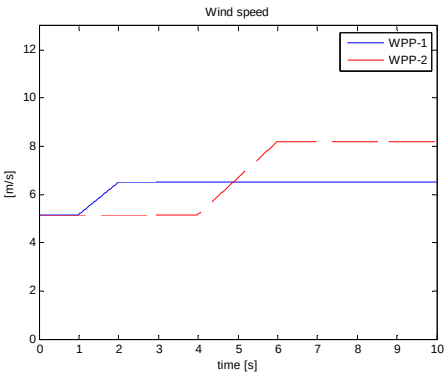

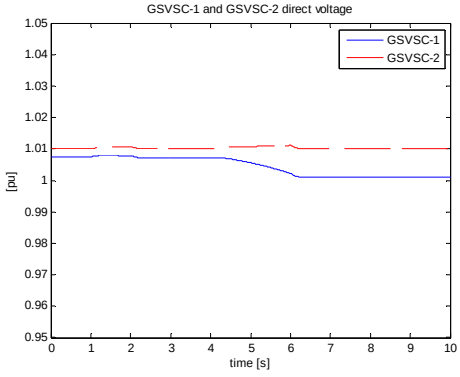

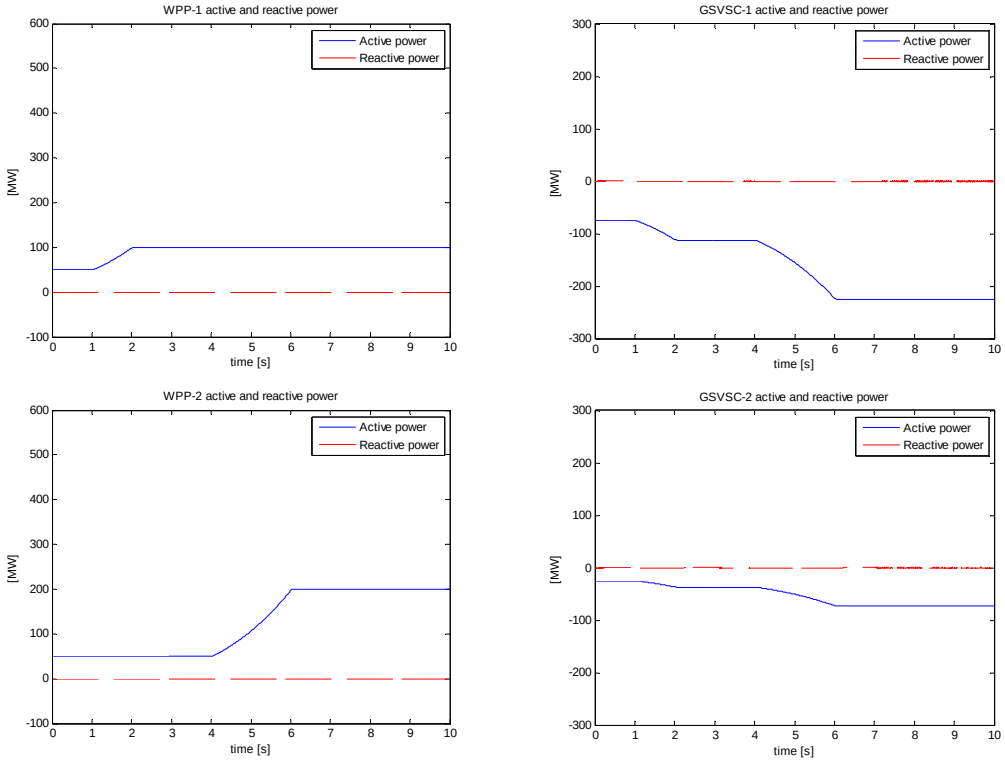

6.2.5 Fixed and proportional power sharing

Simulation scenario

When there is no power from the WPPs, the onshore grid-1 is scheduled to receive fixed power of 200 MW from the onshore grid-2. When there is power from the WPPs, the power is shared among the onshore grids in proportion. Onshore grid-1 and onshore grid-2 are scheduled to receive 75% and 25% of power from the WPPs. Initially, there is no power from the WPPs. GSVSC-1 delivers 200 MW fixed power to the onshore grid-1. GSVSC-2 injects 200 MW plus losses compensation to the offshore network. GSVSC-2 controls the direct voltage at 1.005 pu. At 3s, the WPPs deliver 100 MW to the offshore network. Onshore grid-1 now receives 200 MW from the onshore grid-1 plus 75 MW from the WPPs. GSVSC-2 injects to the offshore network 200 MW plus losses compensation minus 25 MW from the WPPs. At 7s, Power from the WPPs increases to 300 MW. Onshore grid-1 now receives 200 MW from the onshore grid-1 plus 225 MW from the WPPs. GSVSC-2 injects to the offshore network 200 MW plus losses compensation minus 75 MW from the WPPs.

Simulation results

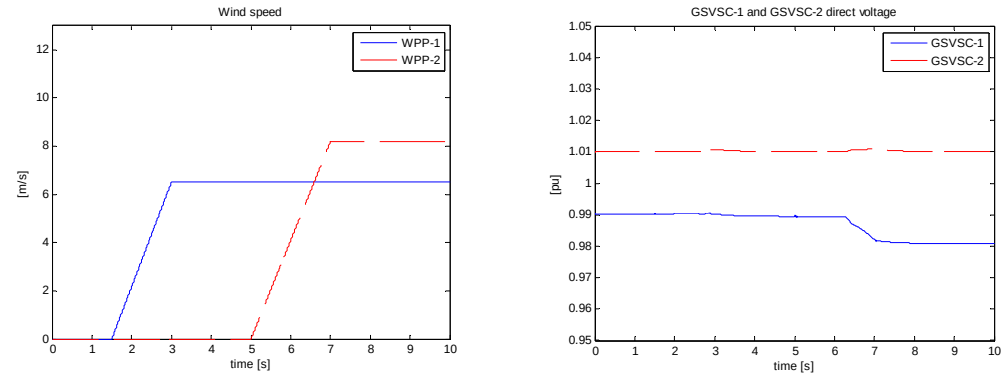

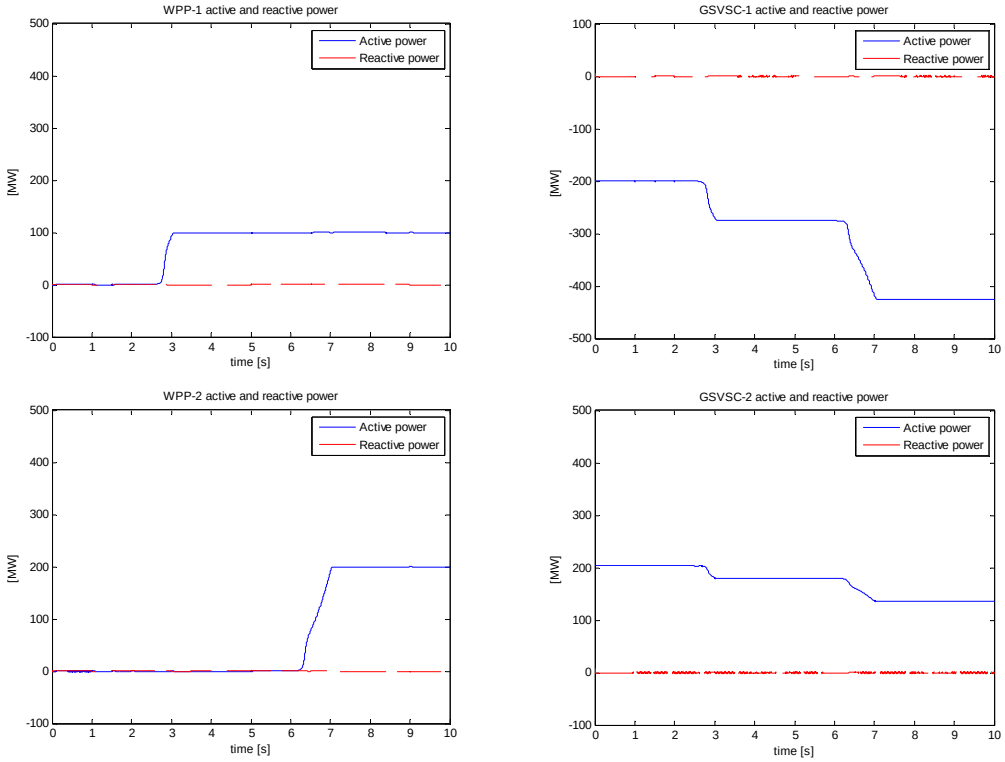

6.2.6 Fixed, priority and proportional power sharing

Simulation scenario

Onshore grid-1 is pre-scheduled to receive fixed power of 200 MW. The source of power delivered to the onshore grid-1 may from the WPPs or the onshore grid-2. The excess power from WPPs is shared to the other onshore grids in priority order. Onshore grid-2 gets the first priority of the first 200 MW of the excess power. The second priority is given to the onshore grid-3 and 4. Between the onshore grid-3 and 4, the power is shared in proportion 3:1. Initially, GSVSC-1 delivers 200 MW fixed power to the onshore grid-1. WPPs deliver 100 MW to the offshore network and therefore GSVSC-2 injects 100 MW to the offshore network. No power is delivered to onshore grid-3 and 4. GSVSC-2 controls the direct voltage at 1.005 pu. At 5s, power from WPPs increases to 300 MW. GSVSC-2 delivers 100 MW to the onshore grid-2. At 8s, power from WPPs increases to 500 MW. GSVSC-2 has reached its power order limit (200 MW). Power from WPPs is now shared between GSVSC-3 and GSVSC-4 in proportion 3:1. GSVSC-3 delivers 75 MW to the onshore grid-3 and GSVSC-4 delivers 25 MW to the onshore grid-4. GSVSC-3 now controls the direct voltage at 1.01 pu.

Simulation results

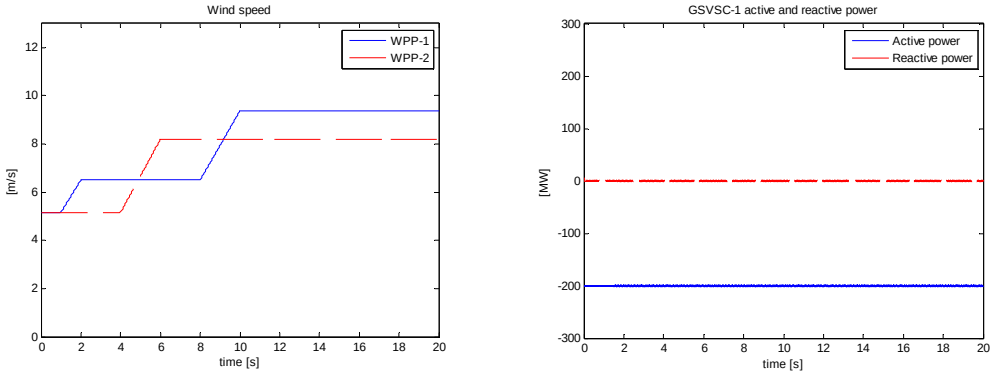

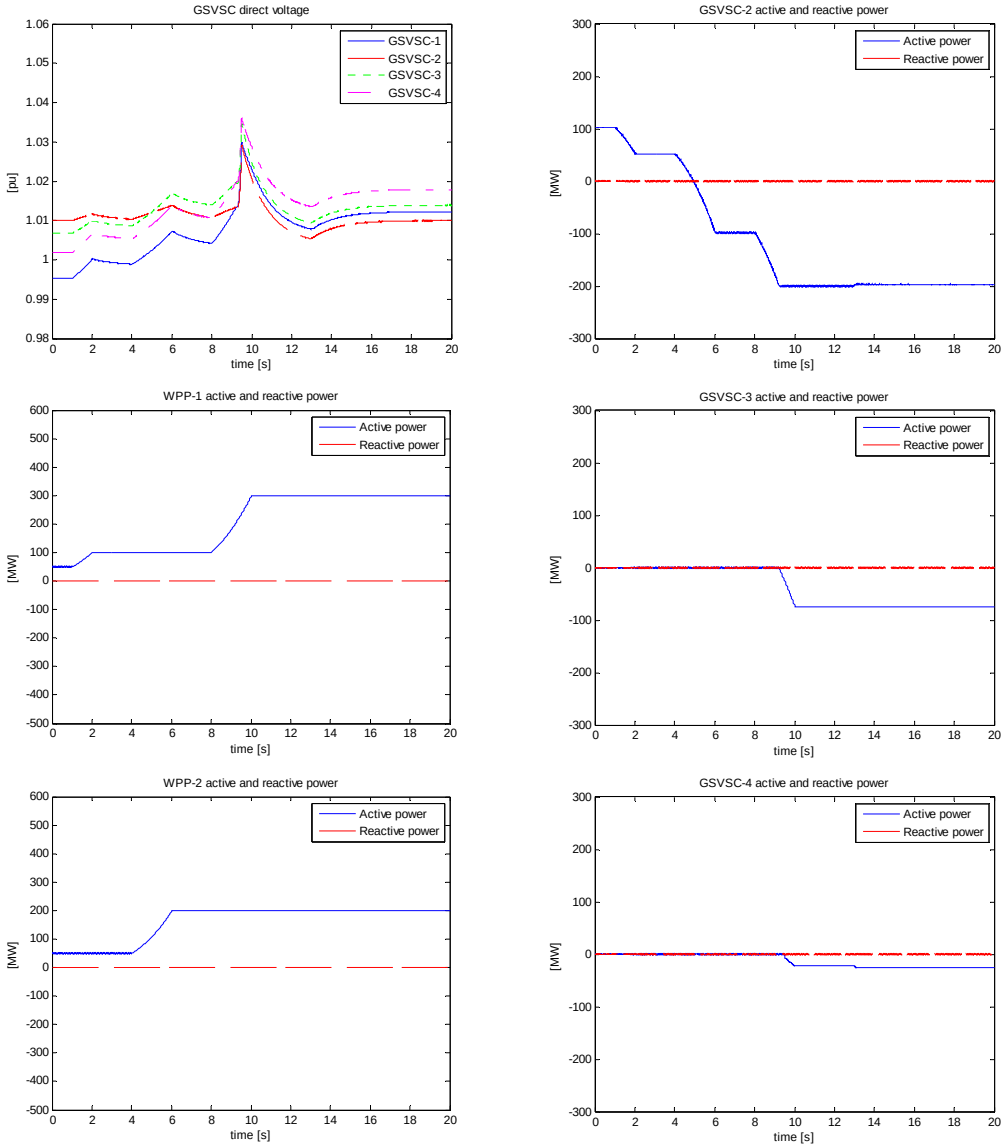

6.3 Loss of an onshore converter

Here, multi-terminal network-1 is used. The capability of the VMM to interchangeably control the direct voltage upon loosing a direct voltage controlling converter will be examined. Each of the three market dispatch schemes will be implemented exclusively as the initial condition. Both of the FRT methods will not be implemented in order to clearly see the response of the control strategy. For each of the market dispatch schemes, event of loosing one of the GSVSC will be presented. The case studies are listed in Table 6.2.

Table 6.2. Case studies for section 6.3

	Fixed power sharing		Priority power sharing	Proportional power sharing
	GSVSC-2 delivers power to the onshore grid-2	GSVSC-2 injects power to the offshore network		
Loss of GSVSC-1	X	X	X	X
Loss of GSVSC-2	√	√	√	√

In the following sections, only the interesting cases (pointed by √ in Table 6.3) will be presented. The rest of the cases (pointed by X in Table 6.3) are shown in Appendix A.1.

6.3.1 Fixed power sharing

Case A: GSVSC-2 injects power to the offshore network; Loss of GSVSC-2

Simulation scenario

Initially, GSVSC-1 delivers 200 MW fixed power to the onshore grid-1. The WPPs deliver 100 MW to the offshore network and GSVSC-2 injects 100 MW to the offshore network. GSVSC-2 controls the direct voltage at 1.01 pu. At 1s, GSVSC-2 suddenly disconnects and thus direct voltage drops. The direct voltage drops lower than 0.98 pu and thus triggers the VMM in GSVSC-1 to adjust its power limit to the lower stage and therefore power delivered to onshore grid-1 is reduced. GSVSC-1 now controls the direct voltage and brings the direct voltage to 0.98 pu.

Simulation results

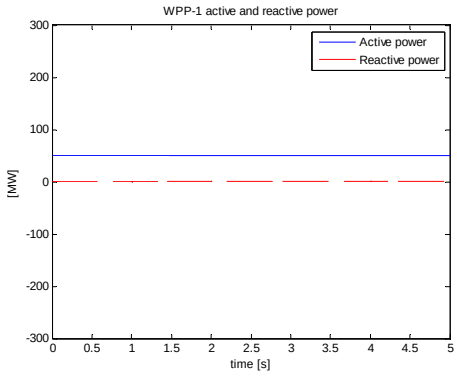

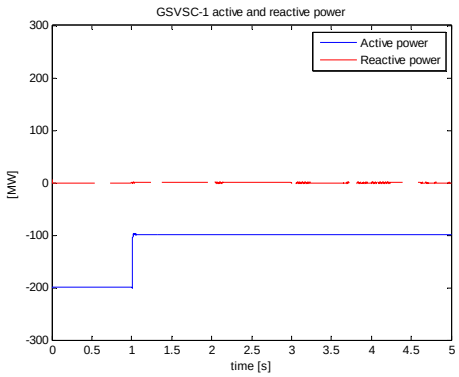

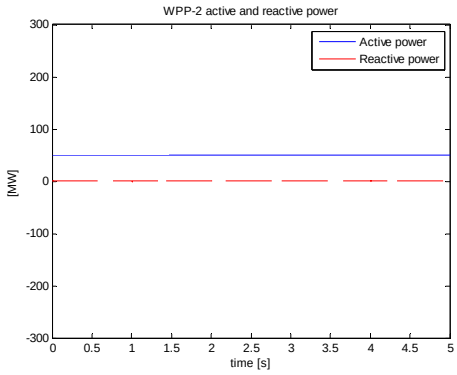

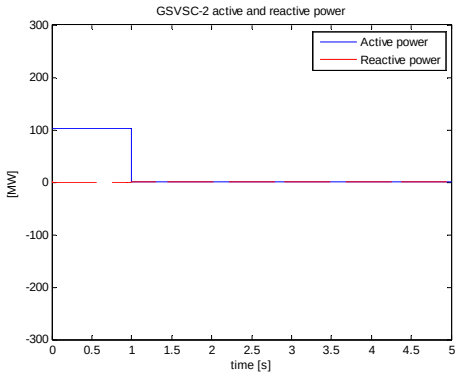

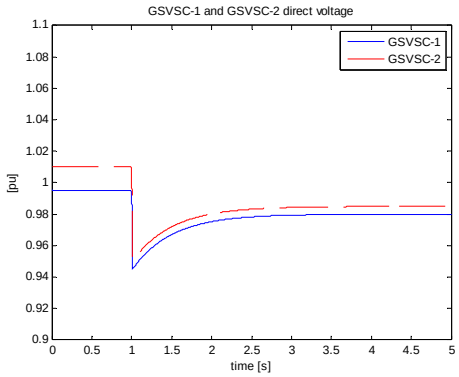

Case B: GSVSC-2 delivers power to the onshore grid-2; Loss of GSVSC-2

Simulation scenario

Initially, GSVSC-1 delivers 200 MW fixed power to onshore grid-1. The WPPs deliver 300 MW to the offshore network and thus GSVSC-2 transfers 100 MW to the onshore grid-2. GSVSC-2 controls the direct voltage at 1.01 pu. At 1s, GSVSC-2 suddenly trips and thus direct voltage rises. The direct voltage rises higher than 1.02 pu and thus triggers the VMM in GSVSC-1 to adjust its power limit to the higher stage and therefore power delivered to onshore grid-1 is elevated. GSVSC-1 now controls the direct voltage and brings the direct voltage to 1.02 pu.

Simulation results

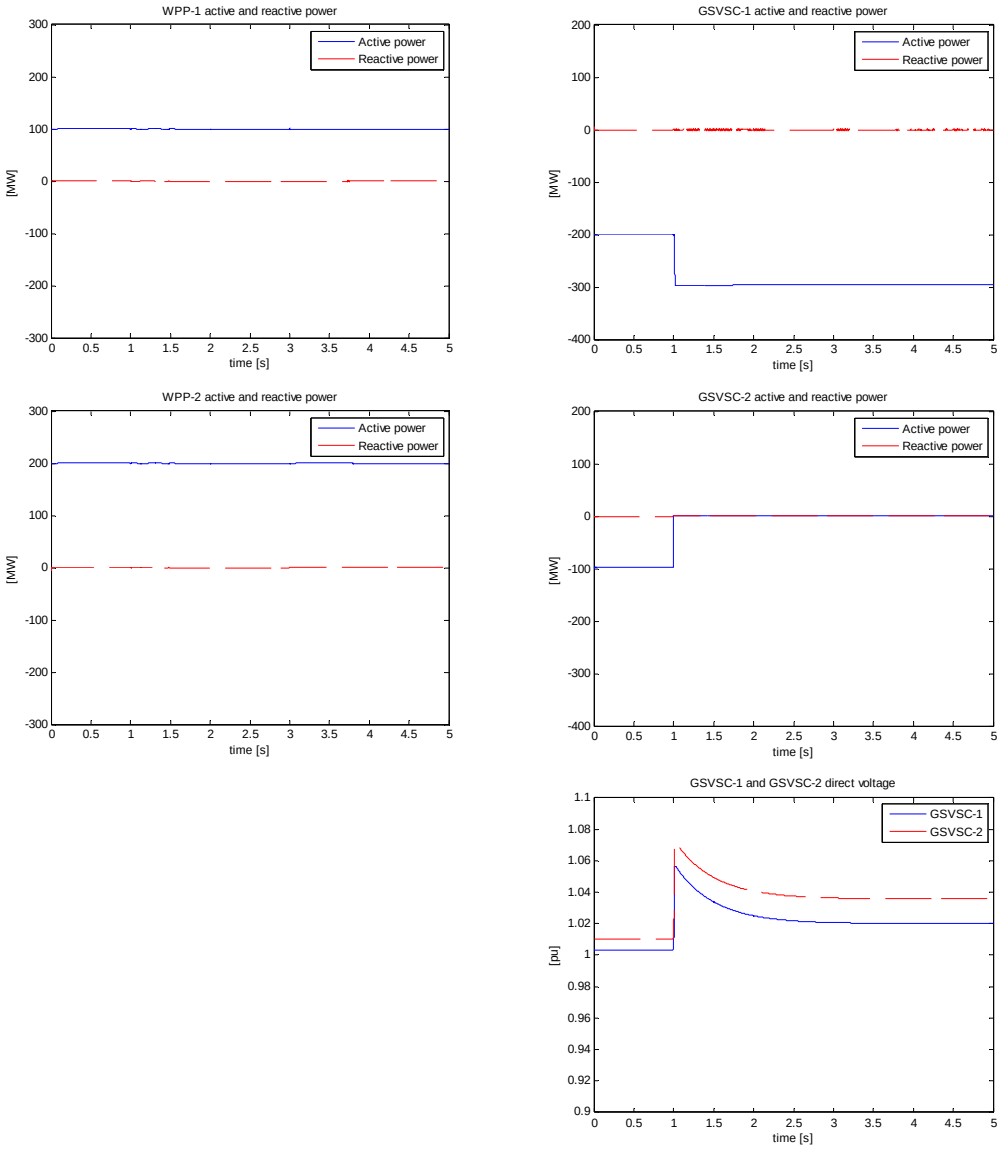

6.3.2 Priority power sharing

Case A: Loss of GSVSC-2

Simulation scenario

Initially, the WPPs deliver 300 MW to the offshore network. GSVSC-1 is pre-scheduled to have the first priority to transfer up to 200 MW to the onshore grid-1 and therefore now

it transfers 200 MW to the onshore grid-1. Since GSVSC-1 has reached its set power limit, GSVSC-2 controls the direct voltage at 1.01 pu. GSVSC-2 delivers 100 MW to the onshore grid-2. At 1s, GSVSC-2 is suddenly disconnected and thus the direct voltage rises. It rises higher than 1.02 pu and thus triggers the VMM in GSVSC-1 to adjust its power limit to the higher stage and therefore power delivered to onshore grid-1 is elevated. GSVSC-1 now controls the direct voltage and brings the direct voltage to 1.02 pu.

Simulation results

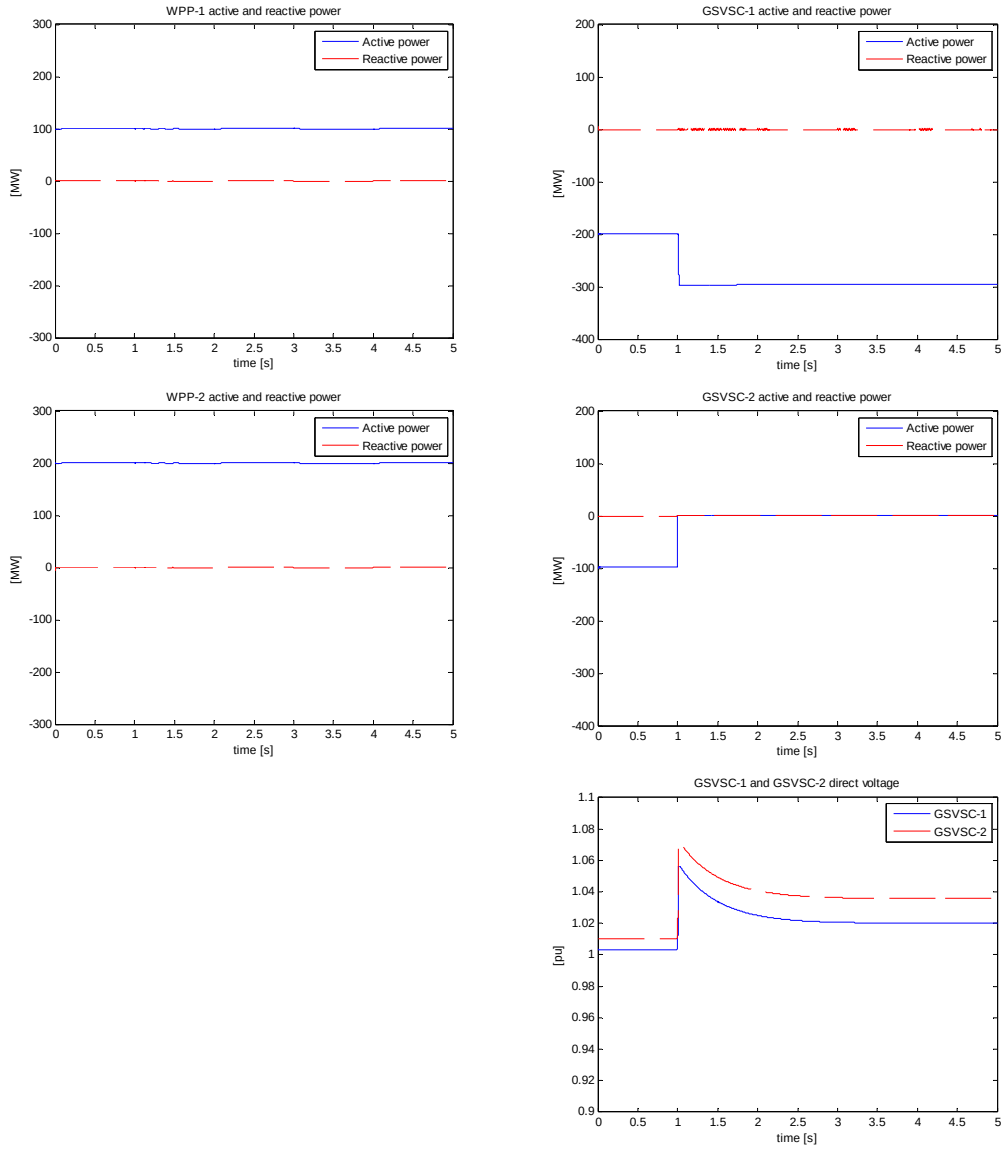

6.3.3 Proportional power sharing

Case A: Loss of GSVSC-2

Simulation scenario

Initially, the WPPs deliver 100 MW to the offshore network. GSVSC-1 transfers 75 MW to the onshore grid-1 and GSVSC-2 transfers nearly 25 MW to the onshore grid-2 regarding proportional power sharing 3:1. Since GSVSC-1 has reached its preset power limit, GSVSC-2 controls the direct voltage at 1.01 pu. At 1s, GSVSC-2 is suddenly disconnected and thus direct voltage rises. Direct voltage which rises higher than 1.02 pu

and thus triggers the VMM in GSVSC-1 to adjust its power limit to the higher stage and therefore power delivered to onshore grid-1 is elevated. GSVSC-1 now controls the direct voltage and brings the direct voltage to 1.02 pu.

Simulation results

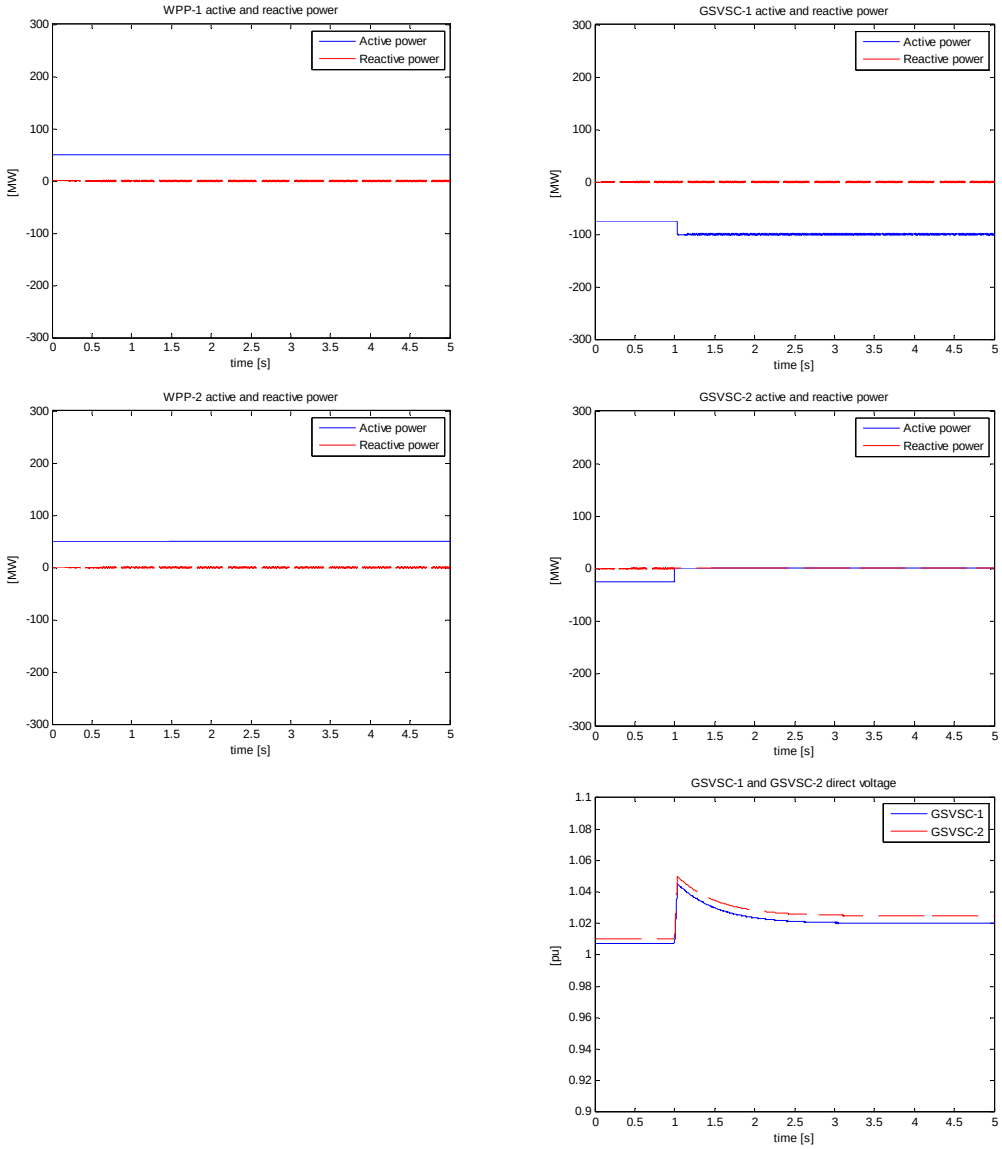

6.4 Fault ride-through

In this section, the multi-terminal network-1 is used and two fault ride-through (FRT) methods are be applied i.e. energy dissipation method by a dc chopper and the WPP grid frequency modulation method. Each of the three market dispatch schemes will be implemented exclusively as the initial condition and voltage dip will be applied at each of the onshore grids. In order to study the influence of onshore grid coupling, the scenario will be implemented for situation where the onshore grids are coupled or not coupled. The case studies are listed in Table 6.3.

In the following sections, only the cases where the onshore grid are not coupled (pointed by √ in Table 6.3) will be presented. The rest of the cases (pointed by X in Table 6.3) are shown in Appendix A.2.

Table 6.3. Case studies for section 6.4

		Fixed power sharing		Priority power sharing	Proportional power sharing
		GSVSC-2 delivers power to the onshore grid-2	GSVSC-2 injects power to the offshore network		
No onshore grid coupling	Voltage dip at onshore grid-1	√	√	√	√
	Voltage dip at onshore grid-2	√	√	√	√
Onshore grid coupled	Voltage dip at onshore grid-1	X	X	X	X
	Voltage dip at onshore grid-2	X	X	X	X

6.4.1 FRT with fixed power sharing

Case A: GSVSC-2 injects power to the offshore network; voltage dip at onshore grid-1

Simulation scenario

Initially, the WPPs deliver 200 MW to the offshore network. GSVSC-1 transfers 400 MW to the onshore grid-1 while GSVSC-2 injects 200 MW to the offshore network. At 0.1s, Voltage dip of 1 pu occurs at onshore grid-1 for 150 ms. Due to direct voltage rises, GSVSC-2 quickly changes its power direction. Neither the dc choppers nor the frequency increase method is triggered. At 0.25s, voltage at onshore grid-1 is back to its nominal. GSVSC-2 quickly restores its power direction.

Simulation results

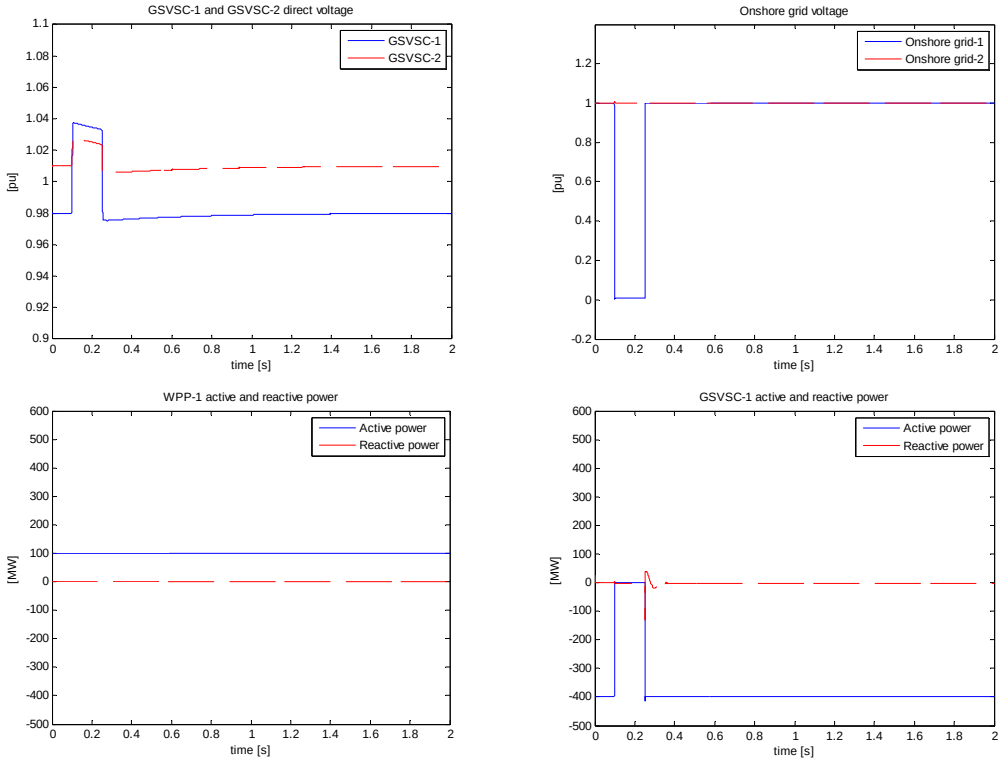

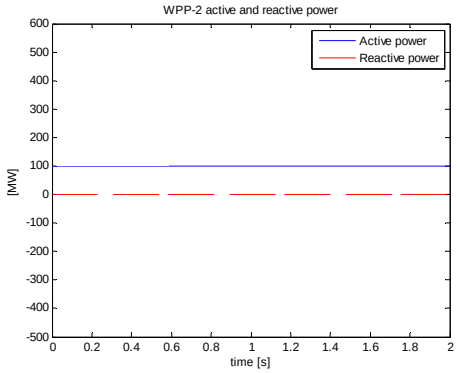

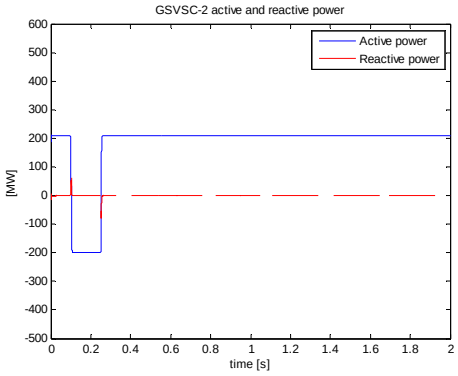

Case B: GSVSC-2 delivers power to the onshore grid-2; voltage dip at onshore grid-1

Simulation scenario

Initially, the WPPs deliver 800 MW to the offshore network. GSVSC-1 transfer 400 MW to the onshore grid-1 and GSVSC-2 transfer 400 MW to the onshore grid-2. At 0.1s, a voltage dip of 1 pu occurs at onshore grid-1 for 150 ms. Dc choppers and frequency increase method successfully work to dissipate the excess power on the offshore network and maintains direct voltage below 1.2 pu at both GSVSC-1 and GSVSC-2.

Simulation results

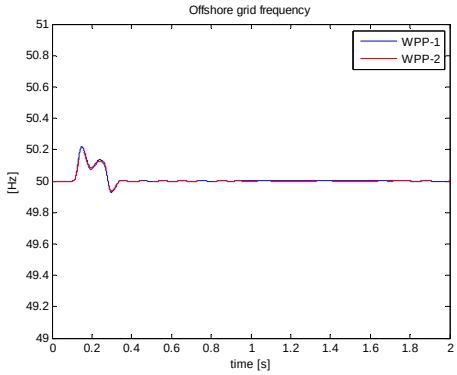

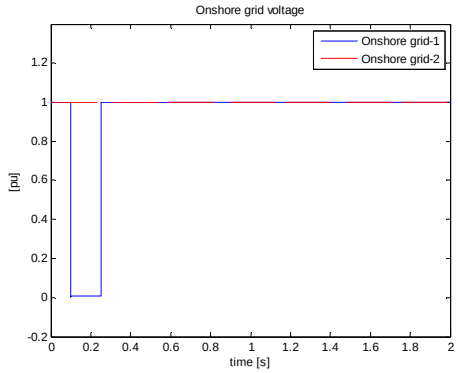

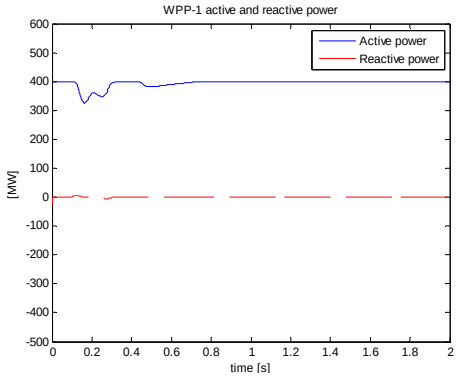

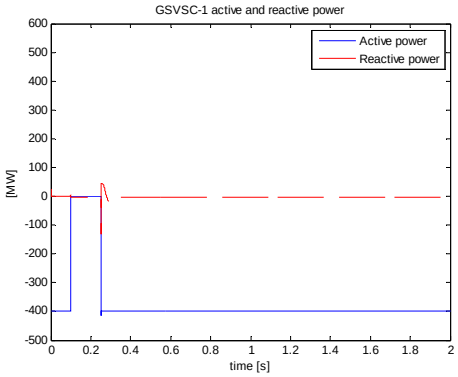

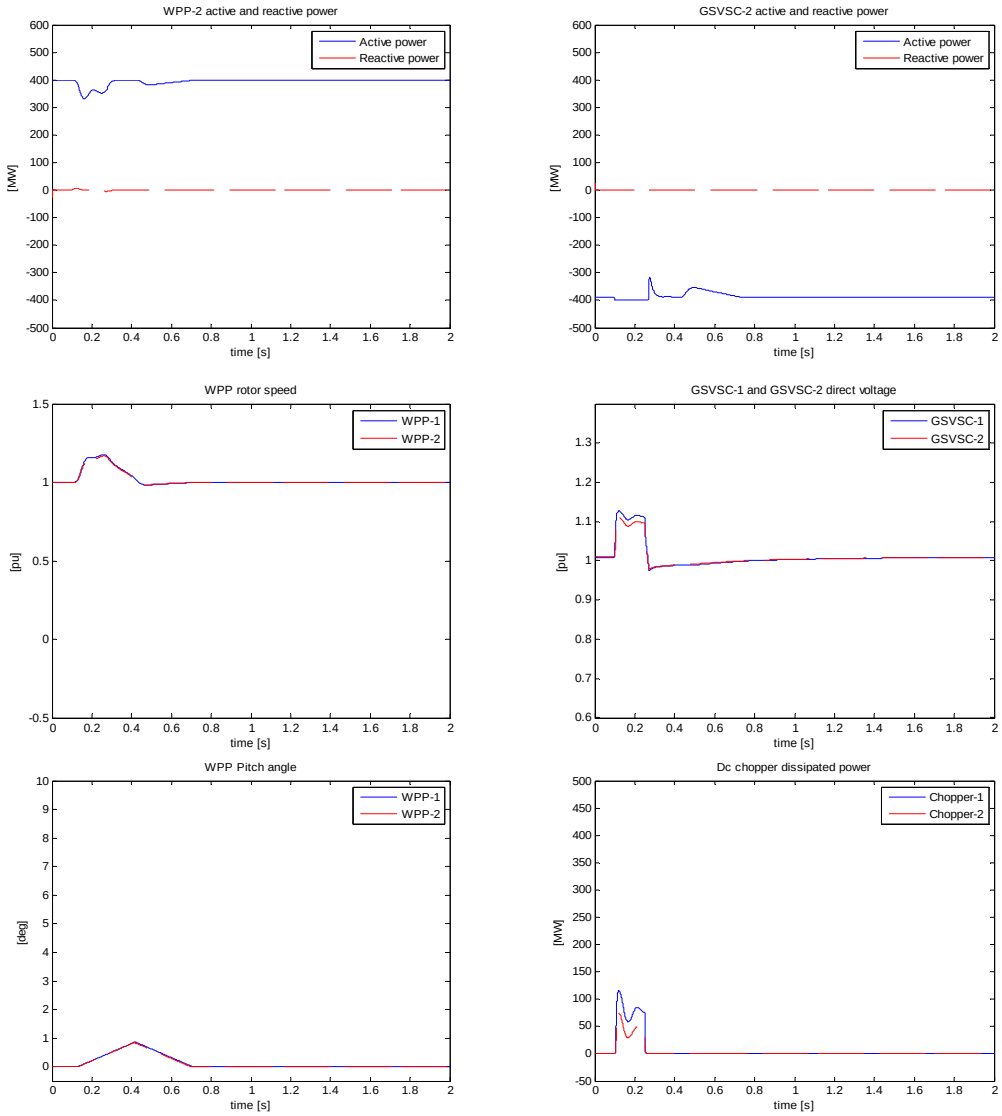

Case C: GSVSC-2 injects power to the offshore network; voltage dip at onshore grid-2

Simulation scenario

Initially, the WPPs deliver 200 MW to the offshore network. GSVSC-1 transfers 400 MW to the onshore grid-1 while GSVSC-2 injects 200 MW to the offshore network. At 0.1s, Voltage dip of 1 pu occurs at onshore grid-2 for 150 ms. This causes GSVSC-2 can not inject power to the offshore network and thus direct voltage drops. Due to direct voltage drops, GSVSC-1 quickly reduces power transferred to the onshore grid-1. Neither dc choppers nor frequency increase method is triggered. At 0.25s, Voltage at onshore grid-2 is back to its nominal. Power injected to the offshore network by GSVSC-2 rises very quickly to restore the direct voltage. As the direct voltage recovers, power transferred to the onshore grid-1 returns to the pre-fault value.

Simulation results

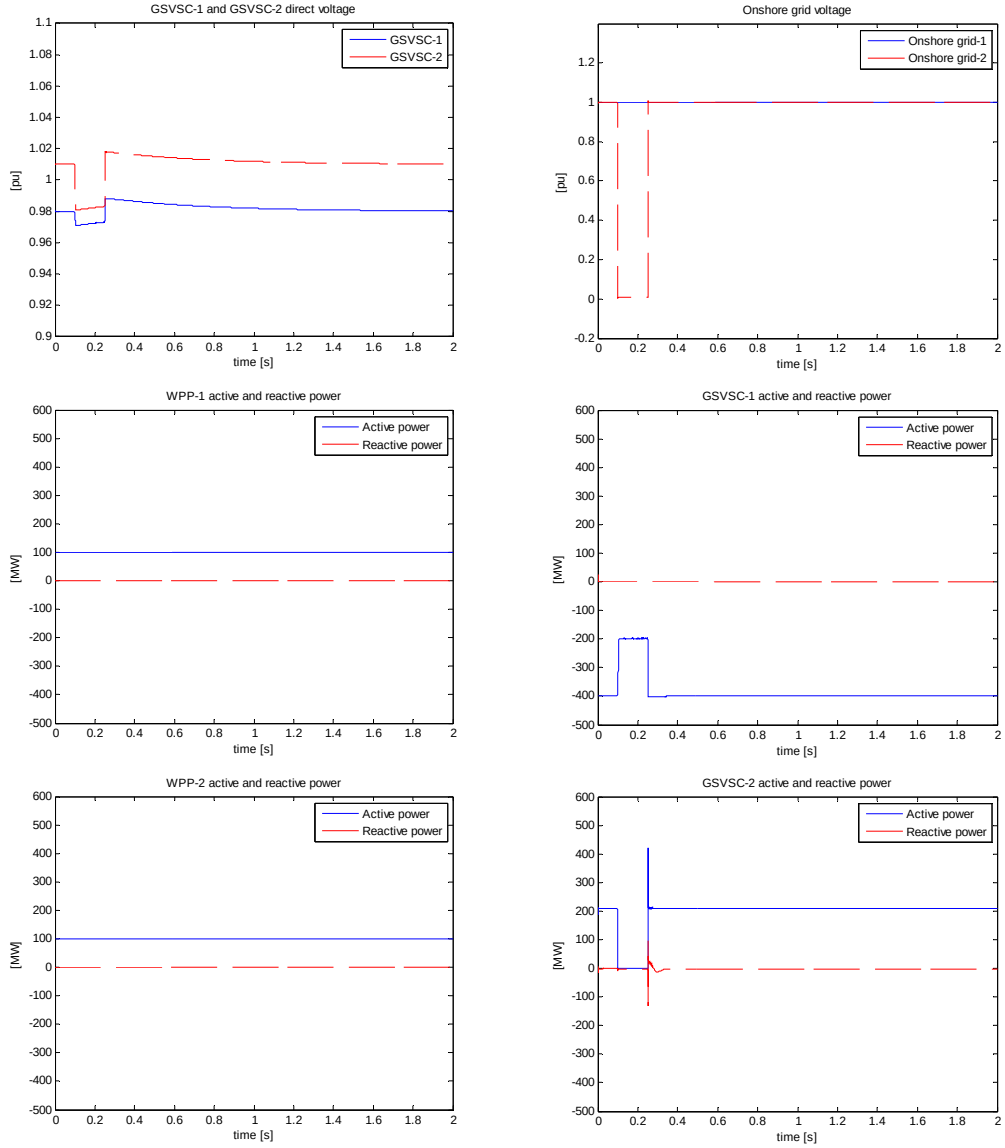

Case D: GSVSC-2 delivers power to the onshore grid-2; voltage dip at onshore grid-2

Simulation scenario

Initially, the WPPs deliver 800 MW to the offshore network. GSVSC-1 transfer 400 MW to the onshore grid-1 and GSVSC-2 transfer 400 MW to the onshore grid-2. At 0.1s, voltage dip of 1 pu occurs at onshore grid-2 for 150 ms. The dc choppers and frequency increase method successfully work in order to dissipate the excess power in the offshore network and to maintain the direct voltage below 1.2 pu at both GSVSC-1 and GSVSC-2.

Simulation results

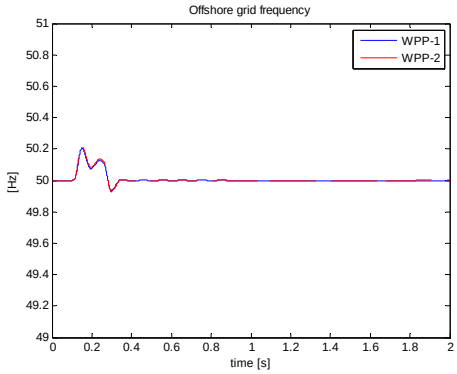

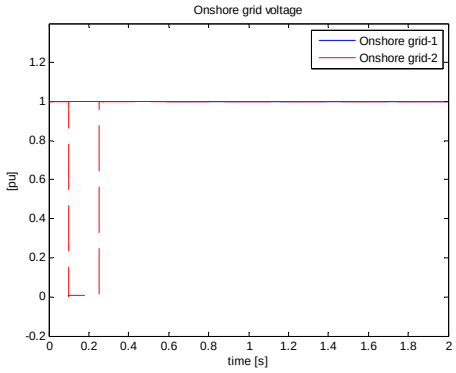

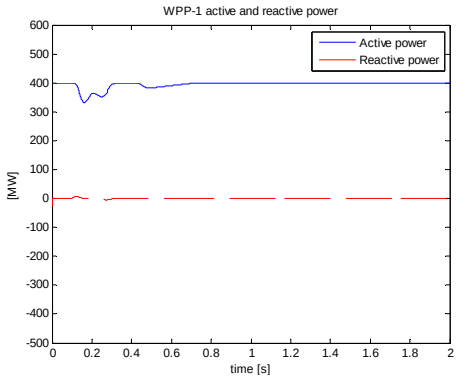

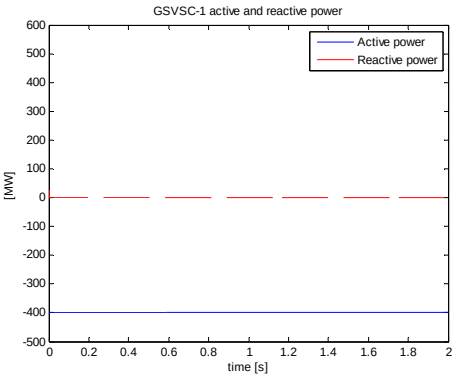

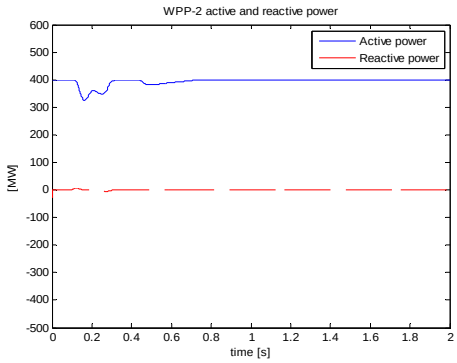

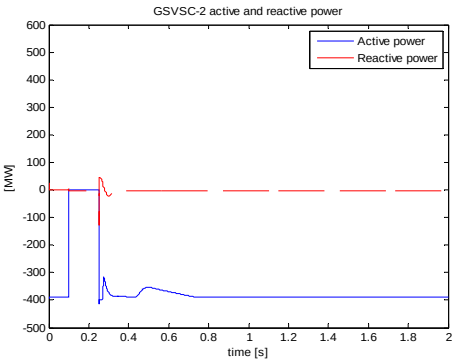

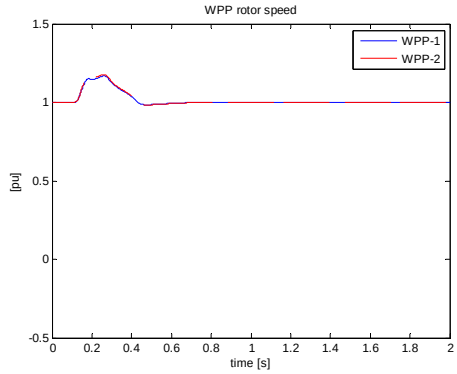

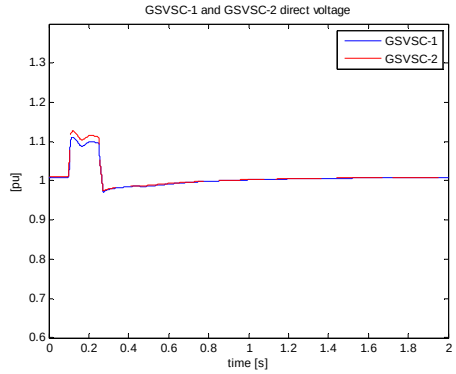

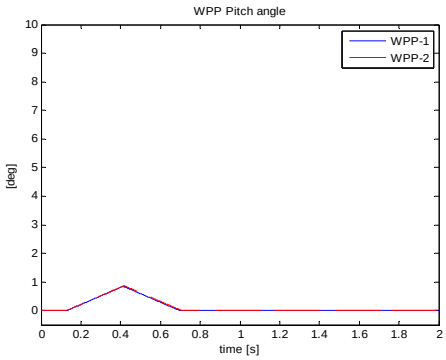

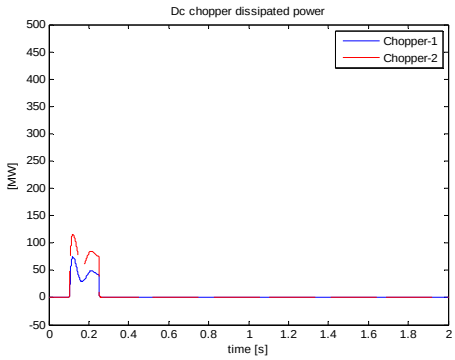

6.4.2 FRT with priority power sharing

Case A: Voltage dip at onshore grid-1

Simulation scenario

Initially, the WPPs deliver 800 MW to the offshore network. GSVSC-1 transfer 400 MW to the onshore grid-1 and GSVSC-2 transfer 400 MW to the onshore grid-2. At 0.1s, voltage dip of 1 pu occurs at onshore grid-1 for 150 ms. Dc choppers and frequency increase method successfully work to dissipate the excess power on the offshore network and maintains direct voltage below 1.2 pu at both GSVSC-1 and GSVSC-2.

Simulation results

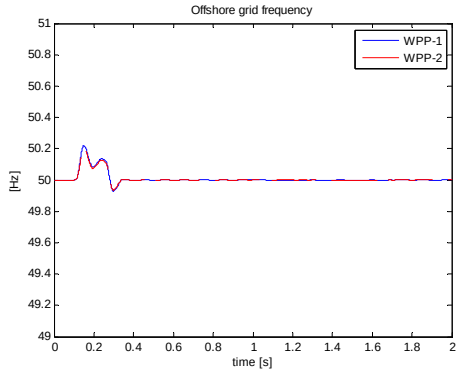

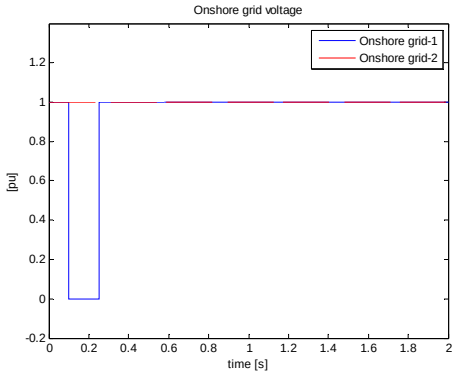

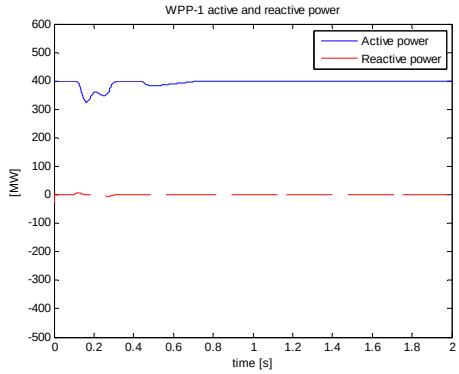

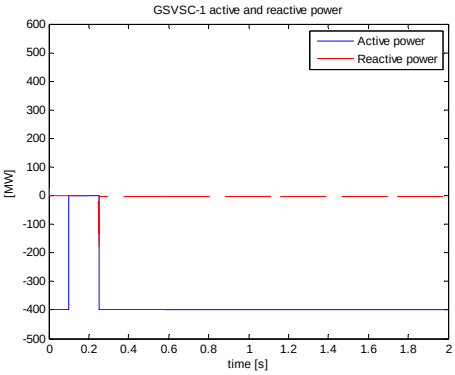

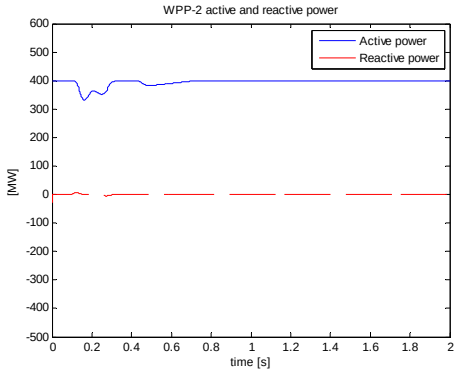

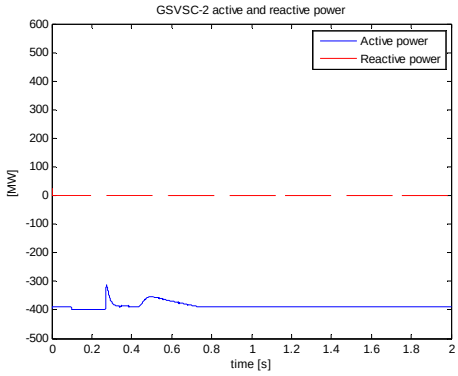

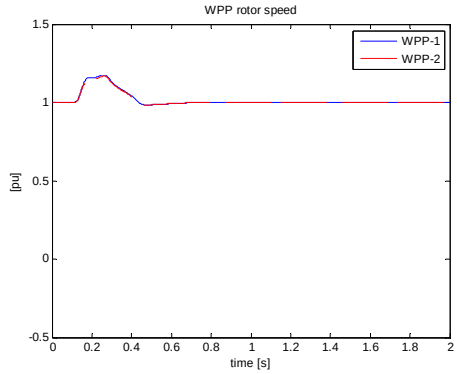

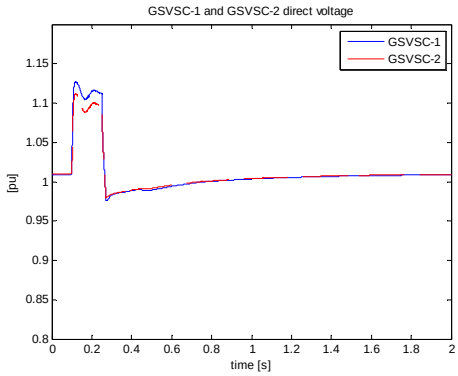

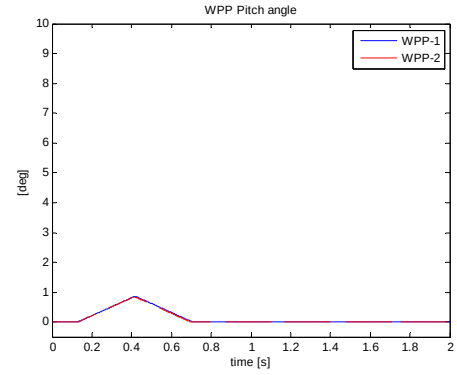

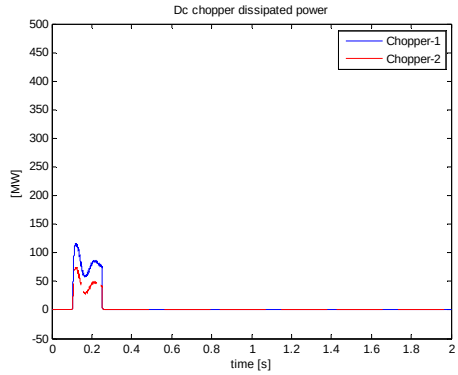

Case B: Voltage dip at onshore grid-2

Simulation scenario

Initially, the WPPs deliver 800 MW to the offshore network. GSVSC-1 transfer 400 MW to the onshore grid-1 and GSVSC-2 transfer 400 MW to the onshore grid-2. At 0.1s, Voltage dip 1 pu occurs at onshore grid-2 for 150 ms. The protection equipment successfully maintain thedirect voltage below 1.2 pu at both GSVSC-1 and GSVSC-2.

Simulation results

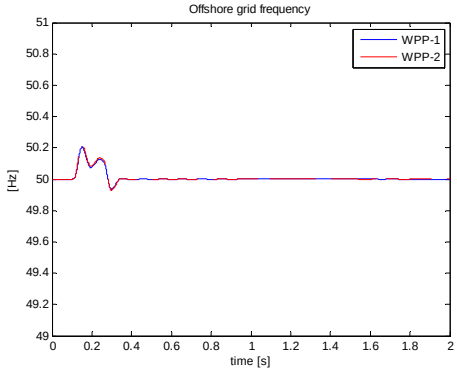

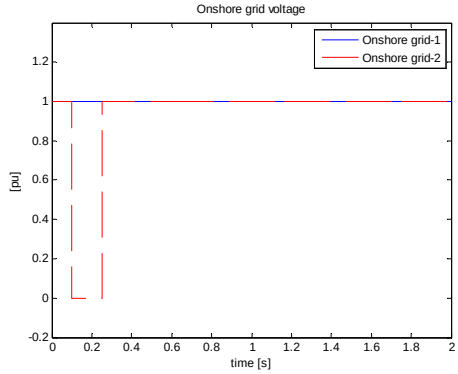

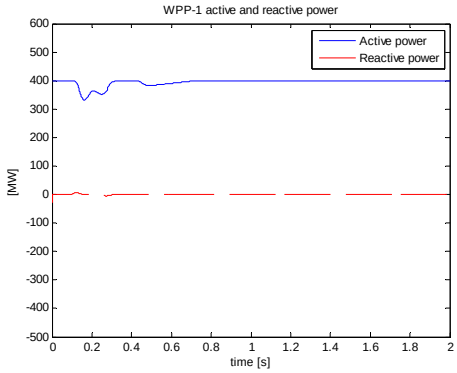

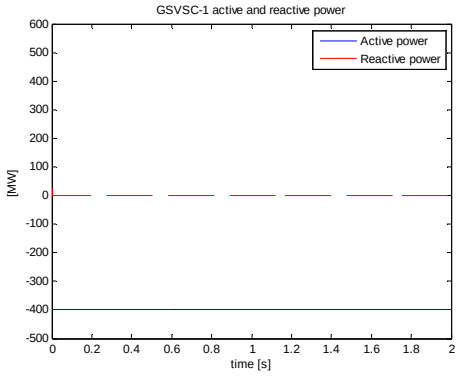

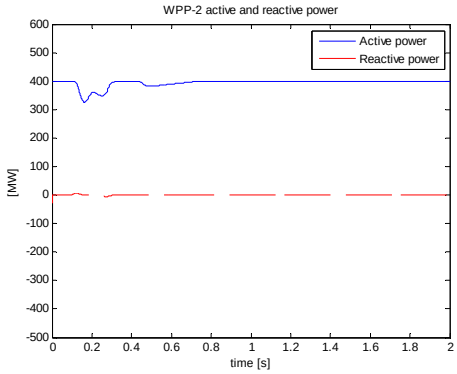

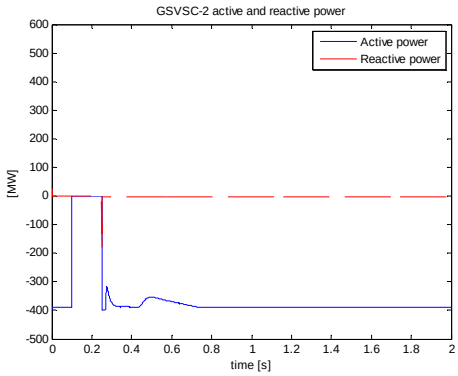

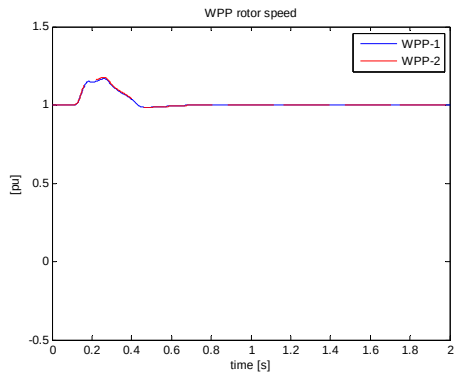

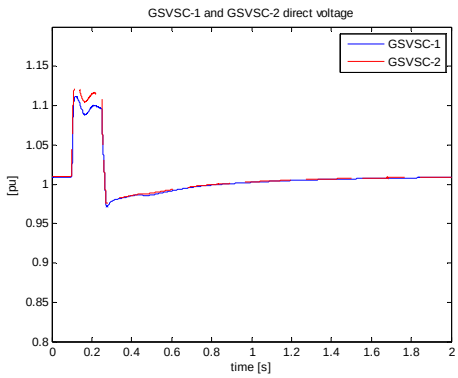

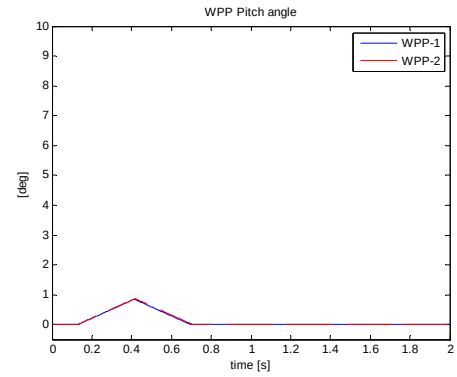

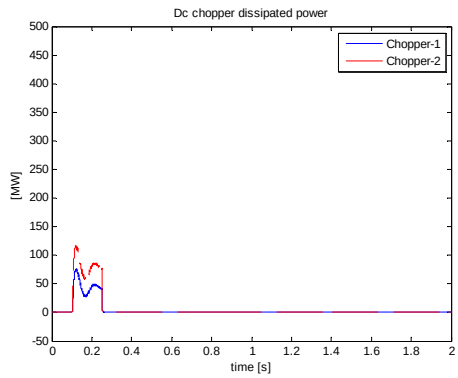

6.4.3 FRT with proportional power sharing

Case A: Voltage dip at onshore grid-1

Simulation scenario

Initially, the WPPs deliver 400 MW to the offshore network. GSVSC-1 transfers 300 MW to the onshore grid-1 and GSVSC-2 transfers 100 MW to the onshore grid-2 regarding proportional power sharing 3:1. At 0.1s, a 0.1 pu voltage dip occurs at onshore

grid-1 for 150 ms. Due to the voltage dip, GSVSC-1 can not transfer power to the onshore grid-1 and thus direct voltage rises. Direct voltage increases higher than 1.01 pu and thus triggers the VMM in GSVSC-2 to adjust its power limit to the higher stage and therefore power delivered to onshore grid-2 elevated. dc choppers and the frequency increase method successfully work to dissipate the excess power on the offshore network and maintain direct voltage below 1.2 pu at both GSVSC-1 and GSVSC-2. At 0.25s, voltage at onshore grid-1 is back to its nominal and power delivered to onshore grid-1 is restored quickly. As power delivered to onshore grid-1 is restored, direct voltage returns to its pre-fault value and so does the power transferred to onshore grid-2.

Simulation results

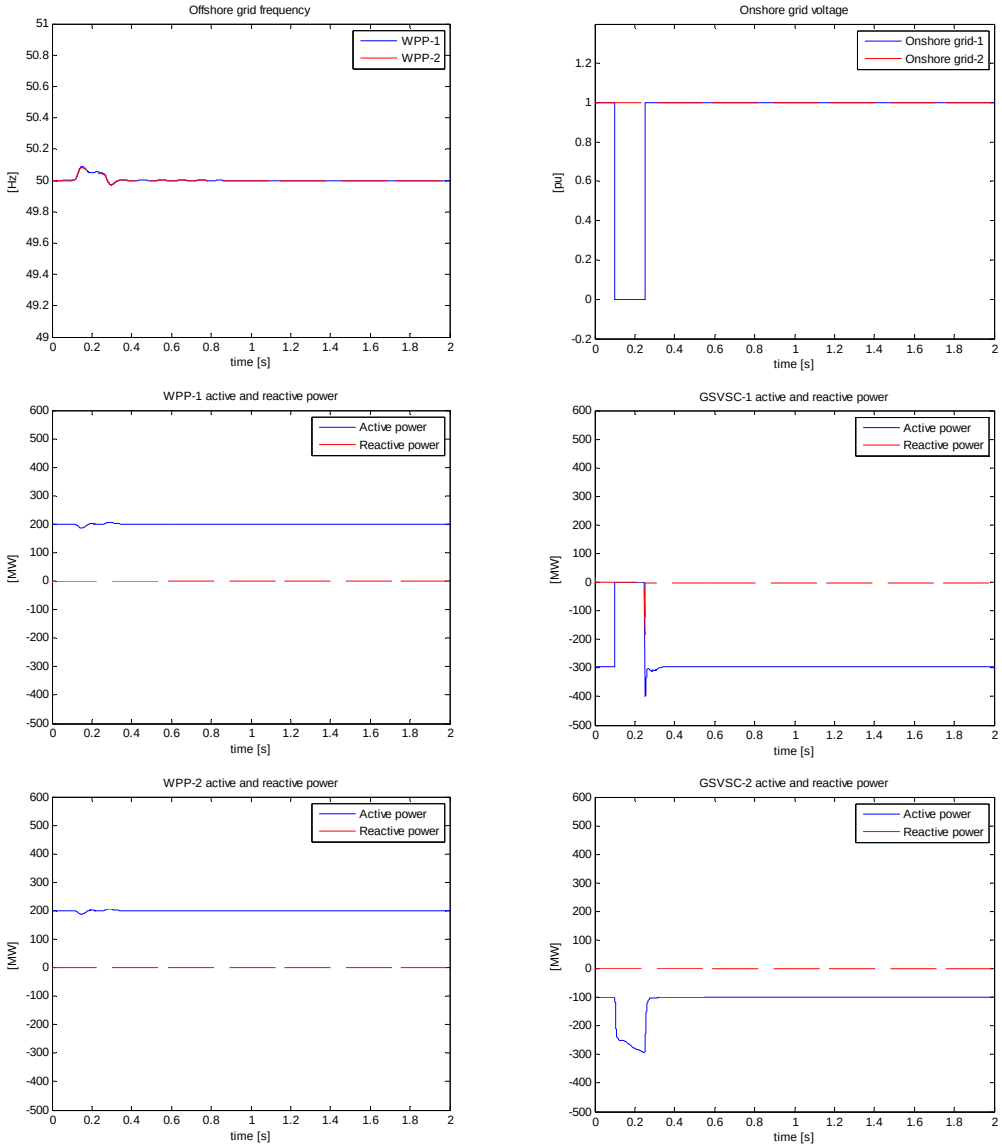

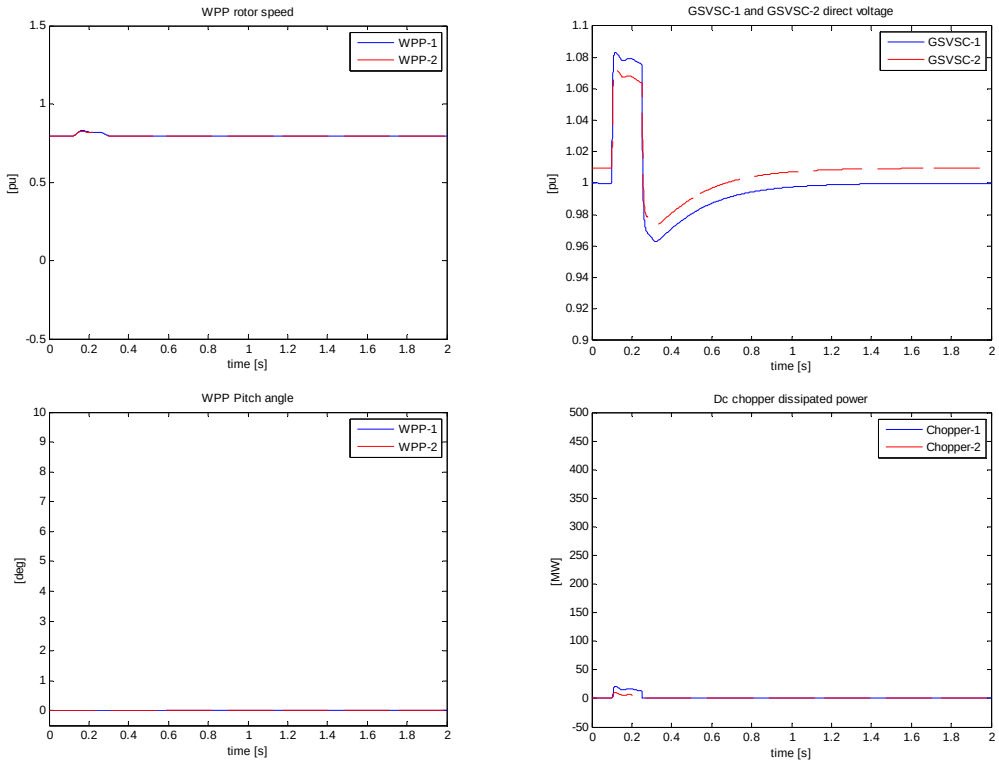

Case B: Voltage dip at onshore grid-2

Simulation scenario

Initially, the WPPs deliver 400 MW to the offshore network. GSVSC-1 transfers 300 MW to the onshore grid-1 and GSVSC-2 transfers 100 MW to the onshore grid-2 regarding proportional power sharing 3:1. At 0.1s, voltage dip 1 pu occurs at onshore grid-2 for 150 ms. Due to the voltage dip, GSVSC-2 can not transfer power to the onshore grid-2 and thus the direct voltage rises. It exceeds 1.01 pu and thus triggers the VMM in GSVSC-1 to adjust its power limit to the higher stage and therefore power delivered to onshore grid-1 is elevated. The dc choppers and frequency increase method successfully work to dissipate the excess power on the offshore network and maintains direct voltage below 1.2 pu at both GSVSC-1 and GSVSC-2. At 0.25 s., the voltage at onshore grid-2 is back to its nominal and power delivered to onshore grid-2 is restored quickly. As power delivered to onshore grid-2 is restored, the direct voltage returns to its pre-fault value and so does the power transferred to onshore grid-1.

Simulation results

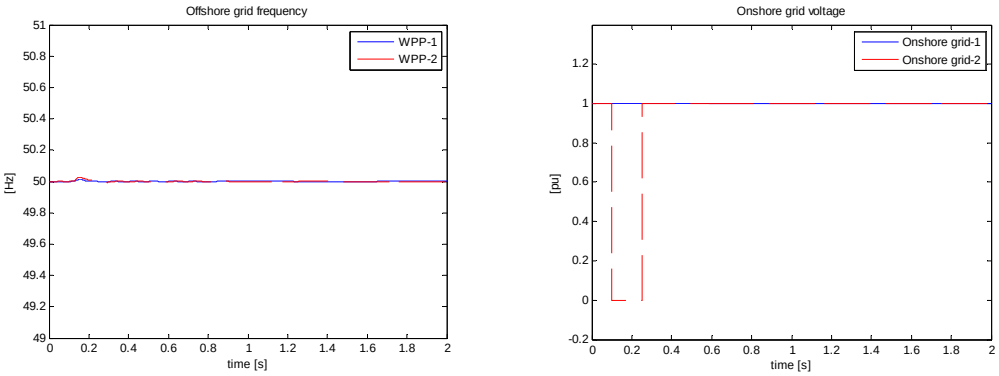

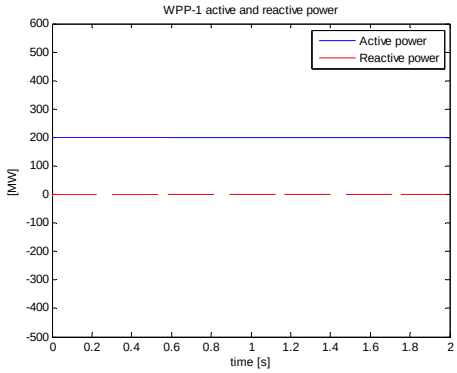
WPP-1 active and reactive power
Active power
Reactive power
[MW]
time [s]

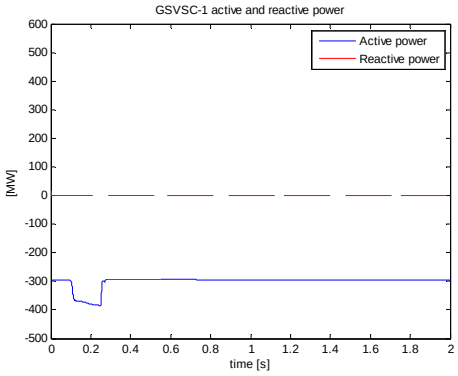
GSVSC-1 active and reactive power
Active power
Reactive power
[MW]
time [s]

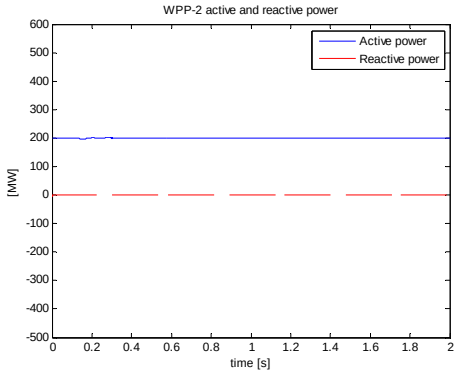
WPP-2 active and reactive power
Active power
Reactive power
[MW]
time [s]

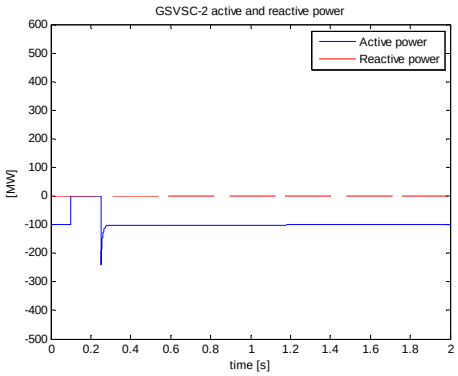
GSVSC-2 active and reactive power
Active power
Reactive power
[MW]
time [s]

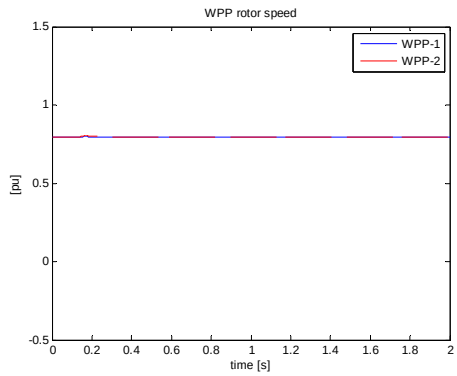
WPP rotor speed
WPP-1
WPP-2
[pu]
time [s]

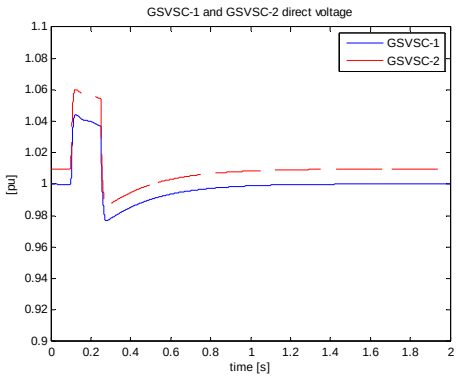
GSVSC-1 and GSVSC-2 direct voltage
GSVSC-1
GSVSC-2
[pu]
time [s]

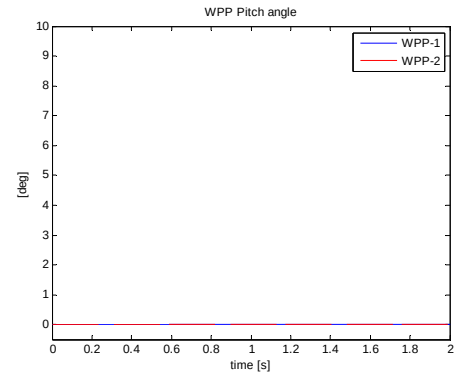
WPP Pitch angle
WPP-1
WPP-2
[deg]
time [s]

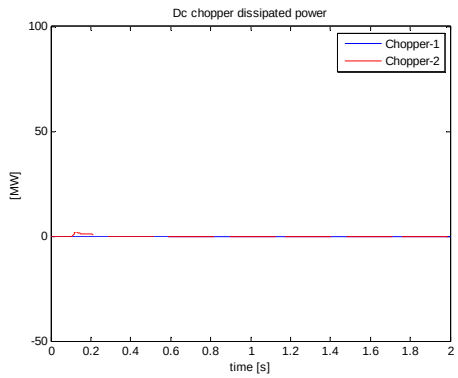
Dc chopper dissipated power
Chopper-1
Chopper-2
[MW]
time [s]

7 Conclusions and Recommendations

7.1 Conclusions

In this thesis project, a control strategy based on the voltage-margin method for dispatching power in future transnational offshore networks has been developed. The capability of the control strategy to perform several market dispatch schemes and to control the direct voltage interchangeably has been explored through simulating several cases. Moreover, the compatibility of the control scheme to work with a particular fault ride-through mechanism during voltage dips in the onshore grid has been studied. Based on the results, several conclusions can be drawn:

a. The control strategy is capable of performing fixed power sharing and priority power sharing without depending on the communication. In order to perform proportional power sharing, however, the control strategy requires a communication with a supervisory controller.
b. For the priority and the proportional power sharing application, the required voltage margin should be set slightly higher than the expected voltage drop between the converter pair.
c. Upon particular changes in the network topology i.e. addition of new converters, the existing converters are able to maintain normal operation without necessarily adjusting their control parameters.
d. The control strategy is capable of controlling the direct voltage interchangeably and maintaining normal operation in the network upon losing a direct voltage controlling converter. During the period when the direct voltage controlling task is exchanged between the converters, a small rise in the direct voltage is observed. This is due to the direct voltage reference value of the converters are displaced one another by a certain voltage margin.
e. During voltage dip occurrence in the onshore network, the control strategy is satisfactory complying with the energy dissipation method and the frequency modulation method of the fault ride-through mechanism.

7.2 Recommendations

In order to further explore the capability of the control strategy, several studies are recommended for future work:

a. In order to perform proportional power sharing, the control strategy requires a communication with a supervisory controller. In this thesis, communication delay is not considered. In practice however the effect of communication delay would be significant. Therefore the capability of the control strategy to perform the proportional power sharing under a communication delay demands further exploration.
b. In this thesis, the response of the control strategy to a disconnection of an onshore converter and to a voltage dip at an onshore grid has been reported. In the future, the response of the control strategy to a circuit disconnection in the dc link should be studied as well.
c. Due to the utilization of the voltage margin between converter pair, the application of the control strategy to a number of converters in a multi-terminal network would result in a large voltage margin between one converter and the farthest converter. Future study is therefore required to determine the maximum number of converters the control strategy can be applied at.

Appendix A – Simulation Results

A.1 Loss of an onshore converter

A.1.1 Fixed power sharing

Case C: GSVSC-2 injects power to the offshore network; Loss of GSVSC-1

Simulation scenario

Initially, GSVSC-1 delivers 200 MW fixed power to the onshore grid-1. WPPs deliver 100 MW to the offshore network and GSVSC-2 injects 100 MW to the offshore network. GSVSC-2 controls the direct voltage at 1.01 pu. At 1s, GSVSC-1 suddenly disconnected. Due to disconnection of GSVSC-1, power cannot be transferred to the onshore grid-1 any longer and thus the direct voltage rises. GSVSC-2 percieves this rise and reacts to change its power direction. GSVSC-2 now supplies power to the onshore grid-2.

Simulation results

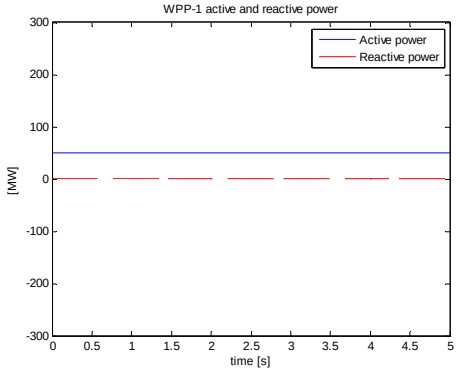

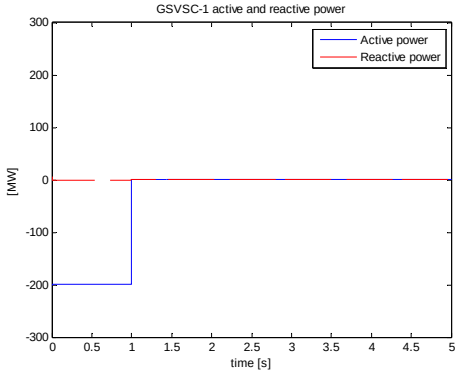

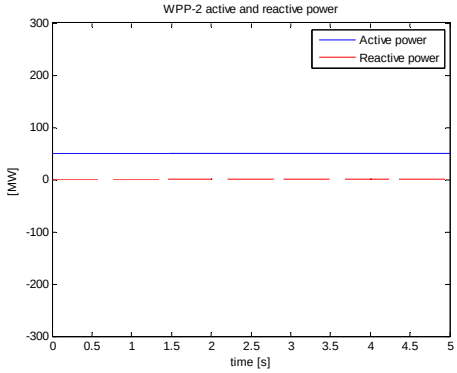

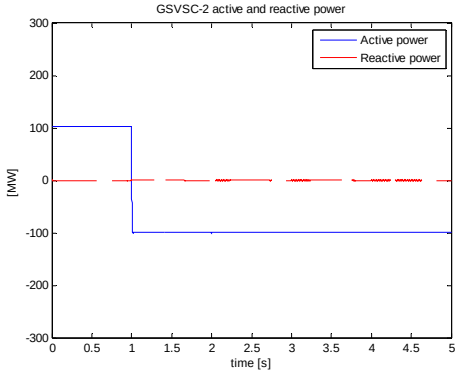

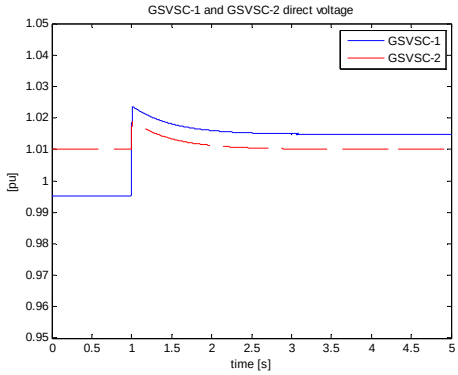

Case D: GSVSC-2 delivers power to the onshore grid-2; Loss of GSVSC-1

Simulation scenario

Initially, GSVSC-1 delivers 200 MW fixed power to the onshore grid-1. WPPs deliver 300 MW to the offshore network and thus GSVSC-2 transfers 100 MW to the onshore grid-2. GSVSC-2 controls the direct voltage at 1.01 pu. At 1s, GSVSC-1 disconnected suddenly. Due to disconnection of GSVSC-1, power can not be transferred to the onshore grid-1 and thus direct voltage rises. GSVSC-2 sees the rise of direct voltage and reacts by increase its power. GSVSC-2 now supplies 300 MW to the onshore grid-2.

Simulation results

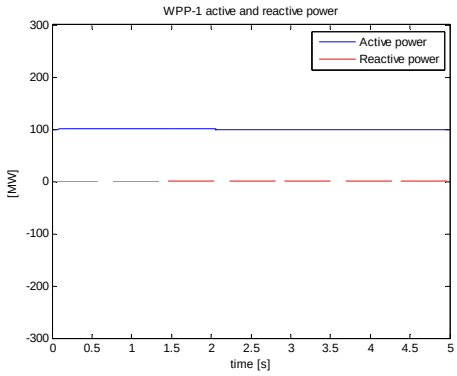

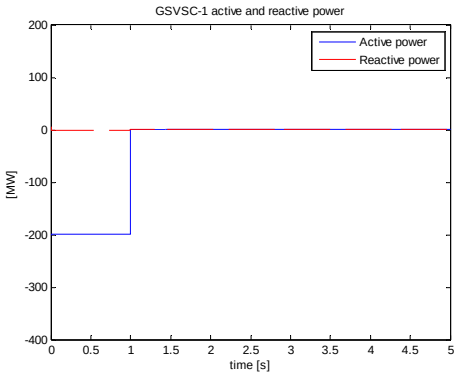

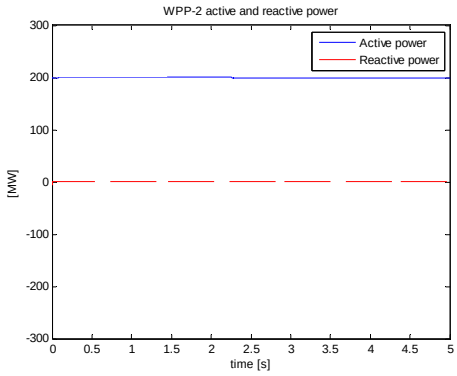

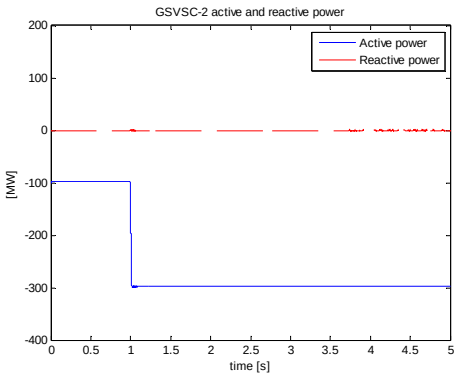

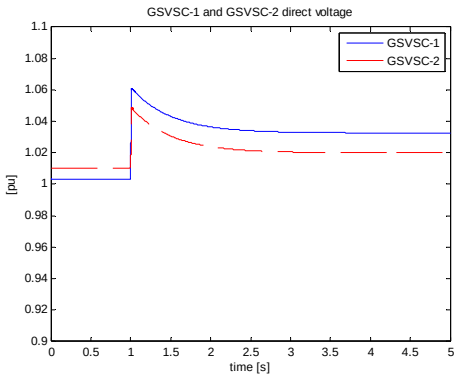

A.1.2 Priority power sharing

Case B: Loss of GSVSC-1

Simulation scenario

Initially, the WPPs deliver 100 MW to the offshore network. GSVSC-1 is pre-scheduled to have the first priority to transfer up to 200 MW to the onshore grid-1 and therefore now it transfers 100 MW to the onshore grid-1. GSVSC-1 controls the direct voltage at 1.0 pu. No power is delivered to the onshore grid-2 by GSVSC-2. At 1s, GSVSC-1 is suddenly disconnected and thus direct voltage rises. It exceeds 1.01 pu and therefore GSVSC-2 reacts by start delivering power to the onshore grid-2. GSVSC-2 now controls the direct voltage and brings the direct voltage to 1.01 pu.

Simulation results

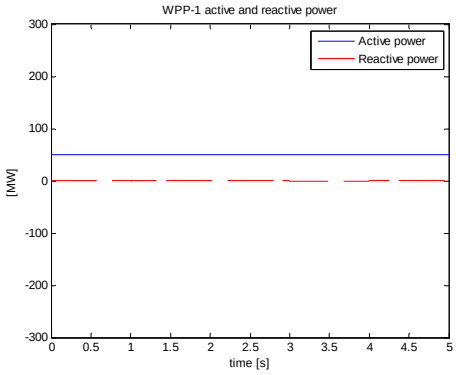

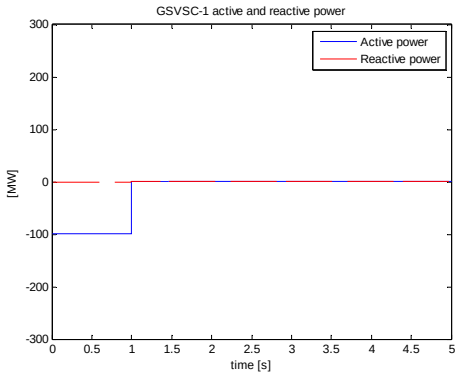

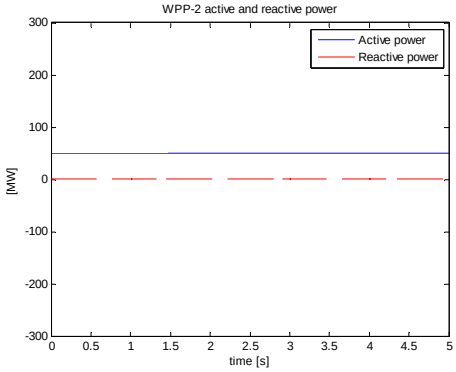

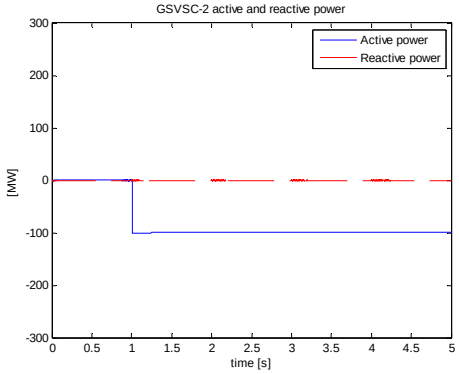

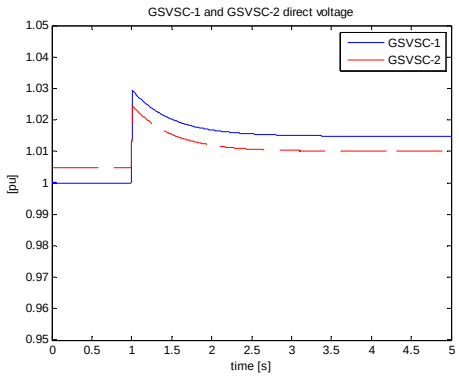

A.1.3 Proportional power sharing

Case B: Loss of GSVSC-1

Simulation scenario

Initially, the WPPs deliver 100 MW to the offshore network. GSVSC-1 transfers 75 MW to the onshore grid-1 and GSVSC-2 transfers nearly 25 MW to the onshore grid-2 regarding proportional power sharing 3:1. Since GSVSC-1 has reached its power order limit, GSVSC-2 controls the direct voltage at 1.01 pu. At 1s, GSVSC-1 is suddenly disconnected and because it was in inverting mode, the direct voltage rises. It exceeds 1.02 pu and thus triggers the VMM in GSVSC-2 to adjust its power limit to the higher stage and therefore power delivered to onshore grid-2 is elevated. GSVSC-2 controls the direct voltage and brings the direct voltage to 1.02 pu.

Simulation results

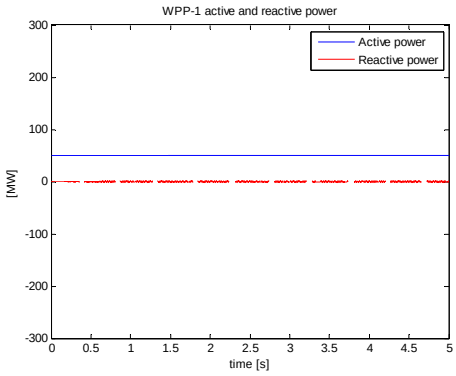

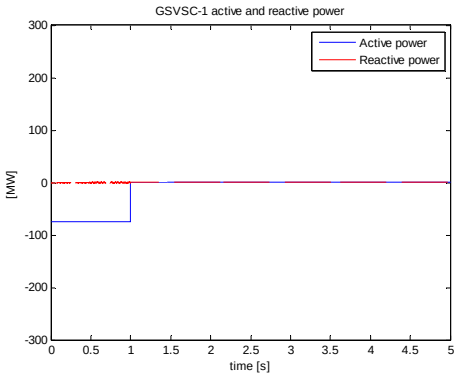

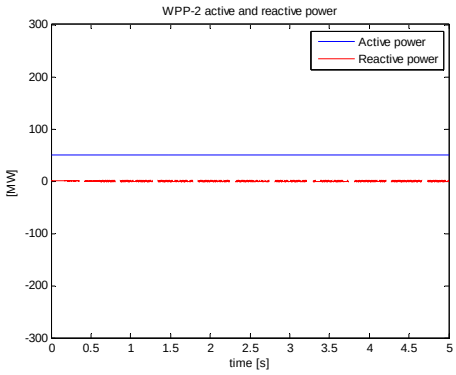

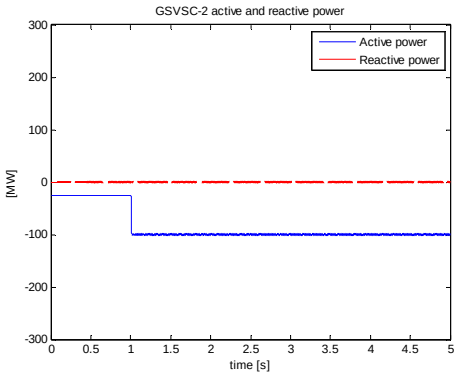

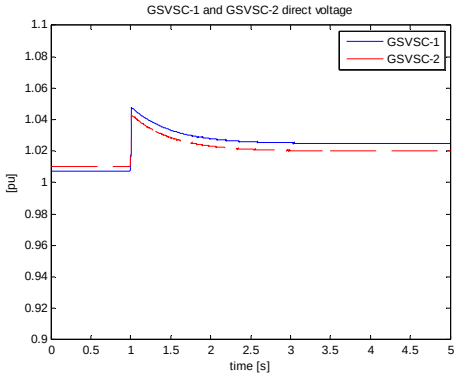

A.2 Fault ride-through
A.2.1 FRT with fixed power sharing (onshore grids coupled)

Case A: GSVSC-2 injects power to the offshore network; voltage dip at onshore grid-1

Simulation scenario
Initially, the WPPs deliver 200 MW to the offshore network. GSVSC-1 transfers 400 MW to the onshore grid-1 while GSVSC-2 injects 200 MW to the offshore network. At 0.1s, voltage dip of 1 pu occurs at onshore grid-1 for 150 ms. Due to direct voltage rises, GSVSC-2 quickly changes its power direction. Neither the dc choppers nor the frequency increase method is triggered.

Simulation results

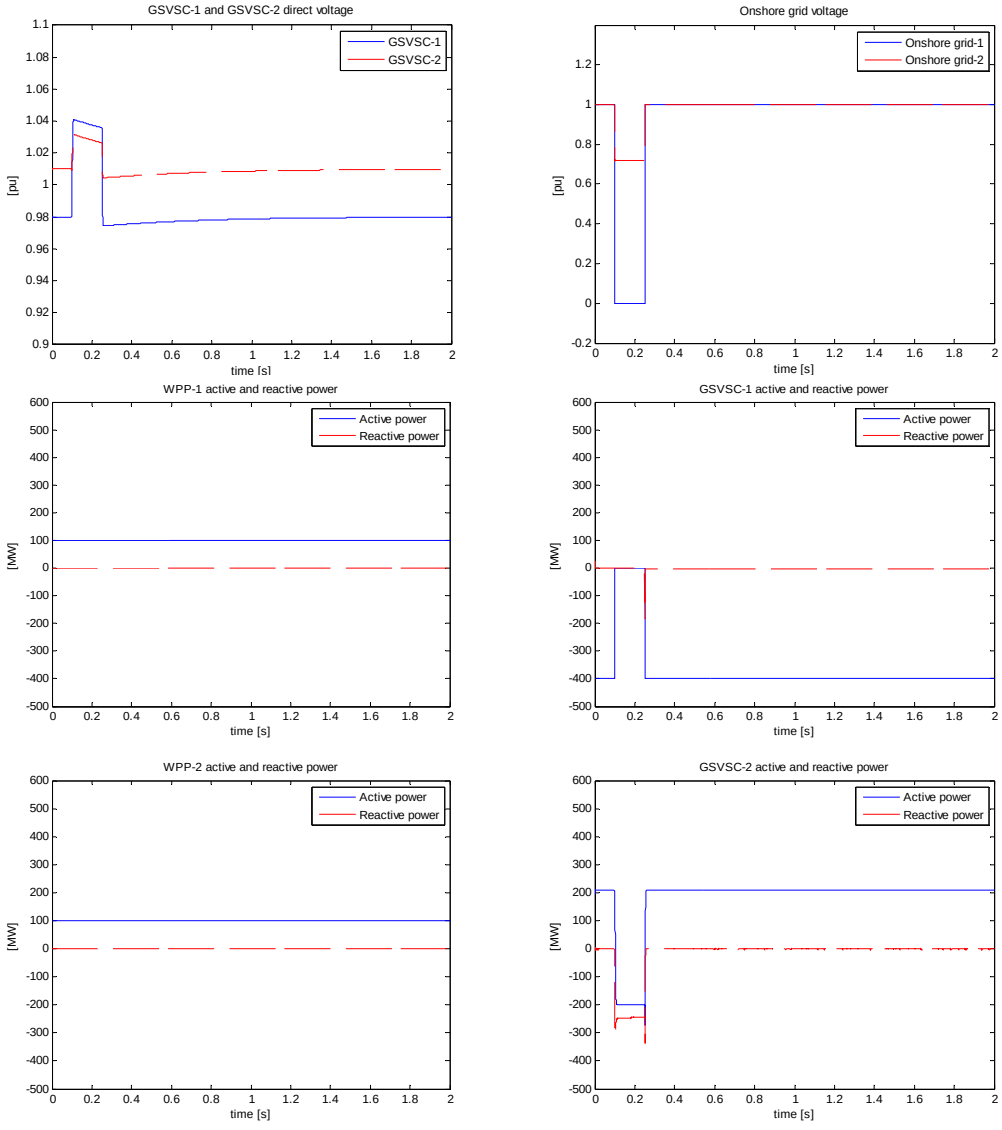

Case B: GSVSC-2 delivers power to the onshore grid-2; voltage dip at onshore grid-1

Simulation scenario
Initially, the WPPs deliver 800 MW to the offshore network. GSVSC-1 transfer 400 MW to the onshore grid-1 and GSVSC-2 transfer 400 MW to the onshore grid-2. At 0.1 s, a voltage dip of 1 pu occurs at onshore grid-1 for 150 ms. The dc choppers and frequency

increase method successfully collaborate to maintain the direct voltage below 1.2 pu at both GSVSC-1 and GSVSC-2.

Simulation results

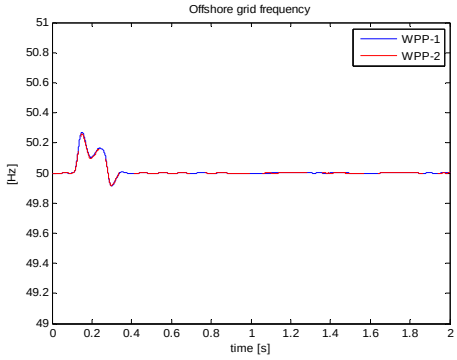

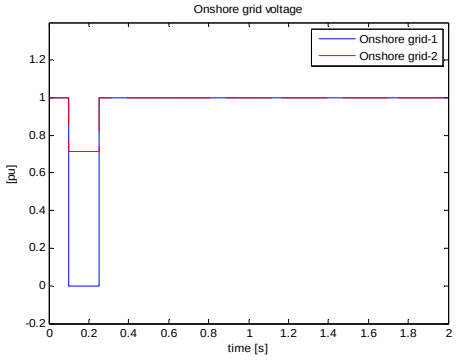

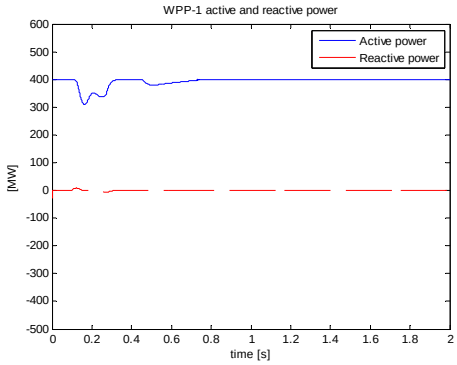

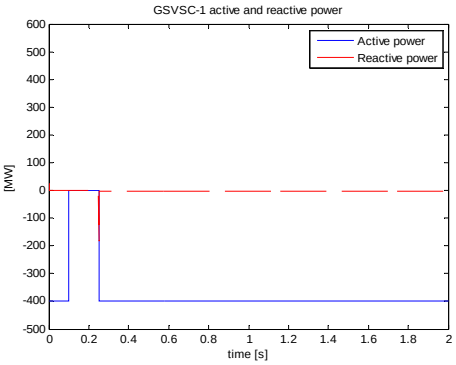

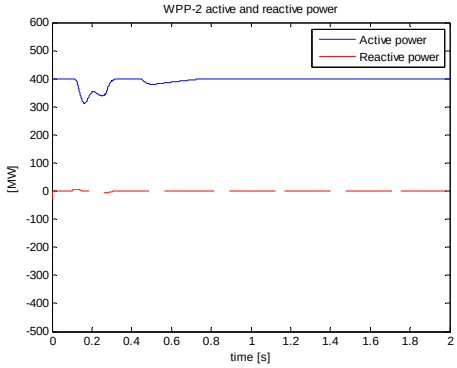

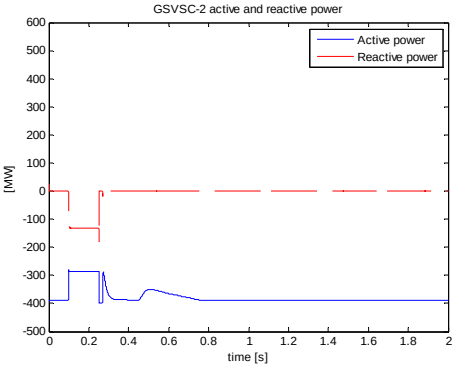

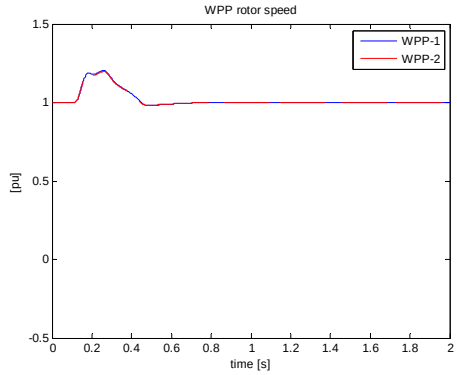

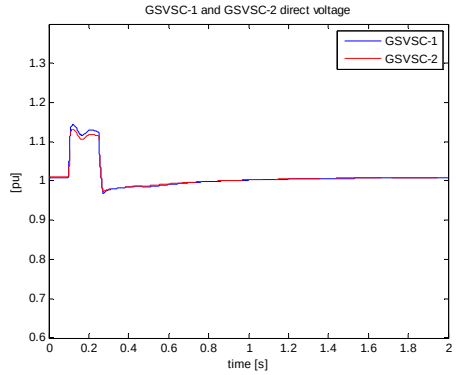

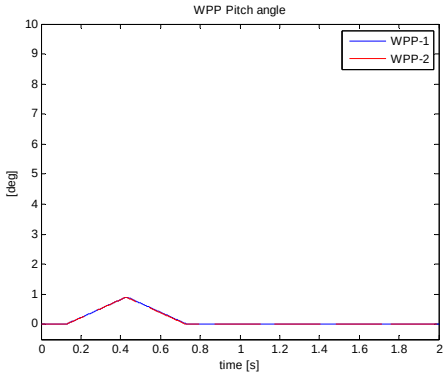

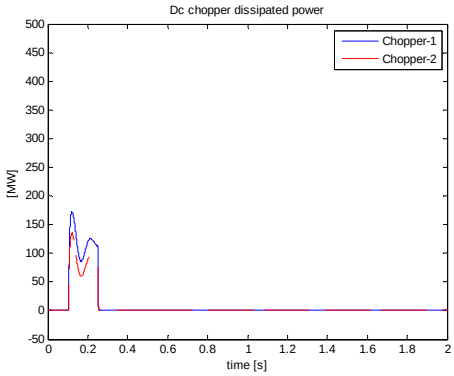

Case C: GSVSC-2 injects power to the offshore network; voltage dip at onshore grid-2

Simulation scenario

Initially, the WPPs deliver 200 MW to the offshore network. GSVSC-1 transfers 400 MW to the onshore grid-1 while GSVSC-2 injects 200 MW to the offshore network. At 0.1s, voltage dip of 1 pu occurs at onshore grid-2 for 150 ms. This causes GSVSC-2 top stop injecting power to the offshore network and thus the direct voltage drops. Due to this, GSVSC-1 quickly reduces the power transferred to onshore grid-1. Neither dc choppers nor frequency increase method is triggered. At 0.25s, voltage at onshore grid-2 is back to its normal operating region. Power injected to the offshore network by GSVSC-2 rises high very quickly to restore the direct voltage. As the direct voltage recovers, the power transferred to the onshore grid-1 returns to the pre-fault value.

Simulation results

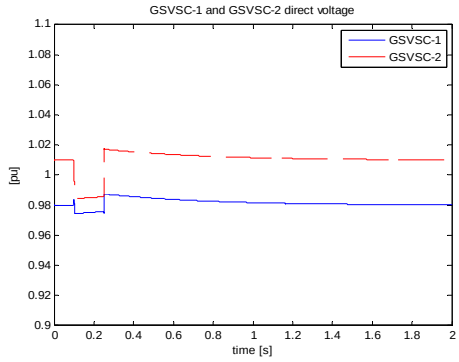

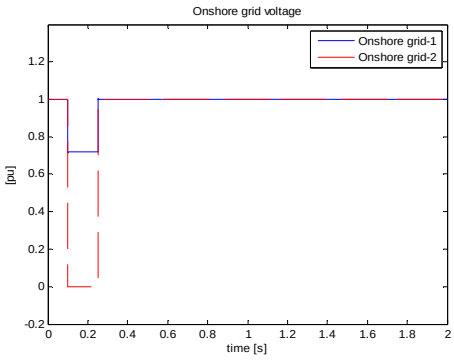

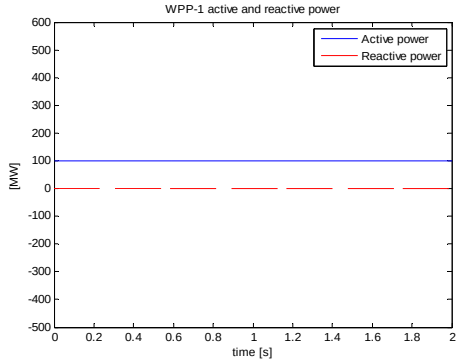

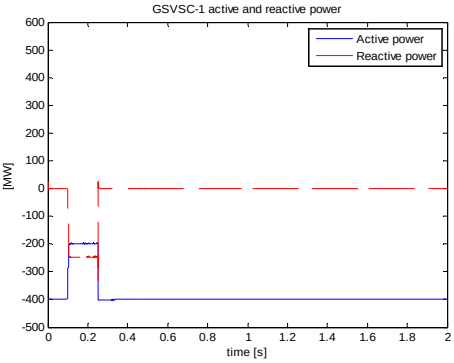

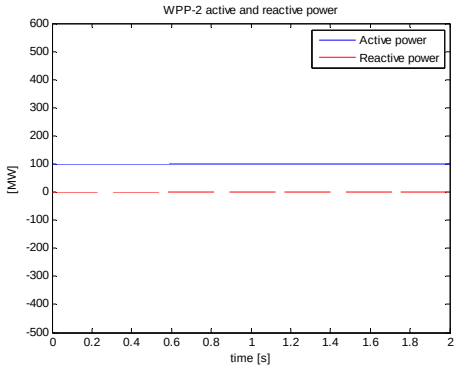

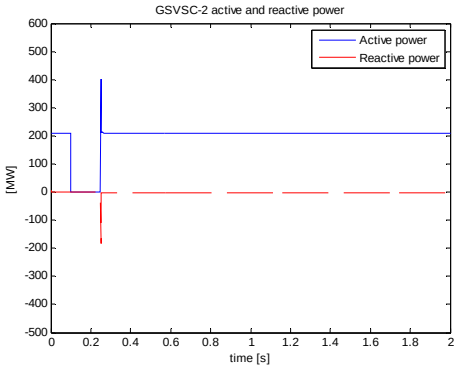

Case D: GSVSC-2 delivers power to the onshore grid-2; voltage dip at onshore grid-2

Simulation scenario

Initially, the WPPs deliver 800 MW to the offshore network. GSVSC-1 transfer 400 MW to the onshore grid-1 and GSVSC-2 transfer 400 MW to the onshore grid-2. At 1.0s, a voltage dip of 1 pu occurs at onshore grid-2, which lasts for 150 ms. The FRT system successfully work to dissipate the excess power on the offshore network and therefore, the direct voltage is kept below 1.2 pu at both GSVSC-1 and GSVSC-2.

Simulation results

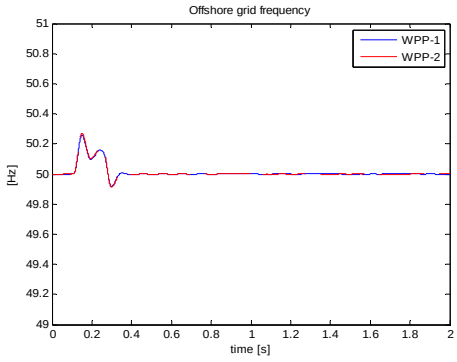

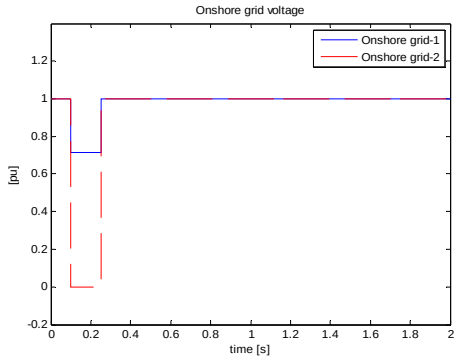

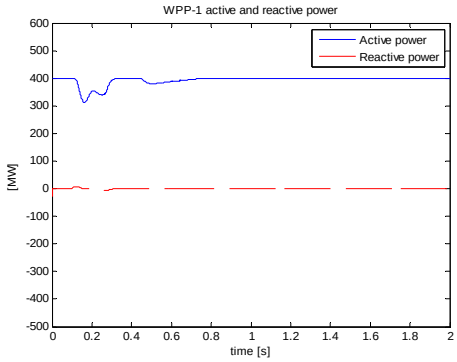

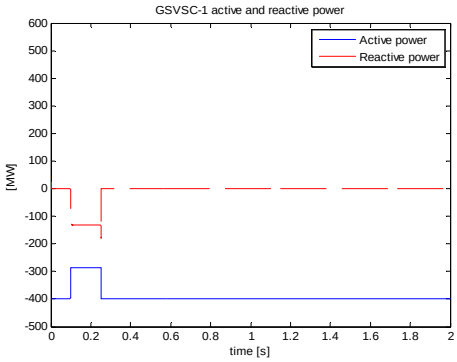

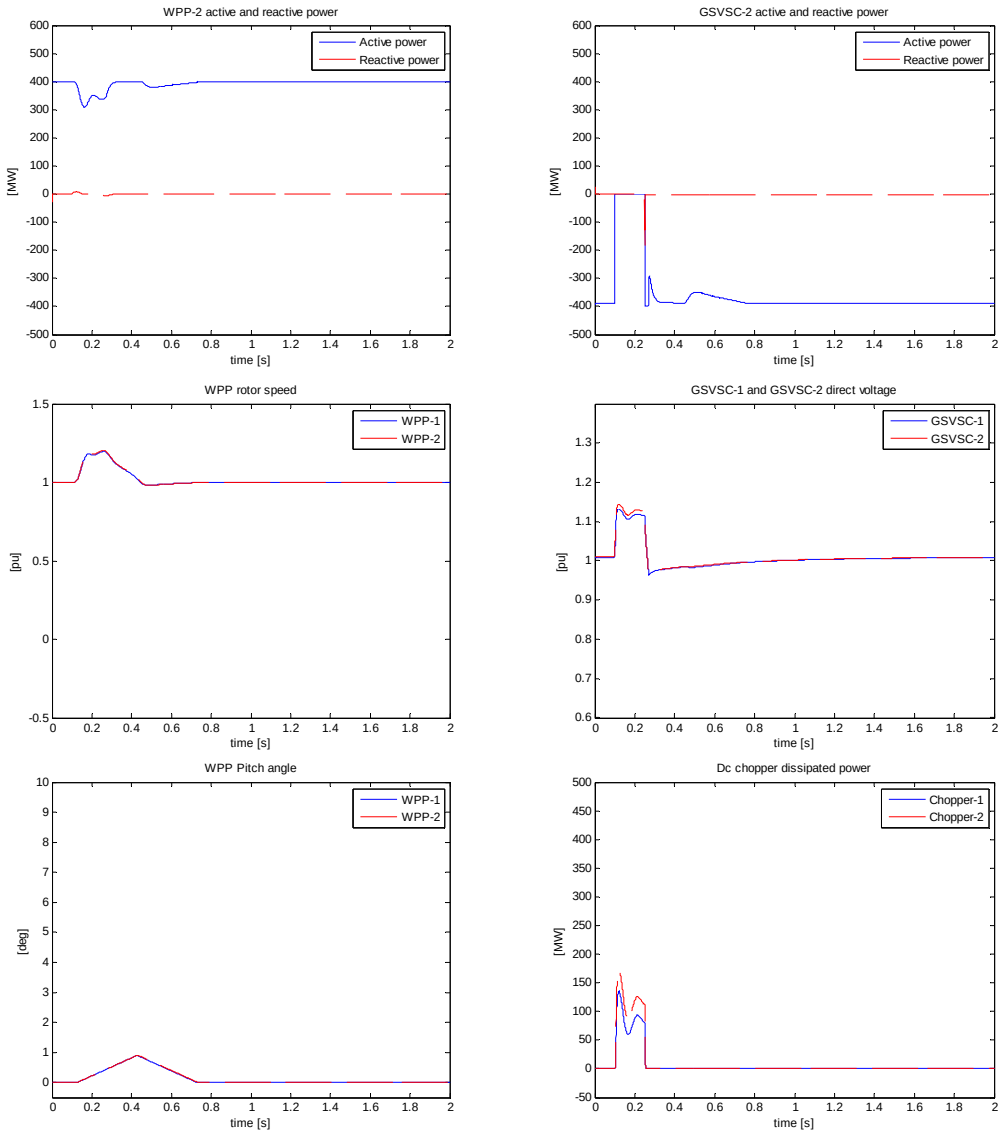

A.2.2 FRT with priority power sharing (onshore grids coupled)

Case A: Voltage dip at onshore grid-1

Simulation scenario

Initially, the WPPs deliver 800 MW to the offshore network. GSVSC-1 transfer 400 MW to the onshore grid-1 and GSVSC-2 transfer 400 MW to the onshore grid-2. At 0.1s, a voltage dip of 1 pu (so a three-phase bolted fault) occurs at onshore grid-1, lasting for 150 ms. Both dc choppers and frequency modulation work together to maintain the direct voltage below 1.2 pu at both GSVSC-1 and GSVSC-2.

Simulation results

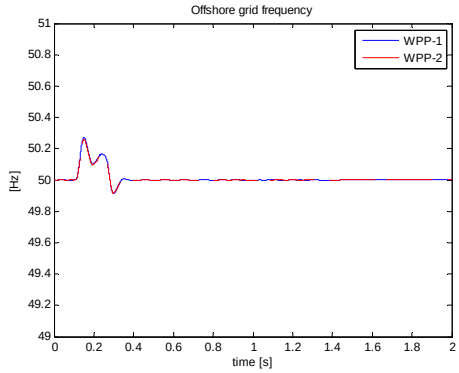

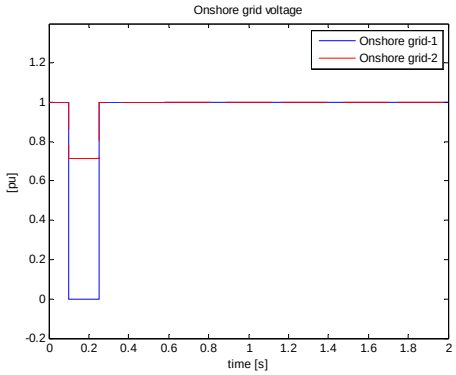

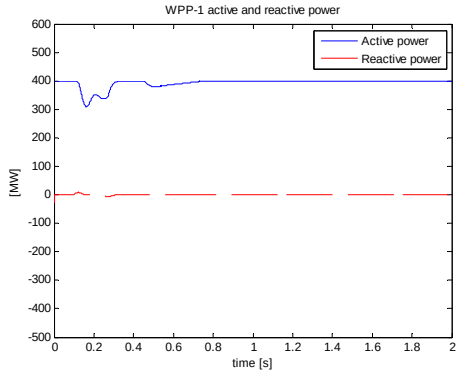

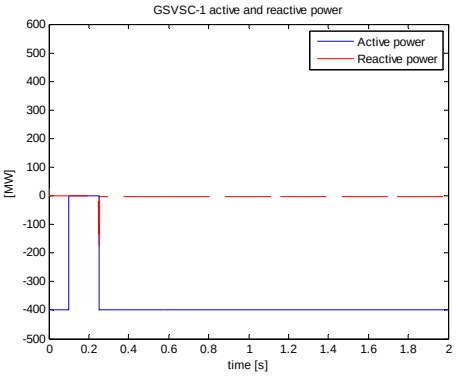

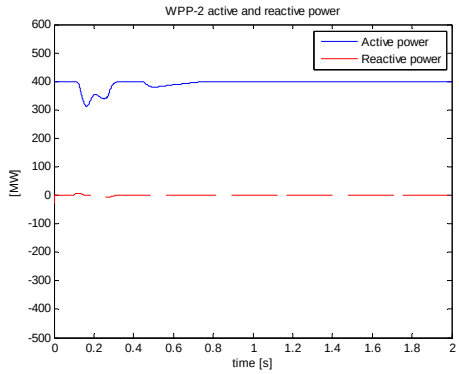

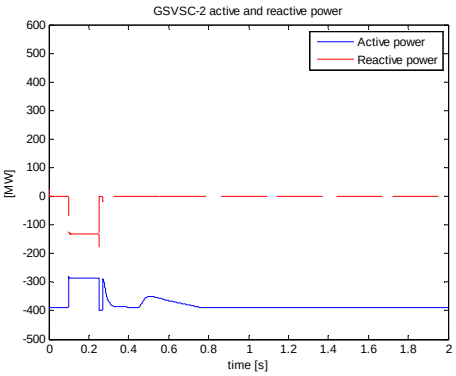

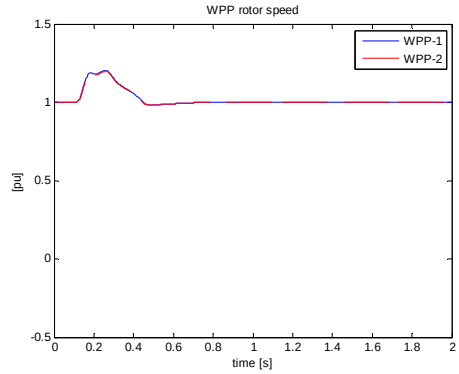

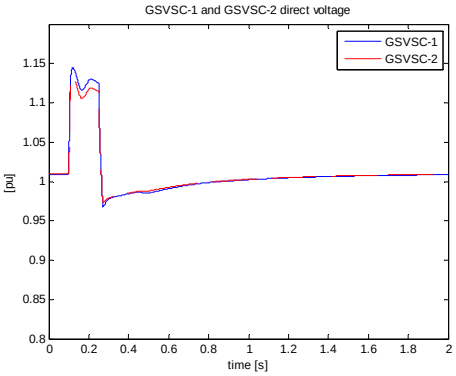

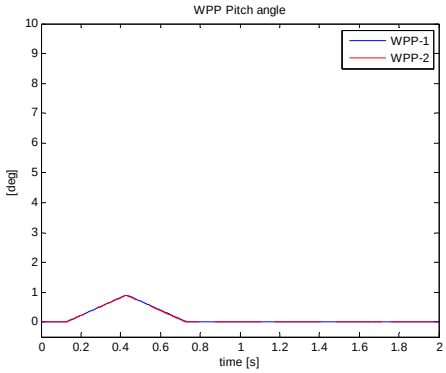

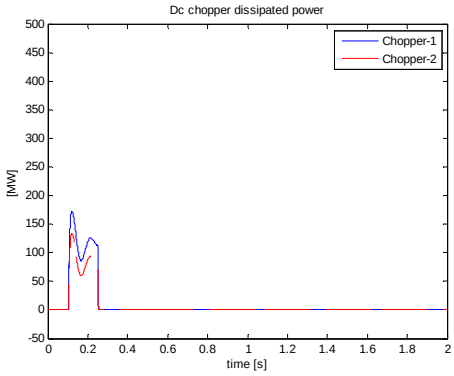

Case B: Voltage dip at onshore grid-2

Simulation scenario

At the outset of the simulation, the WPPs both deliver 400 MW to the offshore network. GSVSC-1 transfer 400 MW to the onshore grid-1 and GSVSC-2 transfer 400 MW to the onshore grid-2. At 0.1s, voltage dip of 1 pu occurs at onshore grid-2 for 150 ms. The dc choppers and frequency increase method successfully work to dissipate the excess power on the offshore network and maintains direct voltage below 1.2 pu at both GSVSC-1 and GSVSC-2.

Simulation results

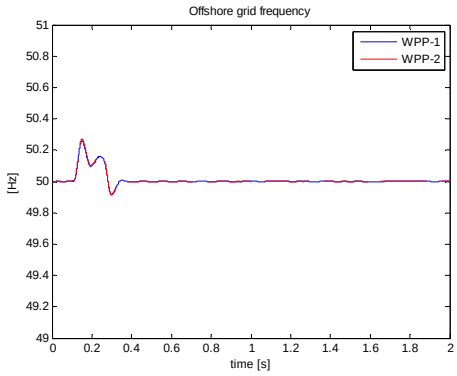

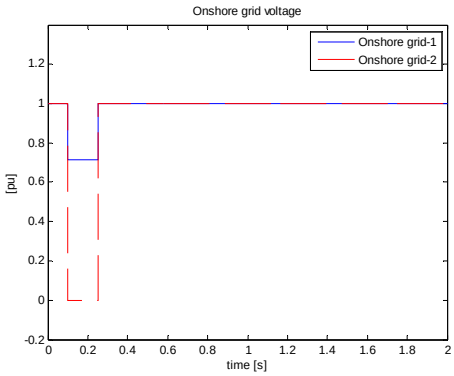

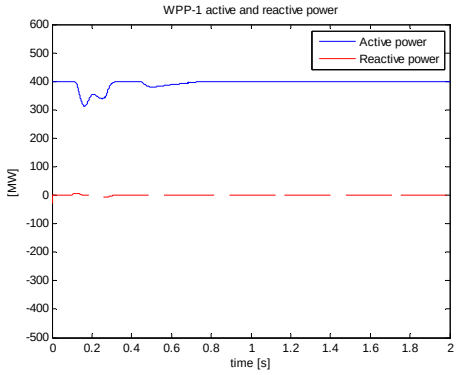

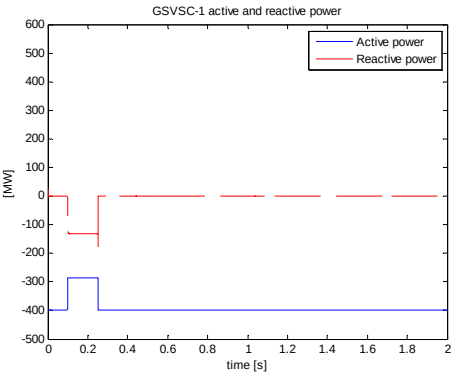

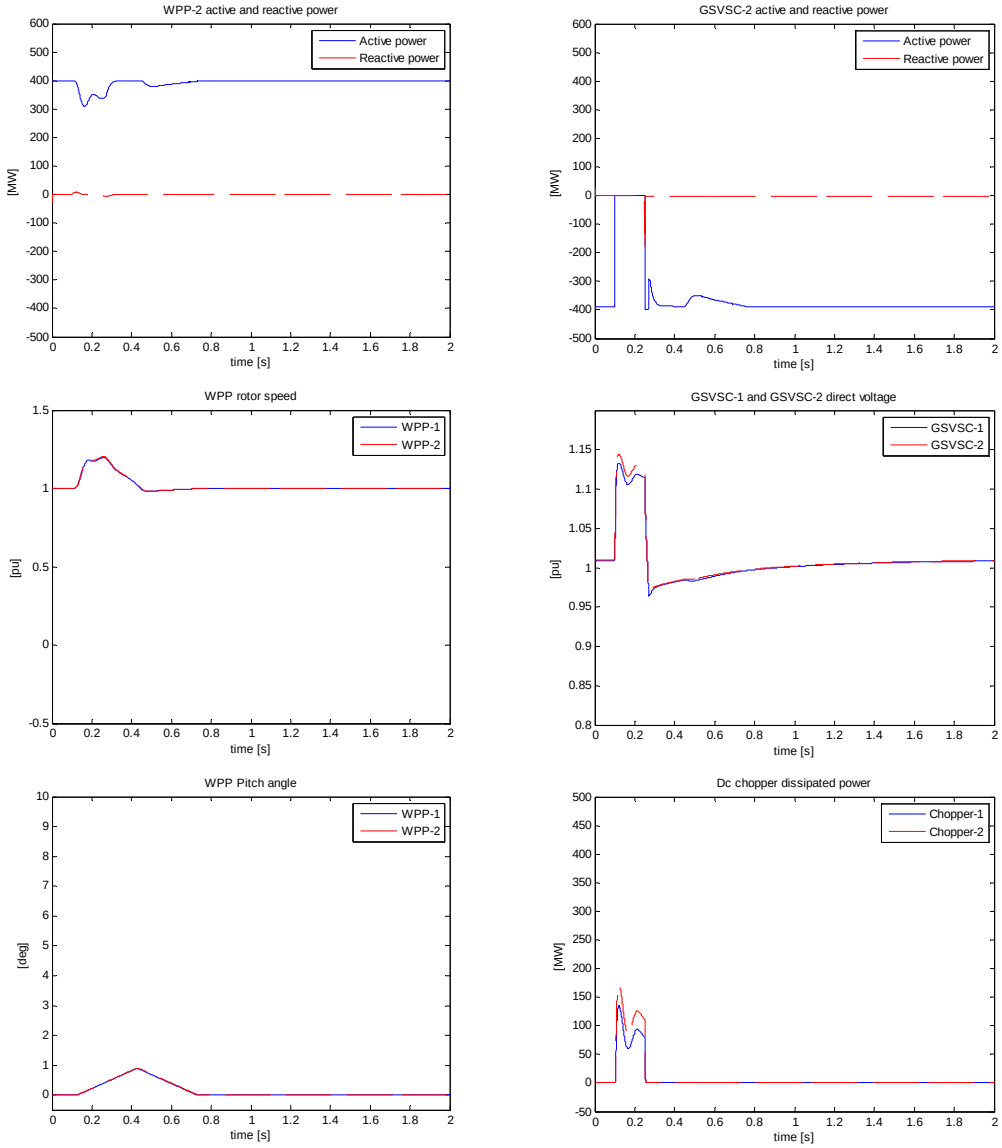

A.2.3 FRT with proportional power sharing (onshore grids coupled)

Case A: Voltage dip at onshore grid-1

Simulation scenario

Initially, the WPPs deliver 400 MW to the offshore network. GSVSC-1 transfers 300 MW to the onshore grid-1 and GSVSC-2 transfers 100 MW to the onshore grid-2 regarding proportional power sharing 3:1. At 0.1s, a three phase bolted fault occurs at onshore grid-1, with a duration of 150 ms. Due to the voltage dip, GSVSC-1 can not transfer power to the onshore grid-1 and thus the direct voltage rises. It exceeds 1.01 pu and the VMM triggers the GSVSC-2 to adjust its power limit to the higher stage and therefore, the power delivered to onshore grid-2 is elevated. However, in this case, due to onshore grids are coupled, voltage at onshore grid-2 drops and thus power delivered to onshore grid-2 is elevated less that that shown in section 5.2.3.1 Case A. As a consequence, the peak of the direct voltage is higher. The FRT methods successfully maintain the direct voltage below 1.2 pu at both GSVSCs. At 0.25 s, the ac voltage at onshore grid-1 is back to its nominal and power delivered to onshore grid-1 is restored

quickly. As power delivered to onshore grid-1 is restored, the direct voltage returns to its pre-fault value and so does the power transferred to onshore grid-2.

Simulation results

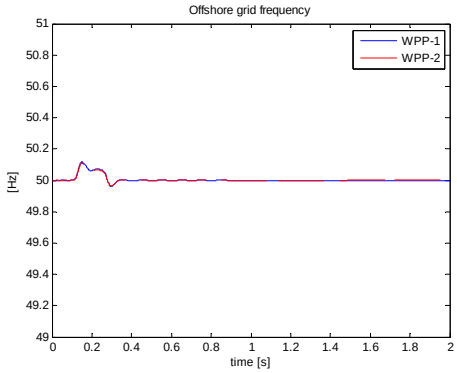

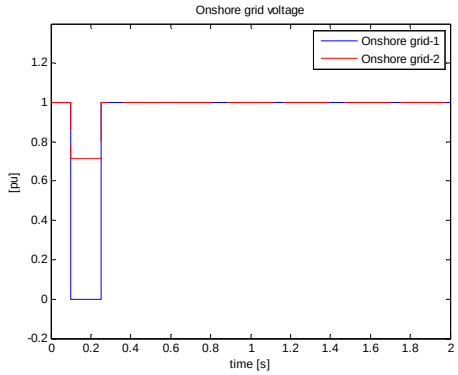

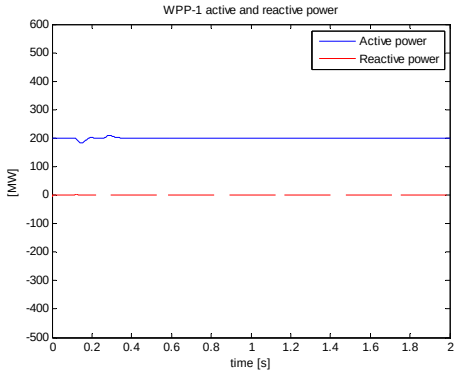

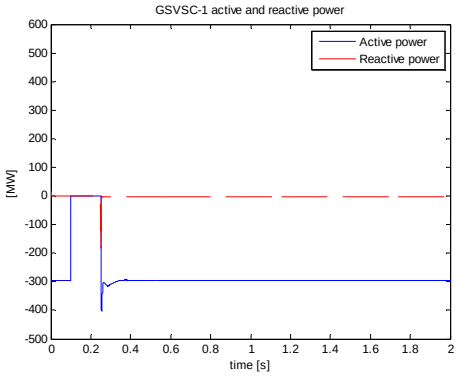

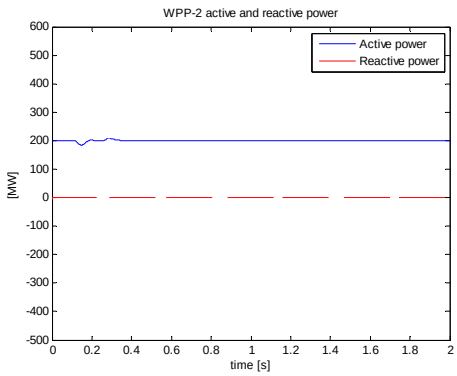

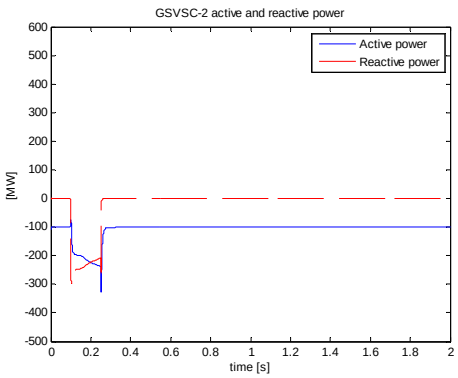

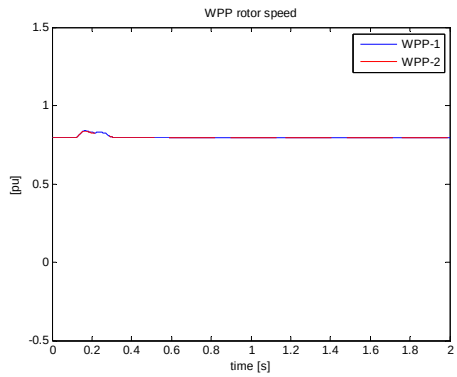

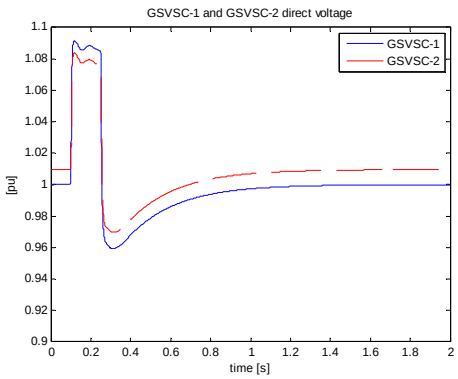

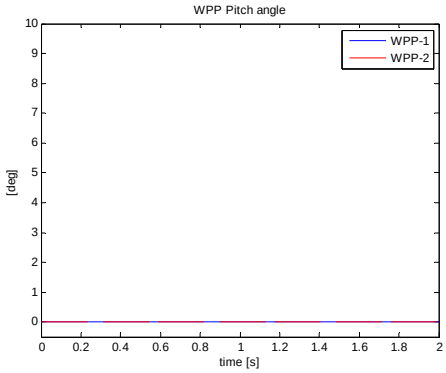

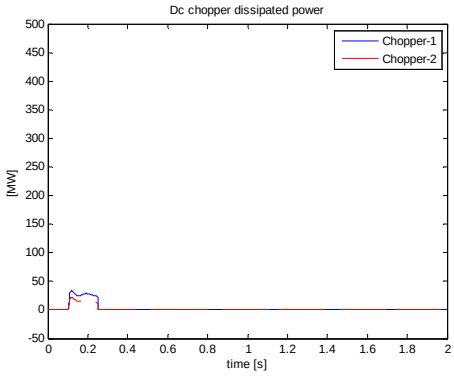

Case B: Voltage dip at onshore grid-2

Simulation scenario

Initially, the WPPs deliver 200 MW to the offshore network each. GSVSC-1 transfers 300 MW to the onshore grid-1 and GSVSC-2 transfers 100 MW to the onshore grid-2 regarding proportional power sharing 3:1. At 0.1s, voltage dip of 1 pu occurs at the onshore grid-2 for 150 ms. Due to the voltage dip, GSVSC-2 cannot transfer power to the onshore grid-2 and thus direct voltage rises. The dc choppers and frequency increase method successfully work to dissipate the excess power on the offshore network and maintains direct voltage below 1.2 pu at both GSVSC-1 and GSVSC-2. At 0.25s, the ac voltage at onshore grid-2 is back to its nominal and power delivered to onshore grid-2 is restored quickly. As power delivered to onshore grid-2 is restored, direct voltage returns to its pre-fault value.

Simulation results

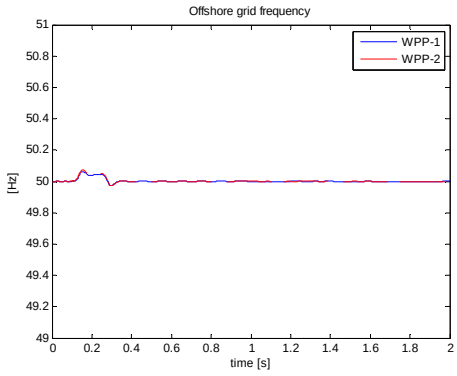

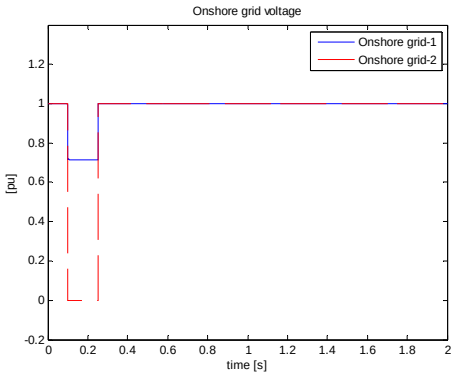

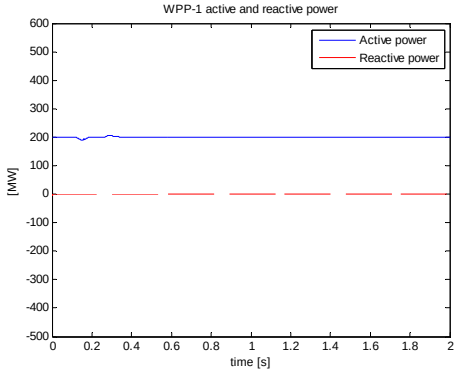

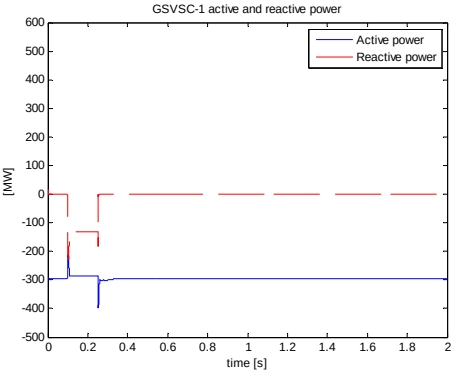

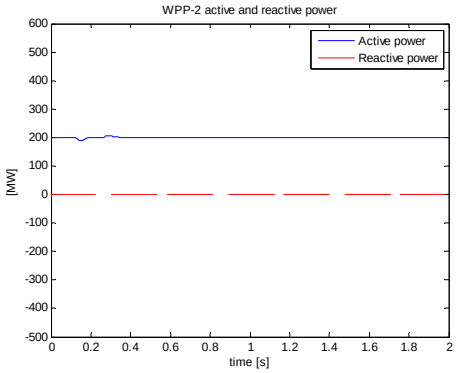
WPP-2 active and reactive power
Active power
Reactive power
[MW]
time [s]

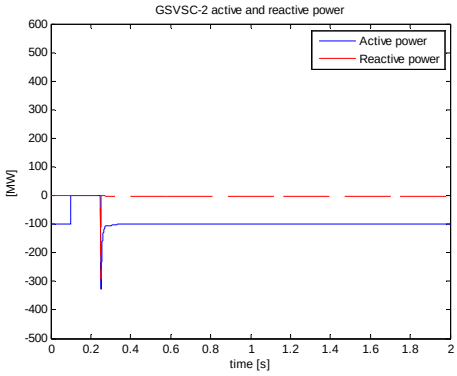
GSVSC-2 active and reactive power
Active power
Reactive power
[MW]
time [s]

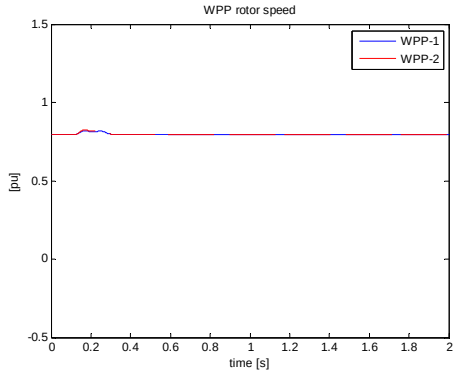
WPP rotor speed
WPP-1
WPP-2
[pu]
time [s]

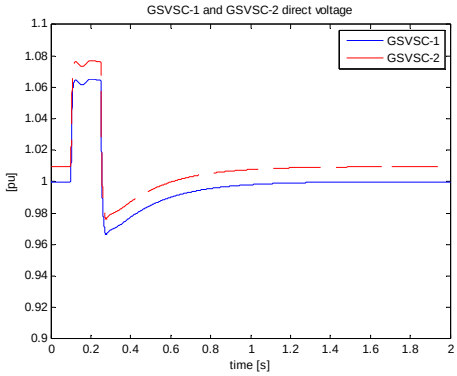
GSVSC-1 and GSVSC-2 direct voltage
GSVSC-1
GSVSC-2
[pu]
time [s]

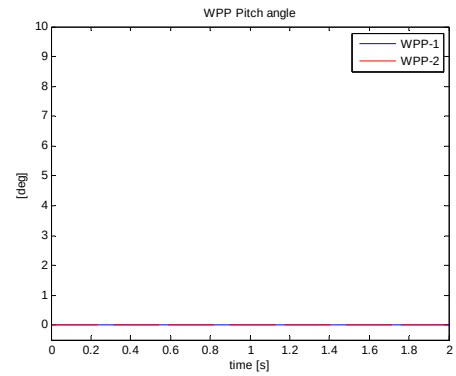
WPP Pitch angle
WPP-1
WPP-2
[deg]
time [s]

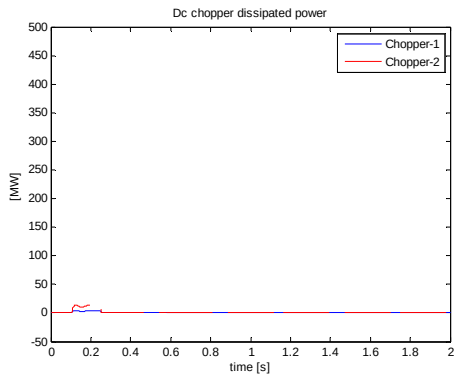
Dc chopper dissipated power
Chopper-1
Chopper-2
[MW]
time [s]

Appendix B - Network Data

Table B.1 Wind turbine data

S_{rated}	2.2 MVA
u_{rated}	0.69 kV
H_t	3.5 s
H_g	1 s
ω_{min}	0.94 rad/s
ω_{rated}	1.88 rad/s
$v_{w,\ rated}$	10.3 m/s
$C_{p,\ max}$	0.48
λ_{opt}	8.1
ρ	1.225 kg/m^3
r	88.7 m
L	0.15 pu
K_{pitch}	330
$K_{p,\ id}$	1
$K_{i,\ id}$	5
$K_{p,\ iq}$	1
$K_{i,\ iq}$	5
$K_{p,\ P}$	0.1
$K_{i,\ P}$	50
$K_{p,\ Q}$	0.01
$K_{i,\ Q}$	1000
$K_{p,\ v}$	0.01
$K_{i,\ v}$	1000
K_f	2

Table B.2 WPPVSC data

S_{rated}	440 MVA
u_{rated}	150 kV
$u_{dc,\ rated}$	300 kV
L	0.15 pu
C	58.7 µF
$K_{p,\ vd}$	0.01
$K_{i,\ vd}$	1000
$K_{p,\ vq}$	0.01
$K_{i,\ vq}$	1000
K_f	20.94
f_0	50

Table B.3 Dc link data

R_{dc}	0.0073 Ω/km
l	200 km

Table B.4 Dc chopper data

$P_{ch,\ rated}$	440 MW
$U_{ch,\ rated}$	360 kV
K_{ch}	6.67

Table B.5 GSVSC data

S_{rated}	440 MVA
u_{rated}	150 kV
$u_{dc,\ rated}$	300 kV
L	0.15 pu
C	58.7 µF
$K_{p,\ id}$	1
$K_{i,\ id}$	20
$K_{p,\ iq}$	1
$K_{i,\ iq}$	20
$K_{p,\ udc}$	50
$K_{i,\ udc}$	100
$K_{p,\ P}$	0.1
$K_{i,\ P}$	50
$K_{p,\ Q}$	0.05
$K_{i,\ Q}$	20
$K_{p,\ v}$	0.01
$K_{i,\ v}$	1000

Acknowledgements

This thesis project was carried out at the Electrical Power System research group as part of the two-year M.Sc. program at the Electrical Power Engineering, Delft University of Technology.

From the beginning until the fulfilling of this project, I have been supported by the following who I owe much gratitude to.

I would like to express my gratitude to prof. ir. W. L. Kling for his willingness to be my responsible professor. I also would like to appreciate my supervisor, dr. ir. M. Gibescu for warmly welcome me to join the Electrical Power System research group and for her continuous supervision. Great thanks to my daily supervisor, ir. A. A. van der Meer for initiating this project, for his guidance and his continuous support during the project. Many thanks to ir. S. W. H. de Haan for taking effort to evaluate this report.

I would like to thank the management of PT PLN (Persero) for supporting me during the program.

Last but not least, I especially thank my parents, my brother and Irene for their love and prayer.

References

[1] U.S. Dept. of Energy. (2008, Sep.). International Energy Outlook 2008. [Online]. Available: http://www.eia.doe.gov/oiaf/ieo/ieoarchive.html

[2] GWEC. (2010, Mar.). Global Wind 2009 Report. [Online]. Available: http://www.gwec.net/index.php?id=8

[3] EWEA. (____,___). Wind Energy - The Facts. [Online]. Available: http://www.ewea.org/index.php?id=178

[4] EWEA. (2009, Mar). Wind Energy - The Facts. [Online]. Available: http://www.wind-energy-the-facts.org/en/home--about-the-project.html

[5] EWEA. (2009, Jun.). Winning with European Wind. [Online]. Available: http://www.ewea.org/fileadmin/ewea_documents/documents/publications/Annual_Report_2008.pdf

[6] TradeWind. (2009, Feb.). Integrating Wind. [Online]. Available: http://www.ewea.org/index.php?id=178

[7] EWEA. (2009, Sep.). Oceans of Opportunity. [Online]. Available: http://www.ewea.org/index.php?id=178

[8] Greenpeace. (2008, Sep.) A North Sea Electricity Grid [R]Evolution. [Online]. Available: http://www.3e.be/publications.php

[9] Bram Van Eeckhout, "The economic value of VSC HVDC compared to HVAC for offshore wind farms," Master thesis, Elektrotechniek Dept., Katholieke Universiteit Leuven, Heverlee, Belgium, 2008. [Online]. Available: http://homes.esat.kuleuven.be/~dvherten/eindwerk_vsc_hvdc_bram_van_eeckhout.pdf

[10] Chuiqing Du, "VSC-HVDC for Industrial Power Systems," Ph.D. dissertation, Energy and Environment Dept., Chalmers University of Technology, Goteborg, Sweden, 2007. [Online]. Available: http://webfiles.portal.chalmers.se/et/PhD/CuiqingDuPhD.pdf

[11] ABB, "Its time to connect," ABB, 2008. [Online]. Available: http://www.abb.com/industries/us/9AAF400196.aspx

[12] Cuiqing Du, Agneholm E., "Investigation of Frequency/ AC Voltage Control for Inverter Station of VSC-HVDC," *IEEE 32nd Annual Conference on Industrial Electronics,* Paris, 2006, pp. 1810-1815.

[13] Siegfried Heier, "Grid Integration of Wind Energy Conversion Systems," John Wiley & Sons Ltd., 1998

[14] J.G. Slootweg, S.W.H. de Haan, H. Polinder, W.L. Kling, "General Model for Representing Variable Speed Wind Turbines in Power System Dynamics Simulations," *IEEE Transactions on Power Systems*, vol. 18, 2003, pp. 144-151.

[15] Greenpeace. (2000, Oct.). Offshore Wind Energy in the North Sea. [Online]. Available: http://www.greenpeace.org/international/en/publications/reports/offshore-wind-energy-in-the-no/

[16] J.G. Slootweg, W.L. Kling, "Modeling of Large Wind Farms in Power System Simulations," *2002 IEEE Power Engineering Society Summer Meeting*, Chicago, USA, vol.1, pp. 503-508.

[17] Z. Lubosny, "Wind Turbine Operation in Electric Power Systems Advance Modeling," Springer-Verlag Berlin, 2003

[18] James Conroy, Rick Watson, "Torsional Damping Control of Gearless Full-Converter Large Wind Turbine Generators with Permanent Magnet Synchronous Machines," *Wind Engineering*, vol. 31, no. 5, 2007, pp 325-340.

[19] Abram Perdana, "Dynamic Models of Wind Turbines," Ph.D. dissertation, Energy and Environment Dept., Chalmers University of Technology, Sweden, 2008. [Online]. Available: http://webfiles.portal.chalmers.se/et/PhD/PerdanaAbramPhD.pdf

[20] Lie Xu, Barry W. Williams, and Liangzhong Yao, "Multi-Terminal DC Transmission Systems for Connecting Large Offshore Wind Farms," *Proc. IEEE PES General Meeting*, Pittsburgh, July 2008.

[21] Lie Xu, Liangzhong Yao, Masoud Bazargan, and Barry W. Williams, "Control and Operation of Multi-Terminal DC System for Integrating Large Offshore Wind Farms," *Proc. of the 7th International Workshop on Large-Scale Integration of Wind Power into Power Systems*, Madrid, Spain, May 2008.

[22] Jun Liang, Oriol Gomis-Bellmunt, Janaka Ekanayake, and Nicholas Jenkins, "Control of multi-terminal VSC-HVDC transmission for offshore wind power," *13th European Conference on Power Electronics and Application*, Barcelona, Spain, September 2009.

[23] Yukio Tokiwa, Fumitoshi Ichikawa, Kenichi Suzuki, Haruhisa Inokuchi, Syunichi Hirose, and Kazuaki Kimura, "Novel Control Strategies for HVDC System with Self-Contained Converter," *Electrical Engineering in Japan*, vol. 113, no. 5, 1993, pp. 1-13.

[24] Tatsuhito Nakajima, and Shoichi Irokawa, "A Control System for HVDC Transmission by Voltage Sourced Converters," *IEEE Power Engineering Society Summer Meeting*, Edmonton, Alta, July 1999.

[25] Temesgen M. Haileselassie, Marta Molinas and Tore Undeland, "Multi-Terminal VSC-HVDC System for Integration of Offshore Wind Farms and Green Electrification of Platforms in the North Sea," *Nordic Workshop on Power and Industrial Electronics*, June 2008.

[26] Ciupuliga, A. R., Gibescu, M., Fulli, G., L'Abbate, A., Kling, W. L., "Grid Connection of Large Wind Power Plants: a European Overview," *Proc. 8th International Workshop on Large-Scale Integration of Wind Power into Power Systems as well as on Transmission Networks for Offshore Wind Farms* , Bremen, Germany 2009.

[27] L. Harnefors, Y. Jiang-Häfner, M. Hyttinen and T. Jonsson, "Ride-through methods for wind farms connected to the grid via a VSC-HVDC transmission," *Proc. Nordic Wind Power Conference*, Roskilde, Denmark, 2007.

[28] R. Hendriks, R. Völzke and W. Kling, "Fault Ride-Through Strategies for VSC-Connected Wind Parks," *European Wind Energy Conference*, 2009.

[29] R. L. Hendriks, G. C. Paap, and W. L. Kling, "Control of a multi-terminal VSC transmission scheme for connecting offshore wind farms," *in Proc. 2007 European Wind Energy Conference (EWEC).*